CAPITAL UNIVERSITY OF SCIENCE AND TECHNOLOGY, ISLAMABAD

Molecular Epidemiology of Antibiotics Resistance Genes in Smog Particulate Matter and its Health Implications

by

Muhammad Imran Khan

A dissertation submitted in partial fulfillment for the degree of Doctor of Philosophy

in the

Faculty of Health and Life Sciences
Department of Bioinformatics and Biosciences

2025

Molecular Epidemiology of Antibiotics Resistance Genes in Smog Particulate Matter and its Health Implications

By

Muhammad Imran Khan

(DBS193002)

Dr. Mashooq Khan, Associate Professor

Qilu University of Technology, Shandong, China

(Foreign Evaluator 1)

Dr. Wen-Jun Li, Professor

Sun Yat-Sen University, Guangzhou, China

(Foreign Evaluator 2)

Dr. Arshia Amin Butt

(Research Supervisor)

Dr. Syeda Marriam Bakhtiar

(Head, Department of Bioinformatics and Biosciences)

Dr. Sahar Fazal

(Dean, Faculty of Health and Life Sciences)

DEPARTMENT OF BIOINFORMATICS AND BIOSCIENCES

CAPITAL UNIVERSITY OF SCIENCE AND TECHNOLOGY

ISLAMABAD

2025

Copyright © 2025 by Muhammad Imran Khan

All rights reserved. No part of this dissertation may be reproduced, distributed, or transmitted in any form or by any means, including photocopying, recording, or other electronic or mechanical methods, by any information storage and retrieval system without the prior written permission of the author.

Dedicated to my beloved parents who sacrifice their comfort for my PhD

CAPITAL UNIVERSITY OF SCIENCE & TECHNOLOGY
ISLAMABAD

Expressway, Kahuta Road, Zone-V, Islamabad
Phone:+92-51-111-555-666 Fax: +92-51-4486705
Email: info@cust.edu.pk Website: https://www.cust.edu.pk

CERTIFICATE OF APPROVAL

This is to certify that the research work presented in the dissertation, entitled "**Molecular Epidemiology of Antibiotics Resistance Genes in Smog Particulate Matter and its Health Implications**" was conducted under the supervision of **Dr. Arshia Amin Butt**. No part of this dissertation has been submitted anywhere else for any other degree. This dissertation is submitted to the **Department of Bioinformatics & Biosciences, Capital University of Science and Technology** in partial fulfillment of the requirements for the degree of Doctor of Philosophy in the field of **Biosciences**. The open defence of the dissertation was conducted on **September 19, 2025.**

Student Name :	Muhammad Imran Khan (DBS193002)	

The Examination Committee unanimously agrees to award PhD degree in the mentioned field.

Examination Committee :

(a)	External Examiner 1:	Dr. Muhammad Imran Professor QAU, Islamabad	
(b)	External Examiner 2:	Dr. Waseem Haider Associate Professor COMSATS University, Islamabad	
(c)	Internal Examiner :	Dr. Erum Dilshad Associate Professor CUST, Islamabad	
Supervisor Name :		Dr. Arshia Amin Butt Associate Professor CUST, Islamabad	
Name of HoD :		Dr. Syeda Marriam Bakhtiar Associate Professor CUST, Islamabad	
Name of Dean :		Dr. Sahar Fazal Professor CUST, Islamabad	

Author's Declaration

I, **Muhammad Imran Khan** hereby state that my PhD dissertation titled "**Molecular Epidemiology of Antibiotics Resistance Genes in Smog Particulate Matter and its Health Implications**" is my own work and has not been submitted previously by me for taking any degree from Capital University of Science and Technology, Islamabad or anywhere else in the country/abroad.

At any time if my statement is found to be incorrect even after my graduation, the University has the right to withdraw my PhD Degree.

(Muhammad Imran Khan)

Registration No: DBS193002

Plagiarism Undertaking

I solemnly declare that research work presented in this dissertation titled "**Molecular Epidemiology of Antibiotics Resistance Genes in Smog Particulate Matter and its Health Implications**" is solely my research work with no significant contribution from any other person. Small contribution/help wherever taken has been duly acknowledged and that complete thesis has been written by me.

I understand the zero tolerance policy of the HEC and Capital University of Science and Technology towards plagiarism. Therefore, I as an author of the above titled thesis declare that no portion of my thesis has been plagiarized and any material used as reference is properly referred/cited.

I undertake that if I am found guilty of any formal plagiarism in the above titled thesis even after award of PhD Degree, the University reserves the right to withdraw/revoke my PhD degree and that HEC and the University have the right to publish my name on the HEC/University website on which names of students are placed who submitted plagiarized work.

(Muhammad Imran Khan)

Registration No: DBS193002

List of Publications

It is certified that following publication(s) have been made out of the research work that has been carried out for this dissertation:-

1. **Muhammad Imran Khan**, Arshia Amin, Wasim Sajjad, Yousef Abdullah M Bin Jardin, "Understanding Smog's Impact on Healthy Male Rat Physiology: A Multi-Dimensional Analysis," *Heliyon*, (2025): e42877, ISSN 2405-8440.

2. **Muhammad Imran Khan**, Arshia Amin, Muhammad Tariq Khan, Hafsa Jabeen & Shafqat Rasul Chaudhry "Unveiling the hidden hazards of smog: health implications and antibiotic resistance in perspective," *Aerobiologia*, 40, 353-372 (2024).

(Muhammad Imran Khan)

Registration No: DBS193002

Acknowledgement

In the name of Allah, the Most Gracious and the Most Merciful, I am deeply grateful for His countless blessings, guidance, and strength that have enabled me to complete this PhD journey.

I would like to express my heartfelt gratitude to my supervisor, **Dr. Arshia Amin Butt**, for her exceptional guidance, unwavering support, and invaluable insights throughout my research. Her mentorship has been instrumental in shaping the direction and success of this thesis.

I am profoundly thankful to **Miss Sana** and **Amjad Ali** from Alpha Genomics Islamabad for their technical support and valuable contributions to my research. I am equally grateful to **Muhammad Huzaifa** from Care Laboratories Rawalpindi for his assistance and collaboration.

Special thanks are extended to **Mr. Muhammad Ejaz-ul-Haq Malik**, whose support and encouragement have been a source of great motivation. I also express my sincere appreciation to **Dr. Tariq Khan**, Assistant Professor, Department of Pharmacy, QAU, for his guidance and expertise, and to **Dr. Jabir Hussain Syed**, Associate Professor of Meteorology, CUI Islamabad Campus, for his insightful discussions and valuable input.

I am also deeply indebted to my parents and family for their unconditional love, prayers, and support throughout this journey. To my brothers and my son, Muhammad Umar Khan, your encouragement and patience have been my constant source of strength and inspiration.

Finally, I extend my gratitude to my colleagues, friends, and everyone who has contributed to the successful completion of this work. This accomplishment is a testament to the collective support and efforts of all those mentioned above. Thank you all for your belief in me.

(Muhammad Imran Khan)

Abstract

The degradation of air quality has emerged as a critical socio-environmental challenge with serious health implications. The present study investigated the impact of prolonged smog exposure in different highly populated areas of Pakistan through an integrated animal model and environmental analysis. The research was conducted in two major components. In the first phase, the effects of continuous smog exposure were evaluated in albino rats with a focus on behavioral, immunological, and histopathological profiles. Two groups were established: a control group maintained under clean air conditions and an experimental group exposed to a smog-laden environment for 60 days. Behavioral outcomes were assessed using the Open Field Test and the Y-Maze Test. Immunological responses were quantified through CD4+ and CD8+ lymphocyte profiling, while histopathological examinations of lung tissues were performed post-sacrifice. Findings demonstrated significant behavioral alterations, heightened immune activation (CD4+ from 25.10% to 37.04% and CD8+ from 15.67% to 28.81%), and notable tissue damage, collectively indicating smog-induced oxidative stress and inflammatory responses. In the second phase, metagenomic approaches were employed to examine microbial communities and antibiotic resistance gene (ARG) profiles in both smog-exposed rat lung tissues and environmental smog particulate matter collected from three densely populated Pakistani cities: Islamabad, Lahore, and Okara. Results revealed a diverse microbial composition with a marked enrichment of high-risk ARGs. Dominant resistance determinants included MCR-3.15, CTX-M-214, and vancomycin-associated genes (vanN and vanG), highlighting the emergence of multidrug resistance potential in smog-associated microbiota. This study provides comprehensive evidence that smog exposure not only induces behavioral, immunological, and histopathological alterations in mammals but also harbors a reservoir of clinically significant antibiotic resistance genes. The findings underscore the urgent need for continuous surveillance, effective mitigation strategies, and targeted interventions to address the dual threats of environmental pollution and antimicrobial resistance.

Keywords: Smog, Health hazards, Behavioral studies, PM 2.5, Histopathology, ARGs

Contents

List of Figures

List of Tables

Abbreviations

AMR	Antimicrobial resistance
AQI	Air Quality Index
ARB	Antibiotic resistance bacteria
ARG	Antibiotic resistance gene
CARD	Comprehensive antibiotic resistance database
CF	Cystic Fibrosis
COPD	Chronic obstructive pulmonary disease
CO	Carbon monoxide
CTAB	Cetyltrimethylammonium bromide
eDNA	Extracellular DNA
EDTA	Ethylene diamine tetra acetic acid
EPA	Environmental protection association
ETS	Ambient tobacco smoke
GLO	Ground level ozone
H&E	Hematoxylin and eosin
HGT	Horizontal gene transfer
iDNA	Internal DNA
LRTIs	Lower respiratory tract infections
MRSA	Methicillin-resistant staphylococcus aureus
NO_2	Nitrogen dioxide
NO	Nitrogen oxide
NPs	Nanoscale particles
PAHs	Polycyclic aromatic hydrocarbons
PCR	Polymerase chain reaction

PM_{10}	Particulate matter between 2.5 micrometer to 10 micrometer
$PM_{2.5}$	Particulate matter 2.5 micrometer or less than 2.5
PM	Particulate matter
PPM	Parts per million
RR	Relative risk
SEM	Standard error of the mean
SO_2	Sulphur dioxide
TAE	Tris-acetate EDTA
TB	Tuberculosis
URTIs	Upper respiratory tract infections
VOC,s	Volatile organic compounds
WHO	World Health Association

Chapter 1

Introduction

1.1 Introduction

Air pollution, a significant threat to public health in the world, contributing to numerous illnesses and deaths worldwide. The primary pollutants in the air include solids, gases, and liquids, each with its own harmful effects. Although the industrial revolution was a major technological milestone, it also resulted in the generation of enormous pollutants that are harmful when emitted into the atmosphere. Even at times when air pollution is low, the health of weak and sensitive individuals may be threatened. COPD, breathing problems, coughing, respiratory diseases, and high hospitalization are all connected with particulate matter exposure. Air pollution does indeed have a negative impact on people who reside in cities, where most air pollution is due to vehicular emissions [1–3]. Few studies have offered fresh perspectives on the correlation between elevated levels of air pollutants and increased mortality rates while taking demographic changes and historical context into account. Although household air pollution has declined, the overall impact of air pollution on global mortality rates has worsened due to increases in outdoor pollutants like ozone and particulate matter. Studies have shown that particulate matter pollution can contribute to higher rates of diabetes and increased mortality from conditions such as ischemic heart disease and stroke in many nations as shown in figure 1.1 [4]. In Asian countries, e.g. China, with

foremost air pollution issues, because of increasing industrialization and overpopulation [5]. Elevated levels of fine particulate air pollution in China have been associated with increased mortality rates from lung cancer [6]. Long-term inhalation of polluted air can lead to serious health problems affecting the heart and lungs [7, 8].

Industrialized countries with significant air pollution tend to have higher rates of cardiovascular disease [9]. India's capital, New Delhi, is one of the world's most polluted cities, with air quality frequently deteriorating to hazardous levels. This alarming trend is driven by factors such as increasing industrial activity, rapid urbanization, and a surge in vehicular emissions [10, 11].

Elevated levels of sulfur dioxide and other air pollutants, such as those from smoking, have been linked to increased mortality rates. Mitigating air pollution by reducing or eliminating harmful emissions can significantly improve public health and environmental quality [12]. Governmental and non-governmental groups and authorities take measures to confirm air quality [13].

Airborne particulate matter with a diameter of $\leq$2.5 micrometers ($PM_{2.5}$), a major component of smog, is linked to respiratory and cardiovascular diseases. Meanwhile, antimicrobial resistance genes (ARGs)—genetic elements that enable bacteria to evade antibiotics—are increasingly detected in urban environments.

Recent studies suggest that $PM_{2.5}$ may act as a carrier for ARGs, facilitating their spread through air and water. Understanding this synergy is critical, as it could exacerbate the global antimicrobial resistance (AMR) crisis [14].

Air quality is assessed by measuring levels of pollutants and comparing them to standards set by the WHO and EPA. The evolution of environmental control, combined with technological innovations triggered the establishment of a debate [13, 15].

The operation of large-scale industrial power plants and combustion engines, particularly in vehicles, is a primary cause of environmental pollution. Because these activities are so widespread, and these are major sources of air pollution, the

automobile sector is responsible for >80% of pollution, they are a significant environmental concern [16].

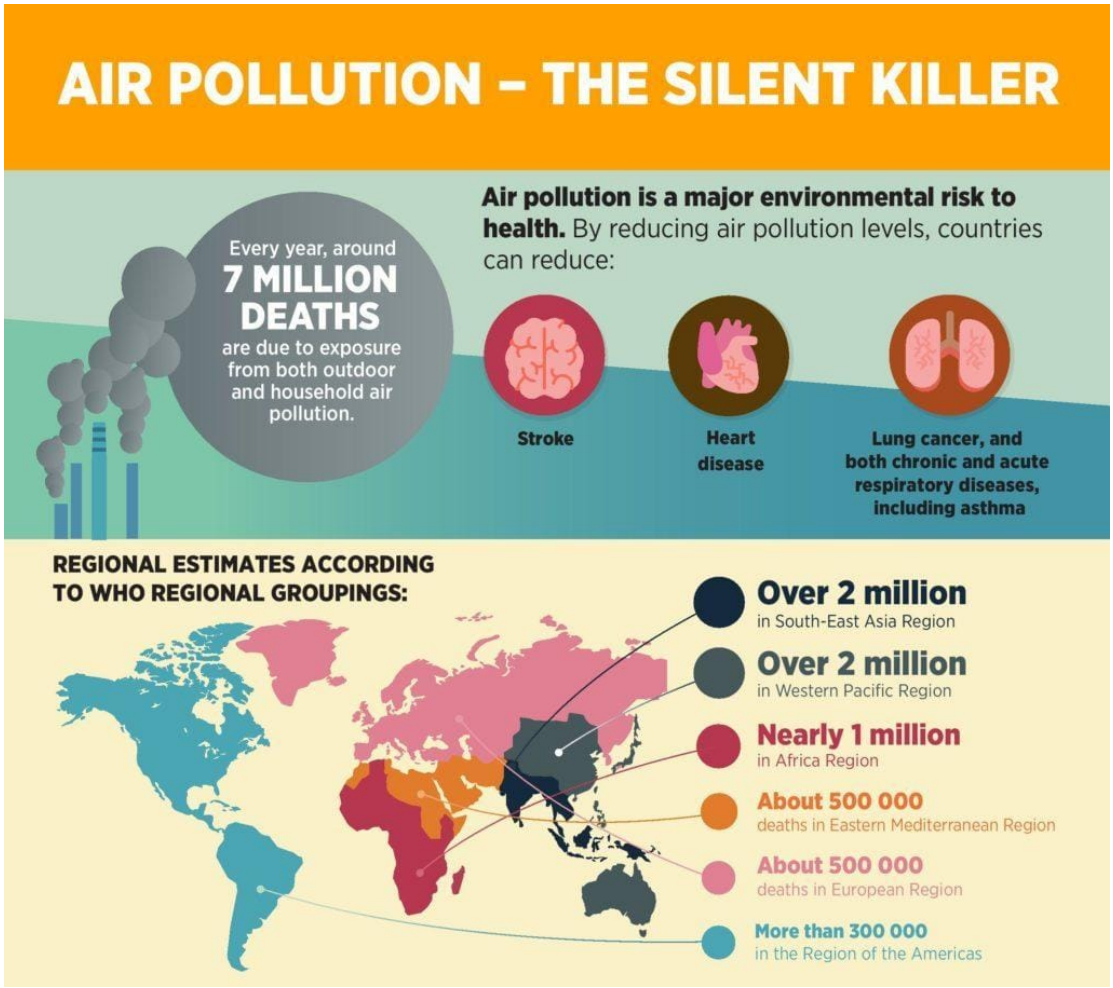

FIGURE 1.1: Global burden of mortality due to pollution as per WHO, 2016 [4]

Air pollution, particularly smog, poses a well-documented threat to public health, exacerbating respiratory and cardiovascular diseases. However, emerging evidence suggests that smog may also play a critical role in the dissemination of antimicrobial resistance genes (ARGs), further complicating global health challenges. Smog components, such as particulate matter and heavy metals, can act as vectors for ARGs, facilitating their spread through environmental and biological pathways.

This interaction may accelerate the evolution of resistant bacterial strains, undermining efforts to combat antimicrobial resistance. While the broader impacts of

air pollution are widely recognized, the specific mechanisms linking smog to ARG proliferation remain underexplored [17].

Furthermore, human activities, including those of petrochemical plants, fertilizer industries, and other industrial facilities, can harm the environment and endanger human health [18].

Many classification approaches are presented, one of which is supported on the addressee of the pollution, for instance the air pollution is defined as the manifestation of toxins at high concentrations in air over extended periods [19]. Aerosol chemicals, due to their microscopic size, can penetrate deeper into the respiratory system compared to gaseous compounds. This increased penetration allows them to cause more significant damage to the lungs, contributing to millions of premature deaths annually. Additionally, it looks as if aerosol acidity encourages further synthesis of secondary organic aerosols [20]. Change of climate is the other side of the issue that is damaging our globe's condition [21].

Particulate matter (PM) pollution in the form of nanoscale particles (NPs) poses serious threats to public health, particularly to brain function. Because of toxicants such organics and metals, both nano-PM(nPM) & sub-PM(sPM) may elicit the neurotoxic consequences in cerebral cortex. During pregnancy, glutamatergic gene expression is specifically impacted by sPM due to its high concentration of water-insoluble PAHs. Because PM, especially PM0.2 ultrafine particles can enter the brain cells through our olfactive system. Many of the recent studies have shown a strong relationship between exposure to these particles and probability of neurodegenerative diseases like dementia, as well as DNA damage, and cognitive deficits [22, 23]. The increasing frequency of natural climate disasters, such as storms, has been linked to outbreaks of disease [24]. These occurrences may influence healthcare and sanitation mechanisms, increasing the possibility of disease transmission through polluted water. This emphasizes how intricately environmental changes and pandemic susceptibility are related [25].

Microscopic airborne chemicals, known as aerosols, have a substantial influence on the environment. Deteriorating air quality is a major societal concern. Industrial

production is frequently associated with elevated levels of pollutants [8]. This means that any increase in output will certainly lead to an increase in emissions, whereas any decline in output, such as during an economic crisis, will result in a decrease in emissions. This is true, but emissions are also lowered as a result of improved production processes, the deployment of new technologies, the outfitting of facilities with more effective emission-reduction systems, and the diversification of legal regulations. Furthermore, higher pollutant emissions do not always equate to greater environmental harm.

Although there is a link, this pollution is influenced by a far broader sum of reasons than just the number of emissions. Environmental pollution arises from alterations in the factors like physical/chemical, & biological properties of the environment. Pollutants can degrade air-quality by increasing the concentration of existing substances or compounds that pose risks to health of human population. The type of primary pollutants emitted directly from the sources, while secondary pollutants come from the reactions involving these primary pollutants.

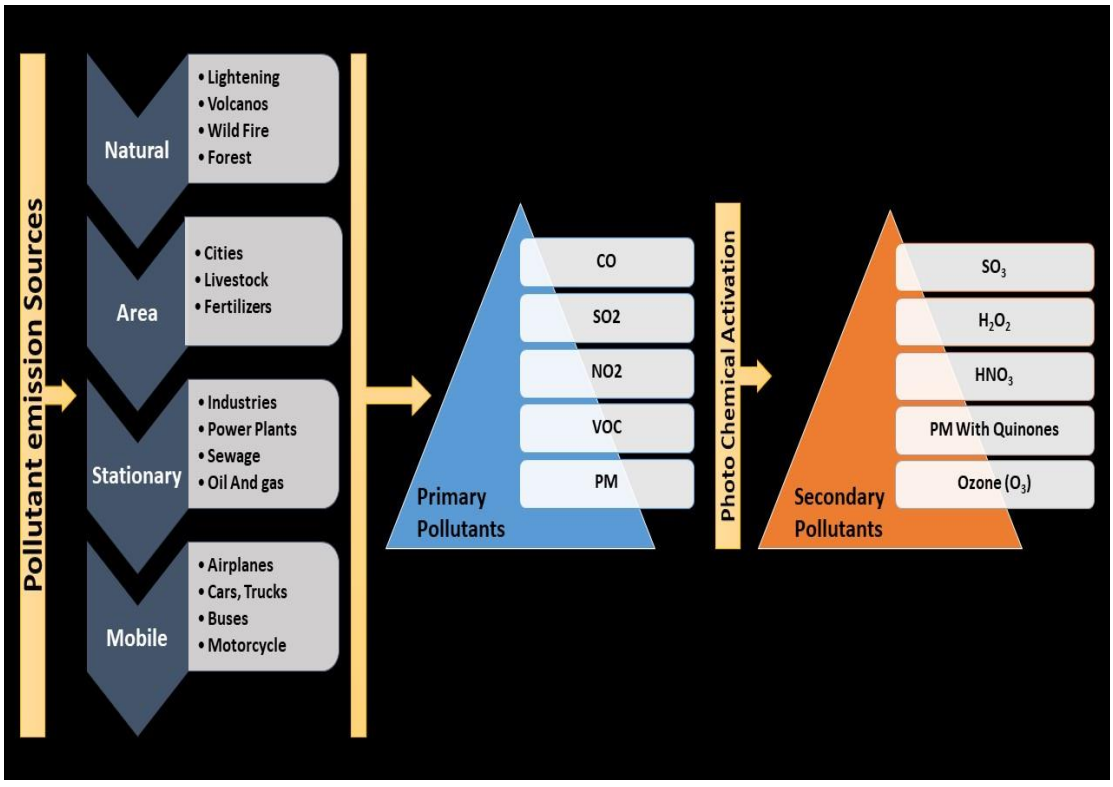

FIGURE 1.2: Basic classification of common air pollutants: Natural, local(Area), capital(stationary), kinetic(mobile), primary and secondary pollutants [26]

Air pollution stems from a variety of sources, including natural, localized, stationary, and mobile origin as shown in figure 1.2 [27, 28]. Primary sources for sulfur dioxide emissions are large-scale combustion industries, including power plants and heat and big power plants. Residential heating (Home boilers) and industrial combustion processes are the second and third largest contributors, respectively. Road transportation, metallurgical industries, and cement production are the key sources of nitrogen oxide productions.

1.2 Problem Statement

Temperature inversions and fog are two effects of smog, an atmospheric phenomenon that results from the simultaneous presence of air pollution generated by humans. One of the main pollutants of smog is PMs. Antibiotic-resistant genes are transcribed on airborne particulate matter, which also acts as a solid surface for a variety of airborne bacteria. The strength of airborne microorganisms may have changed significantly depending on the relative concentration of air particulate matter in smog and non-smog seasons. The spread of antibiotic resistance is facilitated by genes for antibiotic resistance found on particulate matter. Long term exposure to PM is linked to both newborn mortality and cardiovascular illness. Moreover, long-term chronic consequences have been noted, including immune system issues and respiratory illnesses. Pneumonitis, hyperglycemia, and issues with the heart and lungs are among the negative consequences of PM. Because $PM_{2.5}$ and PM_{10} can penetrate indoor areas, they have been linked to several respiratory system ailments. Chronic consequences also include established lung issues. Due to their ability to penetrate, respiratory illnesses are closely linked to $PM_{2.5}$ and PM_{10} levels. Short-term side effects can include neurological issues, asthma, pneumonia, bronchitis, and optical irritation, skin, and throat in addition to coughing and breathing difficulties. Headaches and dizziness are potential side effects for individuals who are momentarily exposed to air pollution. Examining the epidemiology of exogenous ARGs and resistant bacteria on PM during smog is crucial.

1.3 Research Questions

1. What are the hot spot areas for smog with high AQI indexes in Punjab, Pakistan?

2. What is the total bacterial load against the external load of ARGs?

3. What is the impact of smog pollutant on neurological factors, and behavior of animals?

4. How does smog affect the histology of animal organs?

5. How smog effects the levels of pro-inflammatory cytokines and antioxidants?

6. How many amount of ARGs are inhaled by exposed animal group?

7. What are the effects of smog PM with increased ARGs?

1.4 Objectives and Significance

This research is aimed to find out the epidemiology of microbial communities and ARGs concerning the particulate matter in smog and non-smog air. Its health implications will also be explored. Objectives of the study are:

1. To screen the hotspots, based on high AQI indexes across the agricultural and industrial belts in Pakistan.

2. To analyze the effects of smog pollutants on neurological factors and immune response in rat model & to find out the effect of smog pollutants on the histology of lungs in rat model.

3. To estimate inhaled ARGs in exposed animal group & to correlate the effects of smog PM with increased ingraining of ARGs.

4. To estimate resistome in airborne internal and external DNA.

It is necessary to do a thorough investigation into the occupancy of ARGs on particles under an unembellished smog scenario. Smog air is comparable to adjacent air in terms of ARG profiles, but it is different from further environmental channels and more closely associated with soils. The profiles of airborne ARGs can be influenced by physico-chemical factors, the climate parameters, and bacterial ecology. Smog may increase the amount and variety of ARGs, which may be harmful to the health of nearby residents because opportunistic illnesses and some ARGs occur in PM particularly fine PM. The purpose of the current study is to deeply expose the molecular epidemiology of both internal and external ARG,s embedded in smog Particulate matters.

Chapter 2

Literature Review

2.1 The Origins and Modern Impact of Smog

Smog is one of the main classes of air pollution that is formed when the sunlight make contact with air pollutants like nitrogen oxides(NOs) and volatile organic compounds (VOCs) in atmosphere. In this the Photochemical smog is the most common and is a major contributor to urban air pollution. Smog primarily affects the Earth's surface layer, harming both the environment and health of humans. As seen in Table 2.1, it is an atmospheric phenomenon that results in temperature inversion and, occasionally, fog [29, 30]. It is caused by the coexistence of air pollution created by humans.

'Smog' term was first used in 1950s to describe a specific type of air pollution that plagued London. It was derived from the words 'smoke' and 'fog.' Today, we commonly use the term to refer to a broader range of air-pollution caused by activities of humans, markedly in city populations. This pollution often arises from emissions produced by vehicles and residential burning. Under certain atmospheric conditions, such as calm or light winds, these pollutants can become trapped near the surface of earth, making a buildup of harmful substances [31, 32]. A layer of acidic aerosol forms close to the ground, which can be detrimental to human health, the environment, and can cause allergic reactions in certain people [33, 34]. Photochemical smog, primarily composed of nitrogen oxides, carbon

monoxide, and hydrocarbons, is exacerbated by ozone formation through photochemical processes. This environmental issue is widespread, affecting numerous countries and cities, including Poland [35, 36]. In Poland, household boilers are a major contributor to smog, releasing substantial amounts of PM_{10}, $PM_{2.5}$, and other carcinogenic substances. This issue isn't unique to Poland, as similar meteorological conditions and pollution emission patterns are observed in other European nations [37].

TABLE 2.1: Contrast between Smog types: Industrialized and photochemical

Industrial Smog	**Photochemical Smog**
London Smog	Los Angeles Smog
Gray in color	Brown in Color
Produced by burning coal & oil in power industries	Produced from the automobiles & solar radiations
Sulphur oxide mixed with particulate matter	Nitrogen oxide makes reactions with different organic moieties

2.2 Health and Microbial Impact

Chronic exposure to PM is mainly associated with an elevated risk of cardiovascular disease and neonatal death [38]. Due to limited data availability, studies are often confined to specific regions or urban areas, and may not accurately reflect the experiences of the entire population [39]. Recent research has utilized remote sensing to develop a $PM_{2.5}$ model capable of assessing both short-term regional effects and long-term population health effects. These long-term effects can include chronic respiratory and immune system disorders [39].

PM exposure, particularly the $PM_{2.5}$& PM_{10}, can significantly worsen respiratory and cardiovascular health conditions because these $PM_{2.5}$& PM_{10} fine particles can easily penetrate deep tissues like alveoli of lungs, causing chronic inflammation and severe respiratory ailments. [40] [38, 41]. Chronic lung diseases can arise due to Long-term exposure to air pollution. Due to their small size, $PM_{2.5}$ and PM_{10} particles can easily penetrate deep into the lungs, increasing the risk of

respiratory illnesses. [42–44]. Furthermore, these hazardous molecules can be organic or inorganic in nature [45].

TABLE 2.2: The degree of penetration and size of different Particulate matters in human airway system

Degree of Penetration	**Size of PMs**
Alveolar	0.43-0.65 um
Bronchioles	0.65-1.1 um
Terminal Bronchial	1.1-2.1 um
Bronchial area	2.1-3.3 um
Trachea	3.3-4.7 um
Larynx	4.7-7 um
Nasal Cavity	7-11 um
Upper respiratory tract	>=11um

GLOs form when NOs and volatile VOCs, primarily from human activities, react in the atmosphere. Despite increasing urban pollution, levels of ozone in these cities remain relatively low. This potentially harm ecosystems by limiting carbon absorption in forests and vegetation [46, 47]. Ozone primarily enters the human body through inhalation. Once inhaled, it can easily penetrate deep into lung tissues and cells. Additionally, exposure to ozone can damage the skin's outer layers. In urban environments, ozone pollution can result in health issues, including biochemical, morphological, functional, and immunological issues [47].

Carbon monoxide (CO) enters the atmosphere due to incomplete combustion of fossil fuels. Exposure to >CO leads to multiple health complications like headache, weakness, nausea, and vomiting, while at extreme cases even to death. CO is especially deadly because it binds to hemoglobin in the blood more readily than oxygen does, decreasing the amount of oxygen-carrying capacity in the blood. Long-term exposure to high CO levels leads to diseases like hypoxia, ischemic heart disease, and cardiovascular disease.

NO (nitrogen oxide), a pollutant amounting to 65% of the air pollution emitted by automobiles, is highly relevant to health planning. When NO concentration is more than 0.2 parts per million (ppm), the function of T-lymphocytes (especially

natural killer cells) is inhibited and the immune response suppressed. And this is going to cause health problems and health issues.

Higher concentrations, above 2.0 ppm, can further disrupt T-lymphocyte function, specifically affecting CD8+ cells and natural killer cells . Prolonged exposure to NO_2 is connected to chronic lung ailments and can also impair one's sense of smell [44].

In Aotearoa New Zealand in 2016, hospitalizations and premature deaths were projected to have totaled 13,155 and 3,317, respectively, and were linked to the two man-made air pollutants of greatest concern, NO_2 (primarily from vehicle emissions) and $PM_{2.5}$ (primarily from combustion) as demonstrated in figure 2.1 [48].

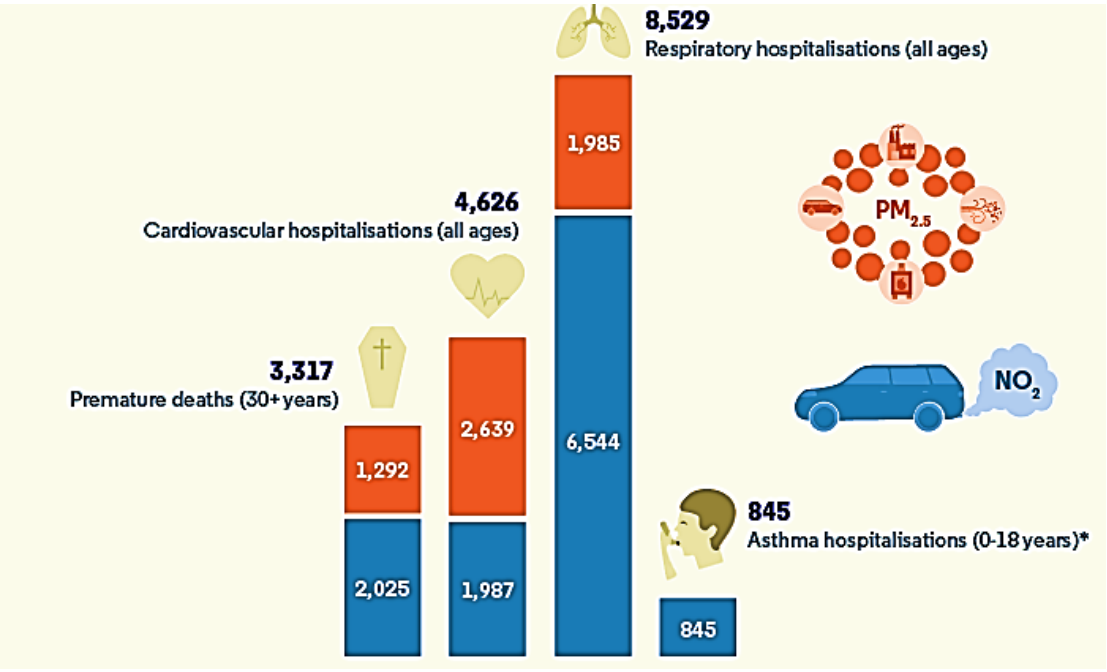

FIGURE 2.1: Estimated annual asthma cases in children attributed to anthropogenic NO_2 and $PM_{2.5}$ in Europe (2015–2020). [48]

A very harmful gas, Sulfur dioxide (SO_2) released primarily from the burning in industrial processes and fossil fuels, poses significant risks to human, animal, and plant life. When inhaled, SO_2 irritates the lungs, transforming into bisulfite and triggering sensory receptors. This reaction can lead to bronchoconstriction, respiratory irritation, and bronchitis [44].

2.3 Air Quality Index

Overall, AQI indicates air quality and purity in the given area. It is however computed by U.S.-Environmental-Protection-Agency (EPA) based on the 5 foremost air pollutants, GLO, PM, CO, SO_2 and NO_2. AQI monitoring systems (which may use sensors to detect particulate matter) can measure current or past air quality. These systems can be used across spaces such as homes, offices, and industrial facilities.

A Higher> AQI value indicates worst air quality and greater> potential health issues and concerns. The Air Quality Index (AQI) ranges from 0 to 500 as shown in table 2.3. An AQI between 0 and 50 indicates good (green) air quality, posing minimal health risks. An AQI between 51-100 signifies moderate (yellow) air quality, which is generally acceptable. However, certain pollutants may affect sensitive individuals, such as people with asthma, who might experience breathing difficulties. Everyone should limit prolonged outdoor activities during these periods. An AQI between 101 - 150 is considered unhealthy for sensitive groups (orange), meaning that certain individuals may experience health effects. Certain individuals, particularly those in sensitive groups, may experience health issues. The general public is unlikely to be affected by air quality within this range. Sensitive groups include the elderly, children, and people with pre-existing conditions like lung disease, heart disease, or chronic respiratory illnesses. Individuals with asthma should adhere to their prescribed action plans and consult with a healthcare provider if they experience worsening symptoms or difficulty breathing. Those with heart or circulatory conditions should monitor for signs such as rapid heart rate, shortness of breath, or unusual tiredness and seek medical advice if necessary [49].

Different anthropogenic and natural sources produce complex matter pollution, which varies in size distribution, chemical composition, and other properties as can be seen in figure 2.2. Depending on which individual's particular afflicted physiological system or organ, the ensuing health implications vary greatly. Furthermore, assessing the correlations between PM pollution and health outcomes is

challenging due to a variety of mixed and, occasionally, synergistic impacts that can be impacted by airborne microbes, heat waves, cold spells, and allergic pollen.

TABLE 2.3: The table below shows the Air Quality Index Chart[50]

AQI Color	**Index Value**	**Concern level**
Maroon	301 & higher	Hazardous
Purple	201-300	Very Unhealthy
Red	151-200	Unhealthy
Orange	101-150	Unhealthy for sensitive group
Yellow	51-100	Moderate
Green	0-50	Good

2.4 Characteristics and Variety of the Airborne Microbiome

The atmosphere contains a significant portion of microbiological bioaerosols, comprising 30-80% of particulate matter (PM). These bioaerosols primarily consist of bacteria, fungi, viruses, cellular debris, and pollen.

While Louis Pasteur first identified airborne bacteria in 1860, recent advancements in DNA-based molecular technologies have reignited scientific interest in these microorganisms [51]. Bacteria are introduced into the troposphere through the aerosolization of various surfaces, including soil and plant matter [52].

Bioaerosol emissions are substantial in both agricultural and wastewater treatment sectors [53]. Bacteria can survive in harsh conditions by attaching to particles or forming clusters, extending their lifespan compared to free-living microorganisms. This ability, combined with their diverse size range (0.0001-100 mm), influences their potential for both short and long-distance dispersal.

While some bacteria may travel short distances, others can be transported over significant distances, especially when associated with particles from desert dust or hurricanes.

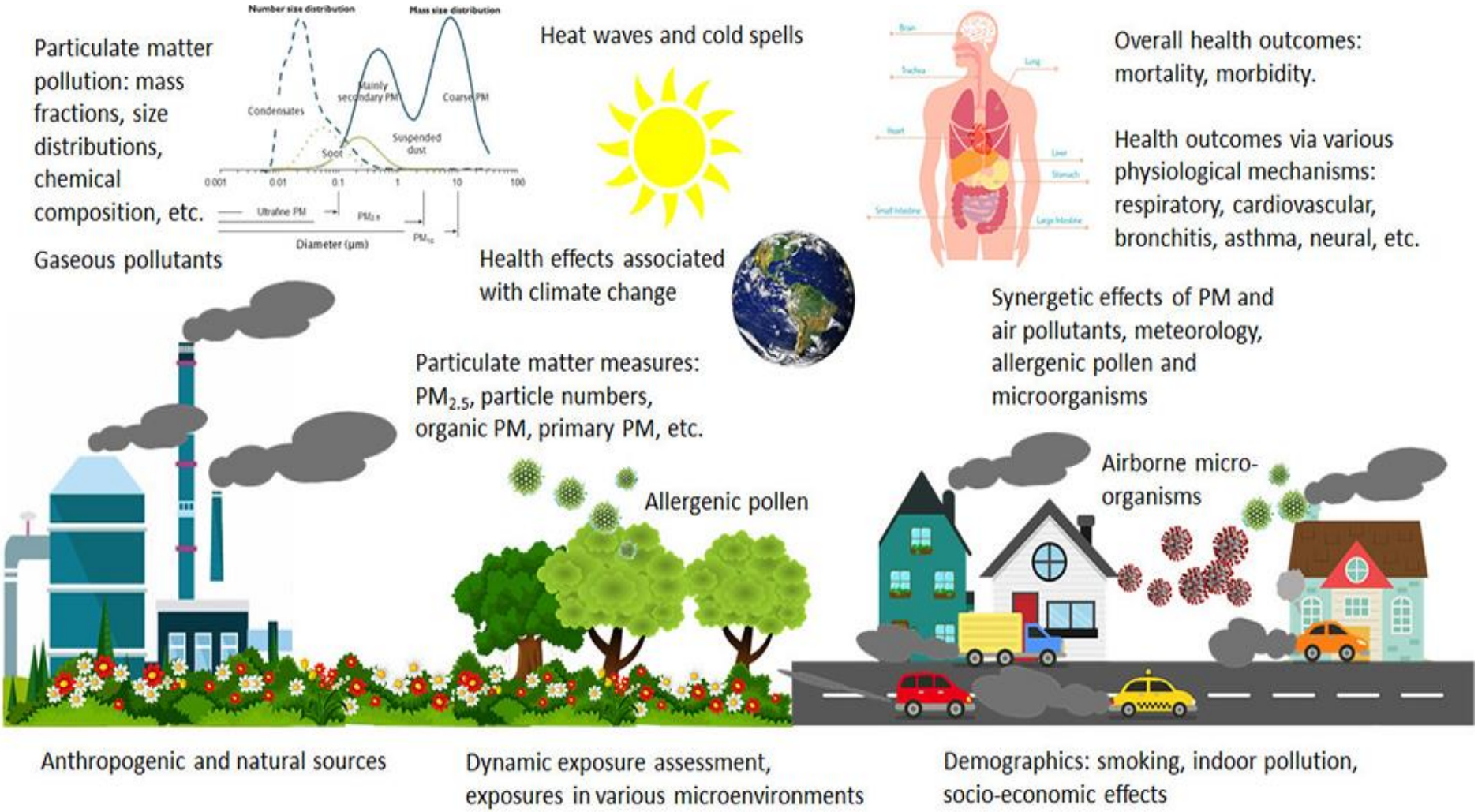

FIGURE 2.2: Key factors in PM exposure and health impacts: sources, pathways, and effects [4][5]

A study found that terrestrial microbes can persist in the air for up to 17 days, with concentrations ranging from 5102 to 8104 cells per cubic meter. The researchers concluded that islands can act as steppingstones, allowing 50% of prokaryotes to survive long-distance transport over 22,000 kilometers [54].

The pulmonary-microbiota contains different microorganisms as well as their genetic material and metabolic by-products. In both the upper & lower respiratory tracts, these bacteria vary in diversity and quantity. Microbial colonization of the human body begins at birth and continues to evolve throughout life.

This dynamic process is influenced by both genetic factors and environmental exposures. Air pollution, both indoors and outdoors, can negatively impact the airway tract microbiota, potentially increasing the risk of airway infections, i.e. pneumonia. Air pollution can present microorganisms, such as pathogens, into the human body through aerial spread. Inhalable PM is one mechanism by which the composition of the human microbiome, especially in the gastrointestinal and respiratory tracts, can be altered [51].

The metagenomic analysis of PM pollutants in Beijing has shown that bacteria are the dominant microbial component during severe smog events. Some of these bacteria are known to cause or contribute to respiratory infections. Qin and co-workers identified 142 novel taxa in the pharyngeal microbiota after smog exposure, originating from diverse sources [55].

These significant shifts in microbial composition suggest that PM particles may act as vectors, transporting microorganisms from various environments to the human respiratory tract. Bacteria are the most prevalent prokaryotic organisms found in $PM_{2.5}$ and PM_{10} pollution.

The abundant phylum on PM, are *Chloroflexi; Firmicutes*, *Actinobacteria; Proteobacteria, Bacteroidetes;* and *Euryarchaeota.* Microorganisms in $PM_{2.5}$ and PM_{10} samples are associated with fecal and terrestrial sources, microorganisms that are found in soil [55]. Given the diverse origins of airborne microbes, their phylogenetic and practical diversity can be analogous to that of soil and water environments [56].

2.5 Health Risks of Air Pollutants from Global and Regional Perspectives

As per the World Health Organization, there are significant health concerns associated with ambient air pollutants such as PM_{10}, $PM_{2.5}$, CO, NO, SO_2, and ozone layer. The main sources of these pollutants are human activities, such as heating operations and car emissions [54]. High pollution exposure increases the risk of developing a number of ailments, especially in the elderly, young children, and people with pre-existing lung or cardiovascular disorders like asthma. The short term exposure to smog laden environment can result in respiratory/airway difficulties and issues such coughing, asthma, pneumonia, bronchitis, and various cardiac issues. Headaches and lightheadedness can occur after a brief exposure to contaminated air [57].

Improvement in air quality is key and essential for safeguarding the human health, as pollutants are linked to a range of different health issues and ailments, including heart disease, skin conditions, and eye disorders. Smog exposure, for instance, triggers inflammatory responses and can lead to ear, nose, and throat (ENT) conditions [58]. Pollutants interact with the tear film, altering its composition, making individuals more susceptible to eye problems like dry eye and infections. Historical examples, such as the 1952 London smog, which caused thousands of deaths due to coal combustion, and photochemical haze in Los Angeles during the 1940s and 1950s, demonstrate the deadly effects of air pollution. Similarly, smog has caused nearly 2 million deaths in China and India [59].

While a strong haze enveloped Lahore, obstructing sunlight, in November 2016, PM_{10} and $PM_{2.5}$ levels in New Delhi were noted as haze, functioning as an indicator of air quality [54, 60, 61]. During this pollution episode, there were reported accidents and health hazards. Deeply ingrained in the respiratory system, $PM_{2.5}$ has been connected to a number of health issues [62]. A decrease in $PM_{2.5}$ levels has been observed in China in recent years as a result of improved knowledge of its physicochemical characteristics. Five to ten percent of airborne particulate matter is made up of bioaerosols, which can be harmful to health, especially if they are

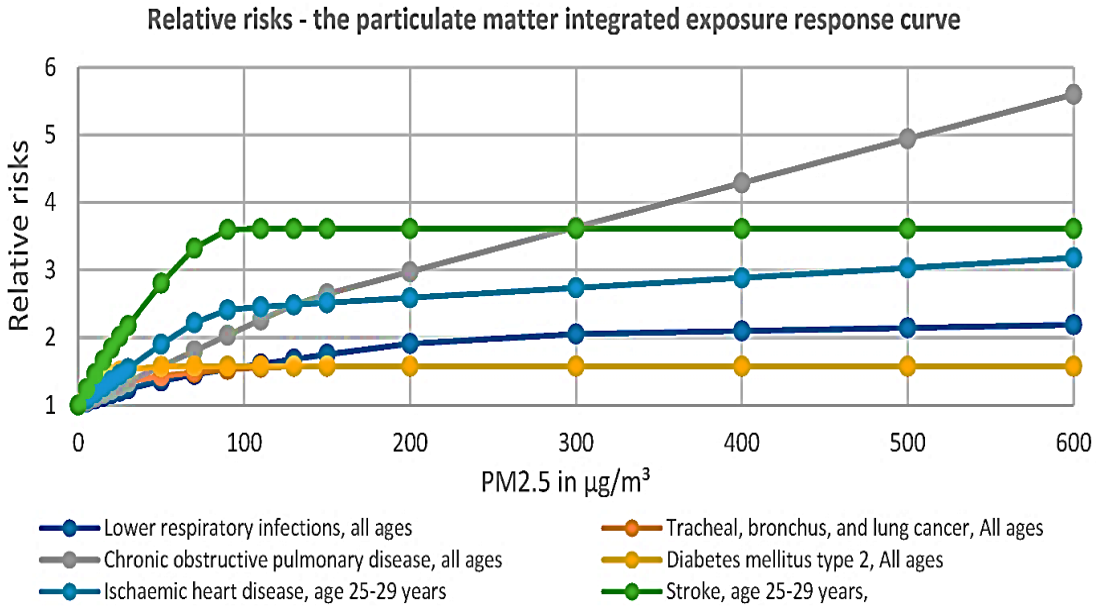

FIGURE 2.3: Integrated exposure–response curve: Relative risk values for long-term $PM_{2.5}$ exposure [64]

smaller than $PM_{2.5}$. Research has demonstrated that respiratory illnesses can be caused by opportunistic bacterial pathogens found in bioaerosols [63].

Pollution exposure during pregnancy and the early years of life has been linked to childhood LRIs. According to one study, there is a correlation between the usage of antibiotics and $PM_{2.5}$ exposure from coal mine fires, which suggests that young children are more likely to get bacterial infections. According to a different study, children who are exposed to pollution during pregnancy are more likely to have lung illnesses from opportunistic microorganisms. Studies conducted on BALB/c mice that were exposed to ambient tobacco smoke (ETS) prior to birth validated that this type of exposure intensifies lung infections caused by *Staphylococcus aureus*, leading to increased inflammation in the lungs [65]. Chronic air pollution exposure has also been linked to cardiovascular complications include myocardial ischemia, heart failure, coronary arteriosclerosis, and stroke [66–69].

Ventricular hypertrophy can result from prolonged exposure to NO_2, and oxidative stress, protein aggregation, inflammation, and dysfunctional mitochondria in neurons have all been connected to neurodegenerative disorders. By causing neuroinflammation and raising immunoglobulin levels, air pollution can compromise immune function [66, 70, 71]. Figure 2.4 shows the effect of air pollutants on

the immune system [8]. Strong evidence that prenatal exposure to air pollution increases children's vulnerability to opportunistic bacterial infection-related lung illnesses was found in a different investigation [71]. A week before to giving birth, the pregnant BALB/c mice in this study were exposed to ambient tobacco smoke [69]. At seven weeks of age, their progeny received an influenza A vaccination and then faced a *Staphylococcus aureus* challenge. Exposure to tobacco smoke in the environment during the perinatal period resulted in heightened susceptibility to *S. aureus* lung infections and consequent pulmonary inflammation [65]. Furthermore, a wide spectrum of cardiovascular effects has been connected to ambient air pollution exposure. Prolonged contact can change red blood cells and impair heart health. Air pollution from traffic has been linked to coronary arteriosclerosis [72], and short-term exposure to it has been linked to myocardial ischaemia, heart failure, and stroke. Ventricular hypertrophy has specifically been linked to extended exposure to NO_2 [73].

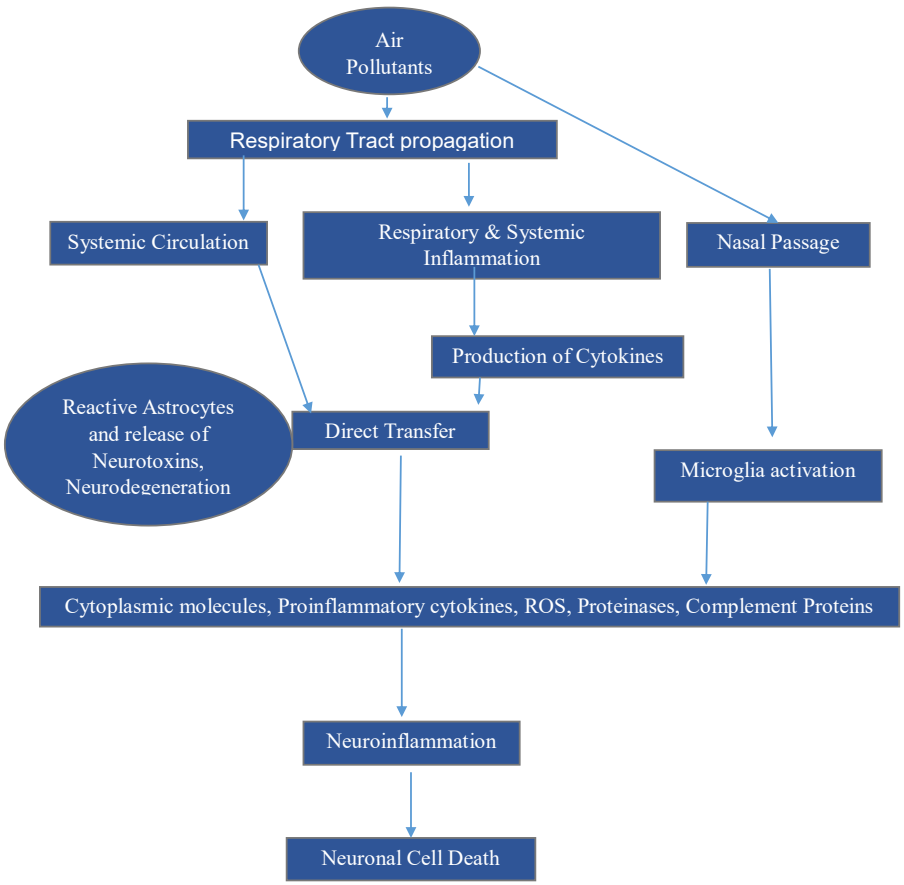

FIGURE 2.4: Key pathways linking air pollution to immune dysfunction [8]

Air pollution affects neurodegenerative disorders as well. These diseases are typified by oxidative stress, protein aggregation, inflammation, and dysfunctional mitochondria in neurons [74]. These toxins set up immunological reactions, which result in inflammation of the nerves [47]. Air pollution has been shown to raise immunoglobulin levels, which can impact antigen presentation by causing macrophages to express co-stimulatory molecules like CD-80 and CD-86 more frequently [75].

2.6 Extracellular DNA

Extracellular DNA (eDNA) refers to genetic material found outside of cells, distinct from intracellular DNA (iDNA) which resides within cells. EDNA can be detected in various environmental samples. It originates from intracellular DNA through mechanisms such as active or passive release or cell lysis [76].

In 1950s, the presence of the extracellular DNA also called as eDNA in the air environment made an interest in its potential role in horizontal gene transfer or (HGT) and the acquisition of antibiotic resistance by bacteria through ARG-genetic modification with foreign DNA, such as plasmids. Subsequent research in the 1980s and 1990s focused on eDNA's ability to persist in soil environments, where it can bind to various soil components and evade degradation by nucleases [77].

Various studies have demonstrated the significance of eDNA in relation to PM and air pollution. For example, it has been shown that eDNA influences the variety and make-up of microbiota—bacteria, fungi, and viruses—that are linked to PM. It has been demonstrated that PM-associated DNA affects the ability of microorganisms to survive, colonies new areas, and spread. Additionally, other creatures can receive genetic information from PM via eDNA.

One worry about antimicrobial resistance (AMR) is the presence of antibiotic resistance genes (ARGs) [78]. Antimicrobial resistance (AMR) ranks among the top ten risks to the health of the world. Global antibiotic abuse and misuse are recognized as important etiologic factors contributing to the emergence of

antimicrobial resistance (AMR). According to statistics, countries with low or middle incomes are driving up AMR rates relative to high-income nations [79].

Concerns are there regarding the potential for horizontal gene transfer and the spread of antibiotic resistance are increased by the discovery of ARGs within PM-associated eDNA. The risk of ARG exposure increases when people and pets inhale the airborne PM, which can travel great distances. This has significant ramifications for public safety and emphasises the need for a deeper understanding of how eDNA functions in PM in ARGs and the transmission of AMR.

Recent studies have examined eDNA in the air using sophisticated molecular techniques like metagenomics. These methods have provided valuable information about the types and quantities of environmental DNA (eDNA) present in particulate matter (PM), as well as how these levels fluctuate over time. Additionally, they have shed light on the sources, transport mechanisms, and potential impacts of eDNA in PM. However, challenges remain in accurately measuring eDNA concentrations, understanding its biological role, and assessing the risks associated with PM-borne eDNA [78, 80].

2.7 Antibiotic Resistance in the Environment

Fine particulate matter (PM), known as $PM_{2.5}$, can have significant contribution to the spread of various microorganisms, like antibiotic resistant bacteria (ARB). The over-use and misuse of various antibiotics may have led to the emergence of drug-resistant "super-bugs," posing a serious public health concern in the 21^{st} century. These super-bugs can render traditional treatments to be ineffective, and making the serious infections more difficult for treatment. [81].

According to research by Algammal and co-workers, *Pseudomonas aeruginosa* is emerged as extremely drug-resistant in grilled chickens, have a very serious concern to public health. It has been highlighted that how virulence, quorum sensing, and resistance genes may co-exist, underscoring the relationship between pathogenicity and antibiotic resistance in chickens [80]. According to another study done by

Lin and coworkers [82], multiple colistin resistance genes were found in multidrug-resistant A study conducted in a Shanghai veterinary clinic found *Escherichia coli* bacteria in companion animals, highlighting a potential risk of zoonotic transmission [79]. The increasing awareness of antibiotic resistance as a major public health threat is driven by concerns about its potential to spread to humans and undermine the effectiveness of existing antibiotic treatments. In several bacterially-caused infectious illnesses, the incidence of antibiotic resistance has increased [82]. Methicillin-resistant *Staphylococcus aureus* (MRSA), first identified in 1962, is a major cause of large-scale healthcare-associated infections. Along with certain Enterococcus species, MRSA is a primary driver of the global antibiotic resistance crisis [83].

Antibiotic environmental factors promote the dispersion of antibiotic-resistance genes [84]. Additionally, ARGs can be airborne and inhaled by humans. Bacteria, originating from soil, are lifted into the atmosphere through wind-driven processes like soil resuspension. These bacteria can attach to particulate matter, often exceeding the typical size of bacteria 1 μm and reaching diameters of approximately 4μm [81]. Airborne bacteria, due to their widespread dispersal, can be exposed to unique physicochemical stressors compared to terrestrial bacteria. $PM_{2.5}$ can contribute to the dissemination of antibiotic resistance genes (ARGs) in the environment. Human exposure to ARGs, inhalation must be considered as a significant route for accurate assessments. A greater understanding of these factors is very crucial for developing effective mitigation strategies to reduce ARG sources and human exposure, as well as addressing public health concerns related to antibiotic resistance and bioaerosols. Research has shown that host bacterial communities, environmental conditions, and human activities can all influence the environmental resistome, shaping the redistribution of different ARGs [85].

These bacteria produce catalase and oxidase enzymes. They are capable of fermenting glucose and liquid gelatin but not inositol. Classified as facultative anaerobes, they can tolerate high salt concentrations ranging from 0.3% to 5% [86]. Among other extracellular hydrolytic enzymes, they can produce amylases, deoxyribonucleases, peptidases, and lipase enzymes [87]. Antibiotic concentrations

in the environment are rising, especially in human waste materials, where these genes are created and coupled with antibiotics and other materials [88]. Horizontal gene transfer (HGT) can occur when bacteria in the environment are exposed to this mixture, enabling them to acquire new genetic material and potentially colonize new environments or hosts [89]. Considering the intrinsic resistance of *Aeromonas* bacteria to beta-lactam antibiotics, treating infections caused by these bacteria is notoriously difficult [90, 91].

Soil environments harbor a significant portion of the resistome, a collective term for environmental bacterial resistance genes [92]. This genetic reservoir, coupled with the potential for horizontal gene transfer, poses a significant threat to global health by facilitating the rapid evolution of antibiotic-resistant bacteria [93]. There are two types of resistome: 1. intrinsic (innate) and 2. extrinsic (acquired). The intrinsic resistome is defined as a set of chromosomic genes that engage in innate resistance, and their presence in strains of a bacterial species is unconnected to HGT and independent of previous antibiotic exposure[94, 95]. Furthermore, the extrinsic is a set of genes acquired through numerous alterations in the genome that can be passed down from generation to generation in a stable manner. Antibiotic resistance genes can be transferred between various bacteria, including both harmful and harmless strains, across diverse environments like humans, animals, and the natural world. The resistome encompasses the entire collection of these naturally occurring genes [92].

The mobilome refers to the collection of mobile genetic elements capable of mobilizing resistance genes in a variety of genetic settings [96]. Key enzymes driving these processes include recombinases, which facilitate homologous recombination, a host-encoded mechanism safeguarding genome integrity. Additionally, transposases catalyze the movement and integration of transposons, enabling the insertion of genetic elements like resistance cassettes into integrons through site-specific recombination [40]. Many enzymes are expressed by mobile elements which can promote gene excision. Knowledge of these genetic material transmission mechanisms in natural settings is becoming increasingly essential due to the implications for a range of businesses, including the food industry, clinic and hospital settings,

and aquaculture, among others. Horizontal gene transfer (HGT) significantly impacts bacterial evolution by facilitating the spread of genes conferring antibiotic and metal resistance. These traits can enhance bacterial fitness by enabling them to utilize novel resources or survive in toxic environments [97]. Prokaryotes primarily exchange genetic material through three primary mechanisms: transformation, transduction, and conjugation. Some of the other methods, such as the transfer of DNA through outer membrane vesicles and nanotubes, also have contribution to horizontal gene transfer in these organisms [98]. Furthermore, Virus like gene transfer agents [99], have recently been discovered but are less well studied and investigated. Several mechanisms may hinder horizontal gene transfer in prokaryotes. One of these mechanisms is the restriction modification system. This system identifies and degrades foreign DNA through the action of restriction of endonucleases, which cleaves double-stranded DNA into smaller fragments. These fragments are subsequently eliminated by other cellular enzymes. Another defense system is CRISPR-Cas, a prokaryotic immune system that targets and destroys invading genetic elements, such as plasmids and phages. CRISPR-Cas systems utilizes the Cas-proteins to cleave and disable foreign DNA [100, 101].

2.8 COVID-19 on PM

COVID-19 (SARS-CoV-2) disease, a severe acute respiratory disorder caused by the virus, is spread by respiratory droplets [102]. Recent studies have indicated a probable relationship between air pollution, mainly NO_2, CO, and fine PM ($PM_{2.5}$), and increased risk and sternness of COVID-19, a disease caused by SARS-CoV-2 virus commonly called as corona virus. This correlation has been observed in regions with high pollution levels, where a significant number of COVID-19 cases emerged during the pandemic. Researchers have hypothesized that air pollution may influence the spread and virulence of the virus. The underlying cellular mechanisms of fine particulate matter and SARS-CoV-2 on lung cells have been depicted in the Figure 2.5 [103]. Several recent systematic reviews have found a strong link between long-term exposure to PM_{10} and $PM_{2.5}$ and increased rates

of COVID-19 infection, severity, and mortality [104] [105]. According to a study, there is a link between increased PM concentrations and COVID-19-related death rates[106]. In previous communications, predicted that the SARS-CoV-2 virus would present day on PM, which is consistent with findings for other viruses. The RNA virus may be discovered on ambient atmospheric PM in stable atmospheric circumstances and at high PM_{10} concentrations, according to an experimental investigation. This data suggests that PM concentrations may be used as a marker indicating a high risk of sickness. The topic of PM-associated microbiota, particularly in cities, is, nevertheless, relatively unexplored, yet no one has conducted experimental tests especially focused on confirming or rejecting the presence of SARS-CoV-2 on PM as of yet[107].

2.9 Smog Analysis in Pakistan

A recent study of smog data revealed a significant increase in nitrogen oxide (NOx) levels, approximately 17 times higher than baseline levels. Additionally, SO_2 and concentrations of ozone were 4-times > higher, while CO, VOCs, and $PM_{2.5}$ levels doubled. Satellite imagery analysis in Pakistan has confirmed elevated NO production during smog events compared to previous years. To mitigate this pollution, strategies such as reducing personal vehicle usage, promoting public transportation, curbing industrial emissions, expanding urban green spaces, and fostering international cooperation to address transboundary pollution are essential. The report also highlights a 60% surge in patients with optical diseases during Lahore's heavy smog [108]. Gujranwala, Lahore, and Faisalabad had air quality levels of 201.6 $\mu g/m^3$, 271.8 $\mu g/m^3$, and 297.2 $\mu g/m^3$, respectively, according to recent IQ-Air numbers from November 2021. The level of air pollution that is deemed acceptable for humans is significantly higher than this [109]. The IQ-Air data from 2018 to 2023 shows consistently high and worsening $PM_{2.5}$ levels in major Pakistani cities, far exceeding WHO guidelines. Islamabad's $PM_{2.5}$ concentration rose from 38.6 $\mu g/m^3$ in 2018 to 42.4 $\mu g/m^3$ in 2023, exceeding guidelines by over 8 times.

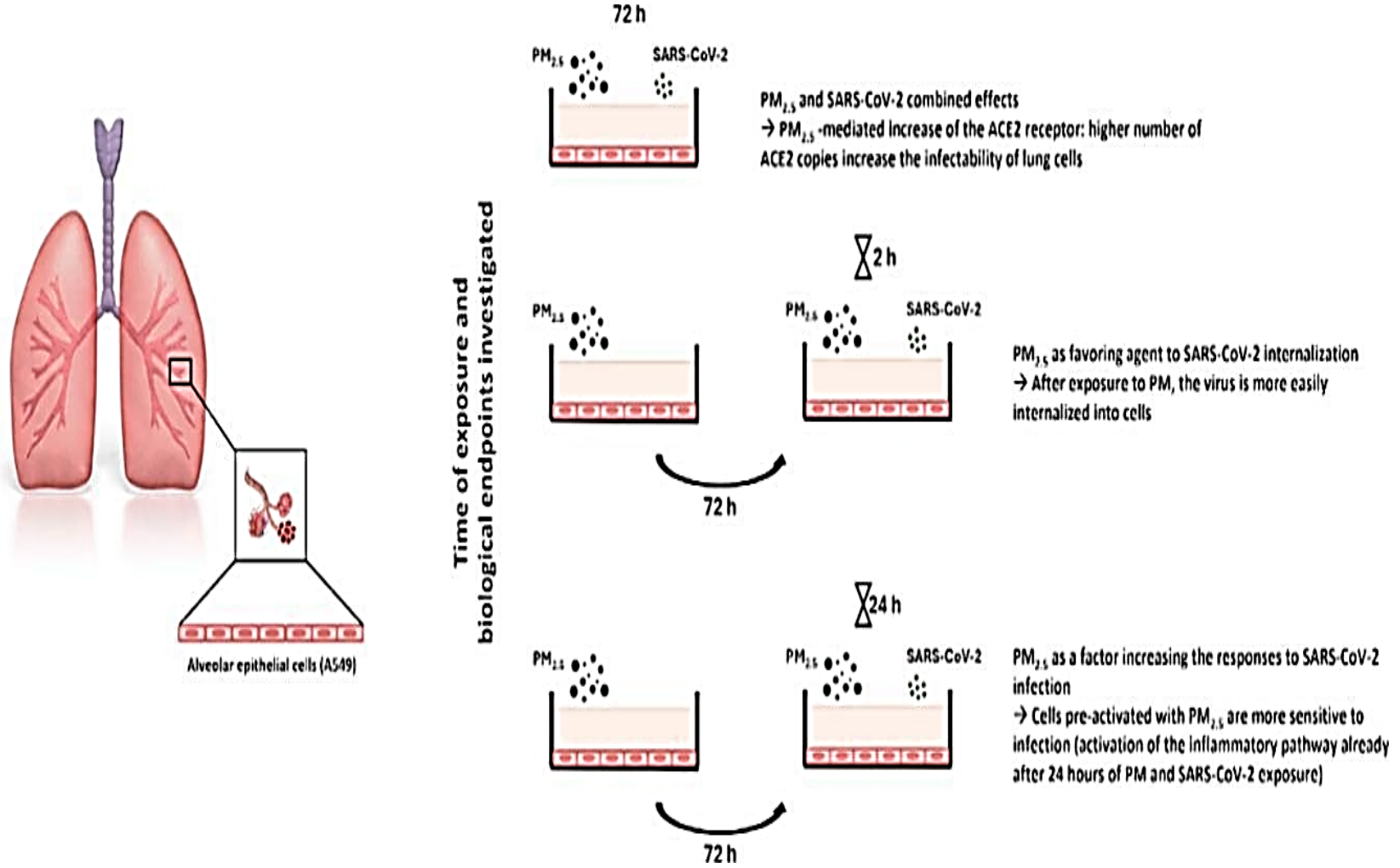

FIGURE 2.5: The underlying cellular molecular mechanisms related to the adverse effects of fine PM and COVID-19 lung cells [103]

Lahore, with the highest levels, saw $PM_{2.5}$ drop from 114.9 $\mu g/m^3$ in 2018 to 79.2 $\mu g/m^3$ in 2020 but then rise to 99.5 $\mu g/m^3$ in 2023, exceeding safe limits by nearly 20 times, reflecting severe air quality issues. Faisalabad also showed fluctuation, with levels dropping to 73.2 $\mu g/m^3$ in 2020 but rising to 88.2 $\mu g/m^3$ in 2023, more than 17 times the WHO guideline. Karachi's air quality has steadily deteriorated, from 33.7 $\mu g/m^3$ in 2018 to 56.4 $\mu g/m^3$ in 2023, exceeding the limit by over 11 times. This data highlights a critical and escalating air pollution issue, attributed to industrial emissions, vehicular pollution, and urbanization, emphasizing the urgent need for stricter air quality measures to safeguard public health.

Negative effects of smog on health and the air, due to a variety of air pollutants that were released and then dispersed into our atmosphere, have significant importance in the globe. As already discussed, the including these, the fine particulate matters$PM_{2.5}$) are of major environmental and health concern. As these enormous, tiny particles of PM can easily enter into the human airway and can penetrate easily to the lung tissues and alveoli, that will lead to shortness of breath, and variety of human airway ailments i.e. severe acute respiratory syndrome (SARS). Components of PM include the different type of inorganic and organic moieties various molecules of hydrocarbons and droplets of water[110]. Construction sites, mining operations, power generating, general combustion, road dust, vehicle emissions, and agricultural activities are the main contributors of $PM_{2.5}$ [111]. One of the significant environmental issues faced by Pakistan in recent years has been air pollution. The situation in Lahore has been deteriorating, which is the 2^{nd} largest city in Pakistan, while Karachi, Pakistan's 1^{st} largest city with AQI 170 & 155 [112].

Human activities that release emissions like from agricultural and automobiles mainly are usually said as key reason to increase prevalence of polluted air and smog specifically in winter season. Therefore, it is essential to make a collective effort to raise public awareness regarding negative impacts of smog on environment and health. Moreover, there has been minimal research conducted on the economic consequences of pollution in Pakistan, and there are limited studies assessing its negative effects on human health [113].

Because of the temporal and spatial diversity in its composition, the chemistry of smog is complicated and impossible to precisely define. Nonetheless, it is typically divided into two categories: photochemical (also known as Los Angeles, or LA) smog and classical (also known as London) smog. Given their harmful consequences on the environment and human health, both are cause for great worry. In addition to these varieties, Polish smog is a unique kind of smog that was discovered more recently[110, 114–116].

London smog, frequently referred to as classical-smog, is a hazardous pollution. This kind of haze formed in London for approx. 5-days in December-1952, resulting in the deaths of thousands of individuals [117].

Because of very high concentrations of sulfur oxides, primarily from burning fossil fuels like coal, this type of smog is referred to as sulfurous smog. The accumulation of high particulate matter in the atmosphere led to the phenomenon known as London Smog.

Increased humidity causes particulate matter in classical smog to grow larger, as they will make the foundation of smog. Acid rain forms when sulfur dioxide oxidizes into sulfuric acid after it dissolves in the droplets of fog. Research showed that the oxidation of sulfur dioxide by nitrogen dioxide in clouds is similar to the formation of classical smog.

The key factors required for the development of classical smog include: primary precursors like SOs, secondary precursors such as aerosols; temperature inversion (TI); high relative humidity (RH) ; & winters low temperature. In the area of the 1^{st} devastating polluted smog episode in London, governments and environmental groups globally implemented Clean Air Acts, including the UK Clean Air Act, introduced by the British government in 1956 [118].

Smog that is triggered by photochemical processes is frequently seen in heavily populated areas as photochemical/Los Angeles (LA) smog. This kind of smog is caused by chemical moieties in the urban air, sunlight, and other particular meteorological factors. High concentrations of a variety of pollutants, such as

aldehydes, carbon monoxide, ozone, and nitrogen oxides, make up the majority of photochemical smog.

Solar light photocatalyzes the nitrogen dioxide from factories and cars to produce nitrogen oxide and free, unpaired oxygen, which is what causes ozone to form in the atmosphere. By interacting with oxygen radicals, this unpaired oxygen creates more ozone. Under typical circumstances, nitrogen dioxide is produced while the cycle proceeds. However, the reaction pathway may instead result in deadly photochemical smog when volatile organic compounds (VOCs) are present [119].

According AQI and studies, Poland country was among the most polluted nations in Europe between 2015-2016 in previously reported data [120]. Because of this, the average life expectancy of European citizens has decreased by nine months, posing major risks. The termed "Polish smog" was different chemically from the smog types that had been previously reported. Household boilers are the primary source of Polish smog, releasing significant levels of $PM_{2.5}$ and PM_{10} along with additional carcinogenic substances like benzo [a]pyrene. Polish smog is unique in that it has high PM_{10} concentrations due to cold temperatures and high atmospheric pressure. Polish fog is the cause of up to 48,000 premature deaths in Poland each year. This kind of fog is not just found in Poland; other European nations with comparable meteorological conditions and pollutant emissions profiles are also experiencing its impacts. Therefore, researchers in other parts of the world need to do further research on this new kind of fog. Since there are numerous contributing components, it is challenging to pinpoint the precise makeup of Pakistani smog. Nonetheless, the chemical makeup of Pakistani haze is comparable to that of other smog kinds [121].

2.9.1 Pakistani Smog Causes and Detection Techniques

Like many other developing countries, Pakistan's AQI is negatively affected by a number of emissions sources, including industrial sector pollutants, vehicle exhaust gases, solid waste management, use, and burning, and agricultural activities. As

the population of Pakistan has increased in last 20-years, so too has the use of motorcars, scooters, and motorcycles, and the countries over 10 million vehicles contribute significantly to air pollution.

The number of automobiles increased dramatically between 1991 and 2012 in Pakistan. According to an evaluation of the photochemical reactions that produce ozone in the Quetta area of Pakistan, car exhaust was proposed as the primary cause of the process [122].

Many enterprises of Pakistan use furnace oil, a major source of sulfur, including factories, power plants, and steel mills, and will contribute majorly to air pollution. Further, burning agricultural-waste is a major factor in the creation of smog in many Pakistani cities. Pakistan produces around 50,000 tons of solid garbage every day, most of which is burned.

PM and harmful gas pollutants (CO, SOx, and NOx) are released into the environment during the incineration process. Additionally, high tropospheric O3 concentrations combined with aldehydes and ketones produce a PAN photochemical fog that can be harmful to health of human beings as already discussed. For instance, the manufacturing of building supplies like cement and hydrated lime may result in the release of harmful gasses [123]. Although cigarette trash has gotten less attention, it contains extremely dangerous and toxic substances (such as Pb, Cd, As, and Cr). Moreover, a considerable amount of wasted food is produced by hotels and restaurants. When the organic materials in this waste break down, they generate biogas, which consist primarily of large quantities of organic gases like CH_4 & CO_2, along with minor amounts of H_2S and NH_3. Consequently, there may be risks of asphyxiation and environmental contamination if these organic wastes are allowed to decay outside of an appropriate facility. Several techniques have been developed & utilized for prompt detection and analyses of these pollutants. Available commercial smog detectors, like the AQS/1-smog-monitor or monitoring system that measures photochemical smog, track the seriousness of smog and its harmful components as inorganic and organic moieties, $PM_{2.5}$, harmful gases CO, SO_2 VOCs and other species. To provide accurate data on haze occurrences, numerous government agencies, NGOs and environmental activities are actively

working in key cities such as provincial capital Lahore, and the Federal city. This assessment was specifically designed to concentrate on the sources associated with smog emissions or major elements of smog, rather than solely on general air pollution causes [123].

2.9.2 Pakistan's General Smog Concerns

Pakistan smog consists of numerous pollutants, such as SOs, NOs, CO, VOCs, O3, PANs, aldehydes, and PM. When present in high quantities, each of these components can be dangerous to the health of humans, plants, animals, and the environment. A recent study highlighted the various health effects that smog events in Lahore can cause in individuals, including headaches, diabetes, and asthma. However, the study only involved medical students [124].

Smog poses significant dangers to the health of the human population. Several recent studies are there that suggest the very harmful adverse effects on the human airway system and CV system. The severity of the risks associated with smog depends on several factors, including the volume inhaled, the specific substances involved, and the characteristics of the individual (such as weight, age, and overall health). In 2005, almost 3,000,0000 people worldwide lost their lives due to pulmonary ailments, cancers of the lungs, and heart conditions that are closely associated tiny matter in the smog i.e. $PM_{2.5}$ and O3, which are the main elements of smog [114]. Any form of particulate matter (PM), which contributes significantly to pollution, is known to lead to premature mortality. Nevertheless, the health issues associated with PM are intricately linked to its particle size. Smaller particles have a greater tendency to enter deeper into the airway tract of human, potentially causing greater damage to the lungs and respiratory function. A recent study that was done in the United States has found a strong connection between levels of airborne PM and the incidence of diabetes in adults. Children are more vulnerable to respiratory conditions when exposed to elevated levels of PM present in smog for prolonged periods, as they have lower immunity to infections compared to adults. Several studies in the United States, China, Europe,

and Pakistan have reported that excessive exposure to $PM_{2.5}$ in smog can act as the main factors for intrauterine inflammation, which can lead to premature births and other neonatal complications. Premature birth of babies can significantly reduce life expectancy over time and is a leading cause of postpartum death in early maturity. Like PM, ozone, once absorbed through the mouth and nose, adversely affects the respiratory and cardiovascular systems, particularly putting women and children at greater risk. Damage to cells and tissues can occur due to secondary oxidation products formed when O3 interacts with elements of the fluid of epithelial lining of lung mucosa. Research indicates that the likelihood of mortality increases by 0.26% for every 10 mg m3 increment in ozone levels. [125].

The levels of tiny particles like $PM_{2.5}$ in Lahore are 9-times more than the recommendations set by WHO, indicating potential serious health risks due to air pollution. According to data from the Pakistan-AQI, the Federal capital, Lahore, Peshawar, and Karachi, all are above the World Health Organization's advised air quality limit of 10mg/m3, recording $PM_{2.5}$ levels of 42, 130, 63, and 40mg/m3, accordingly. Moreover. A recent study reported eye surface disorders in patients at tertiary–care facilities in November-2016 revealed that Lahore had the poorest air quality, noting 28 cases. Smog samples were collected from three well-known locations in Lahore—Mall Road, Gulberg, and Township—both during the smog days that occurred in November-2016. A study also suggests the ocular surface diseases on the basis of data collected from Sheikh Zaid & Mayo Hospitals in November-2016. Using the measurement techniques established by the US Environmental Protection Agency, it was found that NOx was the most concentrated smog component, being 17 times higher than the same measurement in November 2015. Considerable increases in other smog components were also observed, likely exacerbating health issues. The air quality index was recorded at six times its level from 2015 [126].

The smog negatively affects Pakistan's agricultural exports, such as rice, wheat, and cotton. Recent studies have revealed that smog, particularly PM and ozone, has led to a notable decrease in crop yields. Research examined the impact of smog pollutants on two winter wheat varieties. The findings indicated that ozone

was primarily responsible for the 34.8–46.7% reduction in wheat yield. In a related study, it was found that exposure to smog components, chiefly ozone, considerably decreased the photosynthetic efficiency in three wheat varieties that are important sources of food in Pakistan. Additionally, barley that is a very important crop in Pakistan after wheat has also experienced a significant reduction in seed yield (from 13%–44%) due to exposure to smog constituents like NOx, SOx, and ozone. In another study by the same researchers, the yield of two local rice cultivars was decreased by 37–42%. Research focuses on the effect of emissions from brick-kilns, a chief source of air pollution, on wheat production in Punjab that exposure resulted in less yields, shorter plant heights, decreased photosynthetic activity, and metal contamination in the crops. For a developing nation that heavily relies on agriculture, such a significant decline in agricultural productivity is deeply alarming. To ensure adequate food production as the population grows, it is crucial to mitigate the harmful effects of air pollution [127].

A nation's economic development and air quality are linked. Healthy people, thriving enterprises, thriving tourists, and growing employment are all factors that contribute to the economy's success. All of these operations are hampered by air pollution, particularly smog, which slows the economy. Productivity during the working day is adversely affected by the buildup of smog from the morning until the afternoon. Public and private schools in Lahore were recently closed for many days owing to severe pollution (2019). One of the largest economic projects in Asia, the 62 billion USD commercial corridor between China and Pakistan, is also confronting significant obstacles as a result of smog's impact on nearby transportation routes [128]. It is said that if smog is not well controlled, Pakistan's GDP (47.8 USD billion) will drop by more than 5.88%. An economic recession could result from the terrible impacts of smog on Pakistan's agriculture industry and human health (11 million individuals reported headaches and eye irritation). Economic setbacks, including a drop in household income, can arise from the premature deaths and chronic health issues of employed men and women caused by smog pollution. A study by the World Bank in 2016 estimated that air pollution resulted in an economic loss of $5 trillion USD annually. Pakistan and other developing countries are particularly at higher danger, with annual labor income

losses amounting to 1% of South Asia's overall GDP. The total welfare costs linked to air pollution encompass four primary elements: mortality, disutility, indirect costs, and direct market expenses. As reported by the OECD in 2016, the global welfare cost of atmospheric air pollution reached 3.8 trillion USD in 2015 and is forecasted to rise to between 24-31 trillion $ by year 2060. $PM_{2.5}$ and ozone, along with other smog components are largely be attributed to smog, as the primary air pollutants. This indicates that stringent pollution control measures are critically needed to avoid significant consequences in the future[129].

Smog has a negative impact on a nation's tourism industry by seriously damaging tourist destinations like historic structures and monuments. Furthermore, many travelers will steer clear of a nation known for its high levels of air pollution for health reasons. Seeing a country's landscapes, rivers, mountains, and modern or historic structures is one of the primary reasons travelers travel there. However, because haze reduces visibility and the scenic attractiveness of the area, it detracts from the visitor experience. The danger of traffic accidents is increased by smog's loss of visibility. For instance, in November 2017, smog-induced poor visibility resulted in 10 fatalities and several injuries. A 10-percent improvement in-visibility might result as extra 1000000 visitors to park, there are several historical sites and archaeologically significant places in Pakistan. Its tourism business is expanding, and it has the potential to become a highly sought-after international travel destination. Nonetheless, the air pollution caused by fog in major cities like Lahore and Peshawar has raised serious concerns among both the local populace and foreign tourists, including Sikhs who travel to Katarpur to see their sacred shrine [130].

2.9.3 Current Smog Prevention Initiatives in Pakistan

Anthropogenic emissions are the main source of precursors for all forms of smog. Therefore, in order to effectively reduce smog, these pollutants must be properly mitigated. On a local, regional, and even global level, numerous methods have been established. However, preventing smog (to raise air quality indices for a

particular location) usually requires a few abatement strategies that function together rather than relying on a single intervention. These interventions could be technological, social, economic, or regulatory in character.

Increased vehicle use has been a major contributor to smog events in Pakistan because of the country's fast economic and population growth. Vehicles are responsible for almost half of the total emitted volatile moieties that impact quality of air in the various parts of the globe. In this regard, Pakistan is confronted with significant obstacles in the transportation sector, such as the need to replace the fleet of vehicles with cleaner models and the absence of laws pertaining to vehicle maintenance and monitoring now. In Pakistan, the growing number of private automobiles has created significant air quality issues. 6.2 million of the 19.6 million automobiles in Punjab province come from Lahore. Motorbikes, rickshaws, and other vehicles with two-stroke engines are the most dangerous types of fuel vehicles in terms of air pollution and are frequently used for transportation in Lahore. Large volumes of gaseous moieties and harmful compounds, key precursors for development of air pollution and smog, are produced by the enormous number of private vehicles on the road. In this situation, fewer private vehicles must be used, and public transportation must be promoted, perhaps with the help of "low emissions zones" like those in London [123]. Creating a mass transit railway system, for example, by utilizing high-speed electric trains—would significantly improve the quality of the air. Another preventive measure to lessen hazardous emissions and, consequently, the development of smog is the implementation of strategic strategies for monitoring and managing traffic congestion. Second, in order to gradually lower the likelihood of smog events, critical to improve the monitoring and other regulations on cars and encourage the adoption of clean technologies and vehicle powered by renewable energy [131].

Routine vehicle inspections and maintenance can be effective measures for reducing harmful emissions in the transportation sector. The level of air pollution produced by a vehicle is primarily influenced by the state of its engine. Therefore, it is essential to regularly adjust the engine and frequently check the fuel system, muffler, and engine case ventilation system. When considering how to decrease

the volume of hazardous pollutants in exhaust emissions, it is also important to take into account the engine designs, operating conditions, type of fuel used, distance travel, and the amount of work done. To enhance the use of sustainable energy, the automotive industry has recently supported the hybrid engine approach. By integrating advanced-combustion-techniques with hybrid and electric vehicle technology, harmful gaseous and dust can be reduced by 12%–30%. Since consumers often hesitate to change their car preferences until the new option look more better and comfortable than already available technologies, factors such as the operational and production costs of the technology, along with the extended recharging time, must be considered [132].

The main contributors to carbon emissions, especially CO, in households are other oil and gas devices like our home heaters, kitchen stoves, gas/fuel generators, oil pumps, fridge and AC compressors, other high-pressure washers, & high-pressure drills and floor baffles. To cope with this problem, we have to adopt a novel technology that operates on compressed air or electricity, provided that these alternatives are available and safe to utilize. The increase in manufacturing and domestic activities in Pakistan has resulted in a rise in smog levels. Recent advancements like fuzzy-VIKOR offer a way to alleviate the adverse effects of harmful air pollutants, PM and smog by using an effective environmental-strategy. Results of fuzzy-VIKOR models indicate that reducing factories waste and educating our farmers and local communities about the smog and its prevention on lowering their emissions and, in turn, contribution to pollution and smog production can alleviate the impact of smog. Employing this method will assist the Pakistan government in shaping future policies [133].

Contemporary abatement technologies are rarely implemented in Pakistan's industrial sectors due to the country's ongoing economic development. Brick production primarily occurs in brick kilns fueled through coal and agricultural waste. There are approx. twenty thousand operative kilns across Pakistan, most located near urban areas like Lahore and Faisalabad. The emissions from these facilities pose a significant risk to the environmental health of cities in Pakistan. To diminish smog occurrences, it is crucial for the nation's brick industry to cut down on emissions.

Utilizing either wet or dry filtration systems, employing air purifiers, and adopting modern and advanced kilns are potential resolutions to this issue. Additionally, gas bypass systems and specially designed pollution and smog control devices having specific internal-baffle arrangements in their chimneys and boilers can assist in reducing pollution levels. Because they ensure the optimal combustion of coal, Advanced technologies and mechanical feeders like vertical-shaft-kilns(VSK) can also play a role in lowering emissions. The transition from traditional fossil-fuels to these latest energy sources, and like biomass and solid-waste fuels, being explored feasible choice for the forthcoming of industrial power in country as this could diminish CH4 and N2O emissions from conventional sources [134].

Another source of chemical contamination that can spread over great distances and have an impact on the ecosystem worldwide is anthropogenic activity. Coal accounts for over 90% of all industrial emissions worldwide, which is significantly more than the emissions from other man-made sources such cement production, gold-smelting, nonferrous-smelting, iron/steel manufacture, mercurial mining, and household garbage. Solid fuel combustion, which is often a major but unknown source of smog precursors in Pakistan and other emerging nations, is the primary source of emissions from industrial processes like power generation. Therefore, Pakistan's smog generation would be reduced by using alternative industrial fuels like oil and gas and developing techniques for utilizing energy from renewable sources [135].

At present, Lahore faces significant air pollution challenges from November-February every year, thick layer of hazardous smog-haze envelops the whole city and several regions of Khyber Pakhtunkhwa (KP) in Pakistan. Many researchers have highlighted the role of green spaces in mitigating environmental pollutants such as smog. In this context, governments worldwide have begun to introduce new strategies for smog management by creating forests in and around main manufacturing cities to serve as a natural wall between urban areas and industrial zones.

In addition, supplying oxygen to the air, the expansion of forests and plantations helps regulate the local climate and protects communities from heat waves. Shade can decrease extreme smog levels by 5%, amounting to a reduction of 175 tons

of NOx daily, which is twenty-five times more than the four tons/day reduction achieved by cutting down power plant emissions. Although increasing the size of plantations is a beneficial approach, Professor Barry Lefer from the University of Houston notes that "no guarantee that the florae are addressing emissions where drops are necessary." This is due to certain plant species emitting biogenic volatile organic compounds that can negatively affect air quality by increasing ozone and particulate matter, making the timing and placement of the plantations essential. Plants produce pollen grains and fungal spores that can pose health problems and risks to individuals with allergies or other sensitivities [136].

Adopting simple smog prevention techniques like walking, bicycling, and taking public transportation can have a big impact because vehicle emissions are a major source of smog. Switching to environmentally friendly consumer goods including paints, paper, plastics, and sprays with minimal volatile organic compounds (VOCs) is another strategy.

Laumbach and co-workers emphasized individual actions to lower the danger of air pollution, including smog episodes, on one's own health. To safeguard one's health during winter smog, they recommended reducing exposure by remaining inside, using HEPA filters and thus filtering indoor air, and minimizing physical action. Guidelines for wearing masks, avoiding outside activities during smog time specially in winters, and utilizing and spring-cleaning interior air-filters have been released by Pakistan Disaster Management Authority (PDMA) [137].

When tackling these issues, public and knowledge of pollution and smog, its consequences on the environment and health of human being are crucial components that cann't be ignored. Increasing public education and awareness about smog and air pollution can be crucial in reducing smog-related air pollution, according to a survey of 607 carefully chosen people.

Therefore, public awareness sessions and initiatives for preventive actions should be used to educate the public more broadly about the harmful impacts of smog. In a related study, sociodemographic characteristics, especially educational attainment, can be crucial in helping Lahore inhabitants comprehend pollution threats

and smog mitigation measures. The people should be made aware of the seriousness of air pollution through information sources like mobile applications and internet media material, which will enable them to lessen the short term health consequences by remaining indoors and not exerting themselves in the smog events and winter season [138].

2.9.4 Advanced Preventive Measures for Smog

Anthropogenic emissions are the main source of precursors for all forms of smog. Therefore, to effectively reduce smog, these pollutants must be properly mitigated. Numerous tactics have been created at the local, regional, and even global levels. However, preventing smog (to raise air quality indices for a particular location) usually requires a few abatement strategies that function together rather than relying on a single intervention. Due to convenience or a lack of other options, people frequently choose their own cars over public transportation, which worsens traffic congestion and increases dust and exhaust emissions from worn tires and asphalt, further polluting the air. This circumstance emphasizes how important it is to have air quality monitoring systems that can act quickly to restore the quality of the air when it is degraded. Air quality monitoring is essential to the global effort to address air pollution problems, even with advancements in emission reduction and air quality improvement [139]. Modern greenhouses provide increased yields and enhanced planting efficiency, offering a sustainable approach to agriculture with little environmental impact. They are distinguished by their portability and ease of customization. Concerns are raised by the contamination of the immediate human environment, which includes tainted food, water, and indoor air that is contaminated by CO_2, CO, NOx, radon, cigarette smoke, volatile organic compounds, and oxygen shortage. Particularly noticeable is the increase of smog, a type of air pollution, in cities with high energy consumption and exhaust emissions, which are mostly caused by traffic. Innovative technology combinations have been the focus of recent developments in smart greenhouse systems. Data analysis, automation, and monitoring are all integrated into these systems. The automated monitoring framework's four main parts make up the

system architecture. It comprises cloud-based data storage and monitoring of soil moisture, humidity, and climate. Technology notifies the farmer in the case that ideal circumstances are not met, allowing for prompt remedial action. Additionally, the system enables automated irrigation switching based on sensor data. It also makes use of deep learning methods to identify plant illnesses [129].

Dust generated from the construction industry significantly contributes to municipal smog in China, driven by rapid urbanization. A study was conducted to analyze the potential of synthetic natural gas (SNG) as a replacement for coal in Beijing to enhance energy efficiency. Utilizing SNG for heating can decrease haze pollution emissions by 44%. Research findings have shown that hybrid, electric and renewable energy sources, retro-fitting processes, recovering the harmful chemicals and components, and optimizing energy systems offer effective control advantages, with retro-fitting, chemical recovery, and saving energy measures proving to be more effective than renewable energy sources. An assessment was performed to analyze the carbon footprint associated with the oxygen-thermal coal-to-acetylene process, which involved establishing an appropriate boundary, collecting relevant data, and applying suitable allocation principles.

To enhance precision, the activity data was thoroughly verified as mass balance, carbon, and renewable energy balance evaluations of the system. In addition, the distinct contributions of both acetylene and CO to the carbon footprint were factored into the total carbon footprint, highlighting the multi-product characteristic of the coal-to-acetylene process. Ultimately, recommendations were put forward to reduce carbon emissions from the oxygen-thermal coal to acetylene process. Given the difficulties in integrating life cycle assessment with life cycle cost methods to evaluate economic value, a simplified ecodesign approach was adopted, focusing on greenhouse gas emissions alongside material expenses for a product.

A case study involving urban electric railway vehicles (comprising six cars in one configuration) was conducted to validate this method, resulting in favorable outcomes. Moreover, a comparison was made regarding the environmental effects of open-field burning of corn straw versus alternative technologies for utilizing

corn straw through life cycle assessment. The findings indicated that composting methods were more effective and environmentally favorable in terms of air pollution compared to directly returning straw to fields, using it for animal feed, turning it into biogas, or generating electricity, especially in contrast to open burning. Additionally, composted corn straw can act as a viable alternative to synthetic fertilizers. So, two innovative methods, namely Electron Beam Flue Gas Treatment (EBFGT) and Dielectric Barrier Discharge (DBD), were analyzed and compared with conventional technologies for flue gas treatment, including Wet Flue Gas Desulfurization combined with Selective Catalytic Reduction (WFGD + SCR), biofiltration, and adsorption. The comparison was conducted using a comprehensive Life Cycle Analysis (LCA) framework to evaluate the performance of these methods in terms of resource efficiency, environmental impact, and energy consumption. The analysis focused on three key factors: the use of raw materials, the generation of waste, and the total energy required for operation. To quantify and assess the environmental implications of each method, five major impact categories were considered, based on the widely recognized CML2001 method. These categories include global warming potential, which accounts for greenhouse gas emissions; ozone depletion potential, which evaluates contributions to the degradation of the ozone layer; acidification potential, which measures the release of acidic compounds affecting ecosystems; eutrophication potential, which considers nutrient pollution leading to ecosystem imbalances; and human toxicity potential, which examines the effects of toxic substances on human health. This approach provides a detailed comparison to identify the most sustainable and environmentally friendly technology for flue gas treatment [118, 137].

2.10 Antibiotic Resistance Gene in Particulate Matter in Smog Season

A metagenomic approach was employed to assess the quantity and diversity of airborne antibiotic resistance genes (ARGs). While ARGs were less prevalent in airborne particulate matter (PM) compared to fecal samples, their abundance

was comparable to that found in soil and activated sludge. Resistance genes of different environments, such as PM and soil, exhibit similarities, suggesting that environmental factors can influence the airborne ARG profile. Given the bacterial transmission of ARGs, we propose that terrestrial bacteria could be a significant source of airborne ARGs in smog, a hypothesis supported by previous studies [140]. While no significant linear correlation was found between PM concentrations and ARG levels, smog days exhibited higher levels of both total and diverse airborne ARGs compared to non-smog days. This may be attributed to the increased presence of particulate matter during hazy conditions, which can serve as attachment sites for bacteria. Industrial waste, soot, and vehicle emissions can contribute to this phenomenon, as PM particles can easily become airborne and remain suspended, facilitating their dispersal [141].

The airborne transport of microbes carrying antibiotic resistance genes (ARGs) from soil environments may lead to a higher prevalence of antibiotic inactivation resistance in particulate matter (PM). This is because antibiotic inactivation is a common mechanism by which bacteria resist commonly used antibiotics, such as aminoglycosides, beta-lactams, and macrolides [142], and ARGs are abundant in soils and water as well. Research indicates that airborne bacteria can develop novel resistance genes and mechanisms in response to the elevated selective pressure imposed by various pollutants in human-impacted environments [143]. Membrane efflux proteins are capable of transporting a wide range of intracellular pollutants, including drugs and heavy metals, out of cells [144]. Research indicates that increased levels of airborne antibiotic resistance genes (ARGs) during smog events are linked to the accumulation of specific resistance genes, including those associated with tetracycline, lactam, and aminoglycoside antibiotics. Given the extensive use of tetracycline in human and veterinary medicine, as well as its application as a growth promoter in livestock feed, it's plausible that tetracycline resistance genes may be particularly prevalent in these environmental samples [145].

Chapter 3

Materials and Methods

This study was planned in two modules to assess thoroughly the impacts of smog exposure on biological systems and the antimicrobial resistance potentiality of suspended particulate matter ($PM_{2.5}$). The rat model study was conducted in November–December 2023, the smog season, in two major Pakistani cities, Islamabad and Lahore. Experimental rats were segregated into groups by smog and non-smog exposure conditions in both cities, forming control and experimental groups. Following exposure, a series of examinations were conducted that included behavioral studies, immunological studies, lung histopathology, and lung metagenomic analysis. The second module was on the $PM_{2.5}$ filter paper experiment and was done over a span of two years, 2022 and 2023, that is, between November–December when it is normally smog season. PM2.5 were sampled with an air sampler that used quartz microfiber filter papers. Internal and external DNA were then recovered from these filters with the ultimate goal of examining antimicrobial resistance (AMR) gene profiles. The study was segregated into two groups according to DNA type. In the external DNA category, real-time PCR was conducted to analyze the expression of chosen antimicrobial resistance genes. In the internal DNA category, the isolated DNA was subjected to metagenomic sequencing through the Illumina Nova 6000 platform, allowing for a high-resolution and high-throughput analysis of resistance genes contained within particulate matter. Figure 3.1

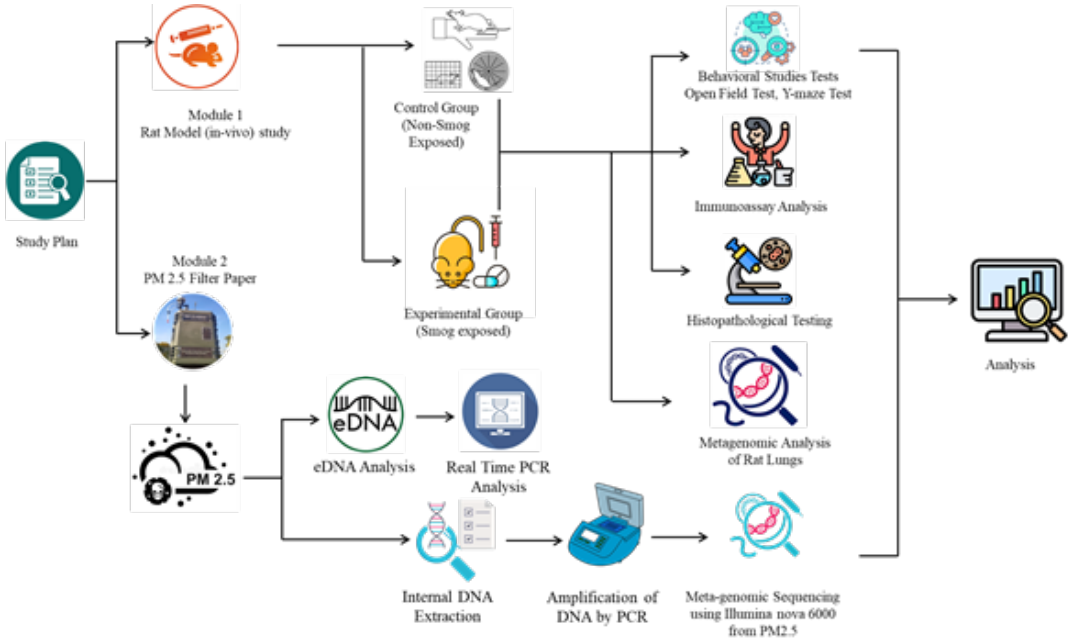

FIGURE 3.1: Overview of the research methodology showing Module 1 (rat model under smog and non-smog conditions) and Module 2 (PM2.5 filter paper analysis)

3.1 Animal Model Studies

Male Sprague-Dawley rats, weighing 200-250gm having aged 8 weeks were taken from the Faculty of Pharmacy, CUST, Islamabad. The whole study protocol was approved by the Research Ethics Committee of the Faculty of Pharmacy, CUST, Islamabad (REC/01/12/22).

To investigate the effects of smog exposure, 24-rats were divided into 2 primary groups: a Islamabad group and a Lahore group, each with 12-rats. The experimental animals were housed in a controlled environment at 22-25∘C and acclimatized for one week prior to the experiment. Both groups had ad libitum access to food and water. Both groups were further subdivided into two subgroups based on smog and Non-smog environment. Rats were divided into Islamabad and Lahore groups (n=12 each), further split into subgroups labeled "Non-Smog exposed (Control)" and Smog exposed (Test) to assess location-dependent smog effects. All rats were reared in a common facility; subgroups were exposed to smog samples collected from each city. The control group was maintained in a smog-free environment,

while the test group was exposed to ambient smog for two hours daily over a 60-day period.

After the exposure period, a series of behavioral and biochemical tests were conducted on both groups. Blood samples were collected from each rat for flow cytometry analysis of CD4 and CD8 T cell levels. Subsequently, the animals were euthanized by cervical dislocation, and their lung tissues were harvested for histopathological examination.

3.2 Behavioral Studies Tests

To check the mental conditions of rats due to smog exposure following behavioral tests were performed on each animal of both groups: (Control & Test)

Open Field Test An open field test was performed to check locomotion, anxiety, and exploratory behavior. In this test each experimental rat was individually placed in the center of a well-lit arena and allowed to freely explore for approximately 5-minutes as depicted in figure 3.2. Parameters such as duration and frequency of grooming behaviors were recorded manually [146].

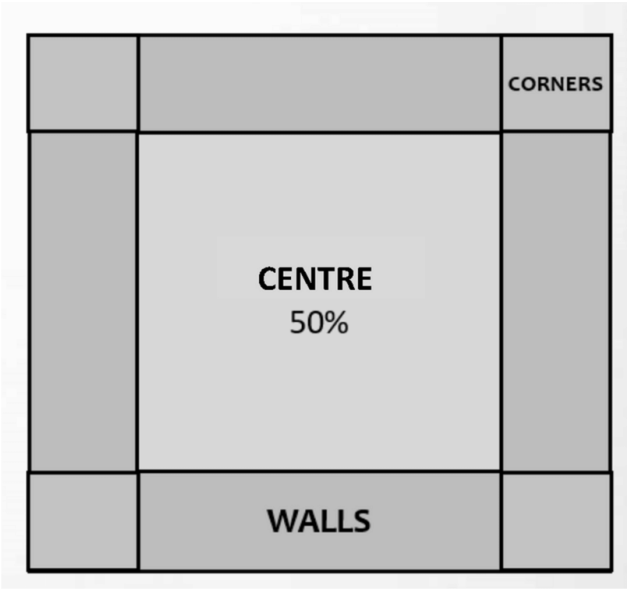

FIGURE 3.2: Different zones of box in open field test for animal behavioral activity

Y-maze Test The Y-maze test was employed for analyzing animals' spontaneous alternation in behavior, a measure of working memory of animal. The random alternation, characterized by the animal's tendency to explore each arm of the maze, is considered a typical exploratory behavior [147]. Both test groups and control animals were individually placed at the start arm of the Y-maze and allowed freely explore the apparatus as depicted in figure 3.3. The entry of each animal into each arm was visually recorded [148].

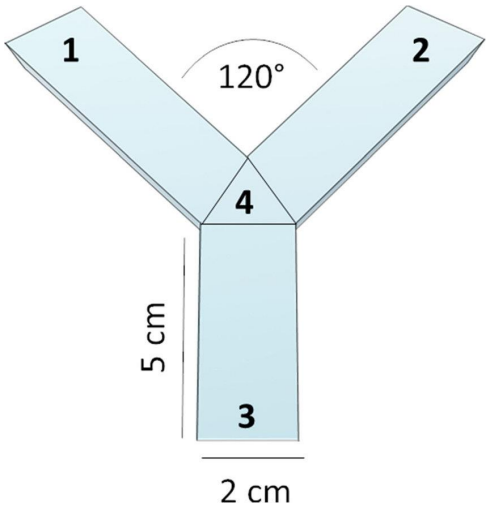

FIGURE 3.3: Y-Maze apparatus for analyzing the animals' spontaneous-alternation in behavior, a measure of working memory of animal

3.3 Flow Cytometry

A 10x concentrated stock solution of Trypan blue was prepared. This Trypan blue stock solution was diluted to a 1xworking solution. Equal volumes (0.1ml) of the 1xTrypan blue solution and cell culture homogenate were mixed together and pipetted thoroughly. The mixture was loaded onto a hemacytometer and immediately examined under a low-power microscope as depicted in figure 3.4 and 3.5 respectively. The number of non-viable the blue-stained cells, and total cells were counted. The total cell count was calculated using the appropriate dilution factor.

$$\frac{No.\,of\,live\,cells\,counted}{No.\,of\,quadrant\,counted} \times 10\,(dilution\,factor) \times 10^{4}_{(Depth\,of\,hemocytometer)\times 0.5\,ml}$$

Each of the four samples was divided into two equal aliquots. One aliquot from each sample was kept unstained as a control. The remaining aliquots were stained with either CD8 or CD4 primary antibodies. Fifteen microliters of the appropriate antibody were added for each sample and then incubated for 15-minutes.

Following incubation, the samples were washed with phosphate-buffered saline (Phosphate saline buffer-PBS, pH 7.4) at 500 xg for 5-minutes at room temperature(RT). The washed samples were then immediately analyzed by flow cytometry as depicted in figure 3.6 [149].

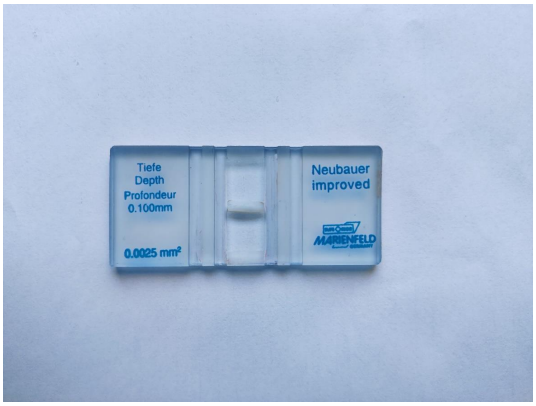

FIGURE 3.4: Neubauer improved hemacytometer for Cells counting

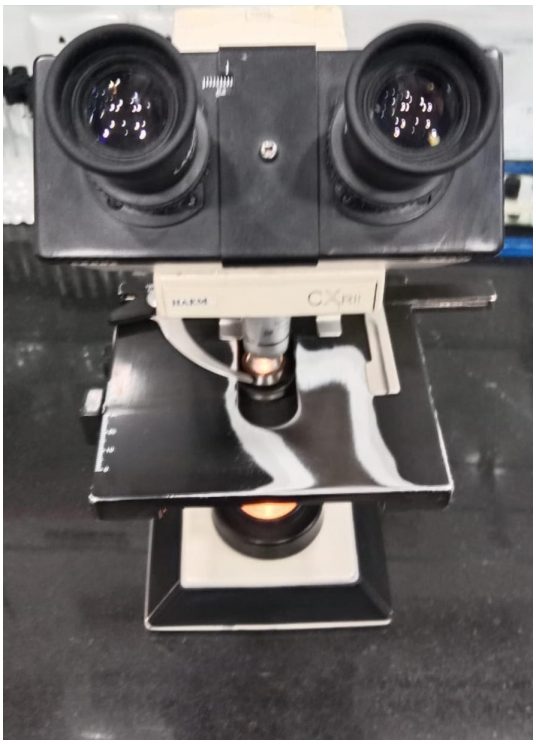

FIGURE 3.5: Microscope for the analysis of viable and non-viable cells

FIGURE 3.6: Analysis of CD4 and CD8 T cells by Flow Cytometer

3.4 Histopathological Testing and Analysis

Following euthanasia, rat lungs were aseptically harvested and preserved in 10% of buffered formalin's solution. The gross inspection involved a visual evaluation of the lung tissue, including its texture, the color, size, shape, and if any abnormalities such as some lesions discoloration, abnormal masses, or congestion. After gross examination the tissue was carried out Fixation, dehydration and clearing by automated tissue processor as depicted in figure 3.7.

FIGURE 3.7: Initial Tissue Processing procedure is being carried out by Tissue Processor

After tissue processing steps the processed tissue was put in the tissue cassette and hot liquid paraffin wax was added in it. Put the cassette on refrigerator for solid block formation. This process is also named as embedding. Now the block is ready for microtomy process as depicted in figure 3.8.

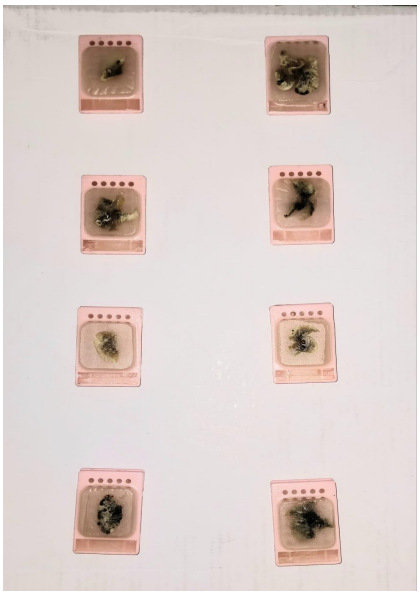

FIGURE 3.8: Embedded rat lungs Tissue in paraffin wax cassettes

The embedded paraffin blocks were then mounted on microtome for microtomy process. Which was done by thin sharp blade and each slice have size of 4microns, which can be adjust by adjusting knobs of blade as depicted in figure 3.9.

FIGURE 3.9: Sledging of Tissue blocks by Microtome for slide preparation

To prepare lung tissue samples for H&E staining, the tissue was first dehydrated by immersing it in a graded series of ethanolic solutions (70%/95%/100%). Each step involved incubation for approximately 1-2 hours. Following dehydration, the tissue was cleared in xylene.

Next, the tissue was infiltrated with molten paraffin wax, which solidifies to form a paraffin block. Thin sections of tissues (4-5μm) were then cut from the paraffin block with the help of microtome and mounted on glass slides. These sections were then finally stained with the help of hematoxylin and eosin(H&E) as depicted in figure 3.10.

Stained tissue section was analyzed under a high resolution imaging microscope (Leica) to check histopathological changes in the lung tissues as depicted in figure 3.11 [150].

FIGURE 3.10: Carrying H and E staining process of Tissue section for microscopic analysis

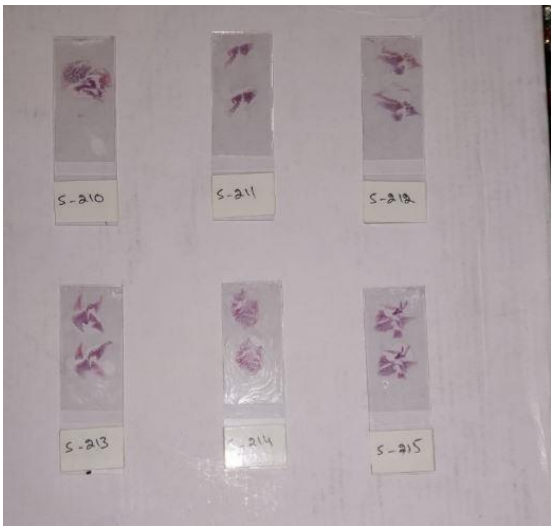

FIGURE 3.11: Prepared and stained microscopic slide for Microscopic analysis

3.5 Metagenomic Analysis of Rat Lungs

A typical phenol-chloroform extraction procedure was used to extract internal DNA from 20 mg of rat lung tissue samples. After lysing the samples for 20 to 30 minutes at 65°C in 500 μL of lysis solution, proteinase K and SDS were added to break down the proteins. Proteins and cellular detritus were then extracted from the lysate using phenol-chloroform. Isopropanol was used to precipitate the DNA-containing aqueous phase, and ethanol was used to wash away any salts. The purified DNA pellet was then kept at 4°C after being resuspended in TE buffer [151, 152]. One gram of agarose was dissolved in 100 milliliters of 1X TAE buffer to create a 1% agarose gel, which was then used for gel electrophoresis. After heating the solution until it became clear, 8 μL of ethidium bromide was added. A comb was used to create wells in the gel in a tray. The gel was moved to an electrophoresis tank containing 1X TAE buffer once it had solidified. After combining 6 μL of extracted DNA with 2 μL of 6X loading dye, the mixture was put into the wells. For 60 minutes, electrophoresis was carried out at 75 volts. A gel documentation system was used to visualize the gel under UV light. In contrast to a 1 kb DNA ladder, the resultant image displays representative DNA bands [153]. Using a Thermo Scientific MultiSkan Go Microplate Spectrophotometer, the amount and quality of DNA were evaluated. The concentration was expressed

in ng/μL, and the purity of the sample was assessed using the 260/280 ratio. Assembly-based and alignment-based methods were the two main strategies used to analyze metagenomic data. The FASTQC tool was used to assess the raw sequencing data's quality [154].

After quality control, the primer obtained the paid end clean reads. To remove the primer information at both ends of the sequence, use the cutadapt software (https://github.com/marcelm/cutadapt/) and fastp (a preprocessor version 0.14.1 (https://github.com/opengene/fastp)) to cut the sliding window quality (- w4-m20) of the two end raw reads data, respectively.

The inconsistent tags should be removed and the original raw tags should be obtained for the data of two terminal sequencing based on the overlap relationship between PE (Pair End) reads (V10 (http://www.drive5.com/usearch/preset) parameters, which include the minimum overlap length set to 16bp and the maximum mismatch allowed in the overlap area of splicing sequence 5bp, etc.).

Kraken 2 was used to taxonomically classify reads against a curated database [155]. After assessing the quality of the sequencing data, a metagenome assembly was conducted using the MEGAHIT assembler.

We first eliminated human readings in order to compile the metagenomic data. We then used MEGA-HIT with default assembly parameters, using a k-mer size range of 21, 41, 61, 81, and 99, and a minimum multiplicity of 2 for filtering (k-mer+1)-mers. We also set the low local coverage criterion to 0.2 and the trimming level to 2. For every iteration, the maximum tip length was set to double the size of the k-mer.

We applied the precise statistical technique Bracken to assess species abundance in the metagenomic dataset. Bracken and Kraken both gave accurate estimates of abundance at the species and genus levels. The CARD database server was used to find antibiotic resistance genes (ARGs). The metagenomic sequencing data from the assembly FASTA files were used as input for the ARG prediction. Phyloseq was employed for data analysis and visualization [156]

3.6 Statistical Analysis

Data received from all methods were analyzed using Graph Pad Prism 6.0 version and were then presented in the form of mean ± standard error of the mean (SEM). One-way ANOVA followed by Tukey's multiple comparisons test was employed to check and analyze the statistical significance. Further, a p-value of less than 0.05 $p<0.05$) was considered statistically significant for all the results [157].

3.7 Air Quality Index and Climate Data Across Cities

Smog sampling was done for two consecutive years in 2022 and 2023 in three cities of Pakistan (Islamabad, Lahore, and okara). The PM2.5 was collected in November and December months of each year. PM2.5 was collected on quartz microfiber filters using an air sampler. At all locations, there was an average of one 24-hour PM2.5 sample taken every day. Before further processing, all the filter samples will be kept in storage at -20 °C. Then two different types of DNA was extracted and processed. One is iDNA & eDNA (Extracellular DNA). The figures 3.12, 3.13, 3.14 showing the air monitoring system, Quartz microfiber filter and site of air sample collection respectively.

FIGURE 3.12: Air monitoring system for collecting smog air samples

FIGURE 3.13: Particulate collection by quartz microfiber filters

FIGURE 3.14: A picture shows the site of air sample Installation in Islamabad

3.8 Internal DNA Analysis of Antibiotic Resistance Genes

Internal DNA Extraction: Internal DNA was isolated, employing CTAB method. The extracted DNA was subsequently analyzed on a 1% agarose gel to evaluate its integrity, purity, and concentration as shown in figure 3.15.

Polymerase Chain Reaction (PCR) Amplification: Internal DNA was amplified by PCR using region-specific primers with barcodes. Takara Premier Taq Version 2.0 (Takara Bio, Dalian, China) was used as the DNA polymerase. Takara Premier Taq Version 2.0 is a thermostable DNA polymerase that amplifies complicated and GC-rich templates with great precision and efficiency.

Primer Corresponding Region: Primer corresponding regions include the 16S V4 primers (515f and 806r) that identify bacterial diversity,18S V4 primers (528f and 706r) to identify the diversity of eukaryotes & ITS1 primers (its5-1737f and its2-2043r) to identify the diversity of fungi

PCR Reaction System

TABLE 3.1: Reagent name and dosage

S.No	**Reagent Name**	**Dosage**
1	Primer-R	10 mM
2	Primer-F	10 mM
3	Nuclease-free water	Add to 50μL
4	DNA	60 ng
5	2x Premix Taq	25μL

PCR Reaction Conditions: Following a 5-minute initial denaturation at 94°C, 30 cycles of 9°C for 30 seconds, 52°C for 30 seconds, and 72°C for 30 seconds were carried out for the PCR reaction cycles. Then a 10-minute extension step at 72°C, followed by a hold at 4°C. The Biorad S1000 (CA) PCR apparatus was used to combine the PCR results after each sample was run three times. The Bio-Rad S1000 thermal cycler, which provides accurate temperature control and consistent

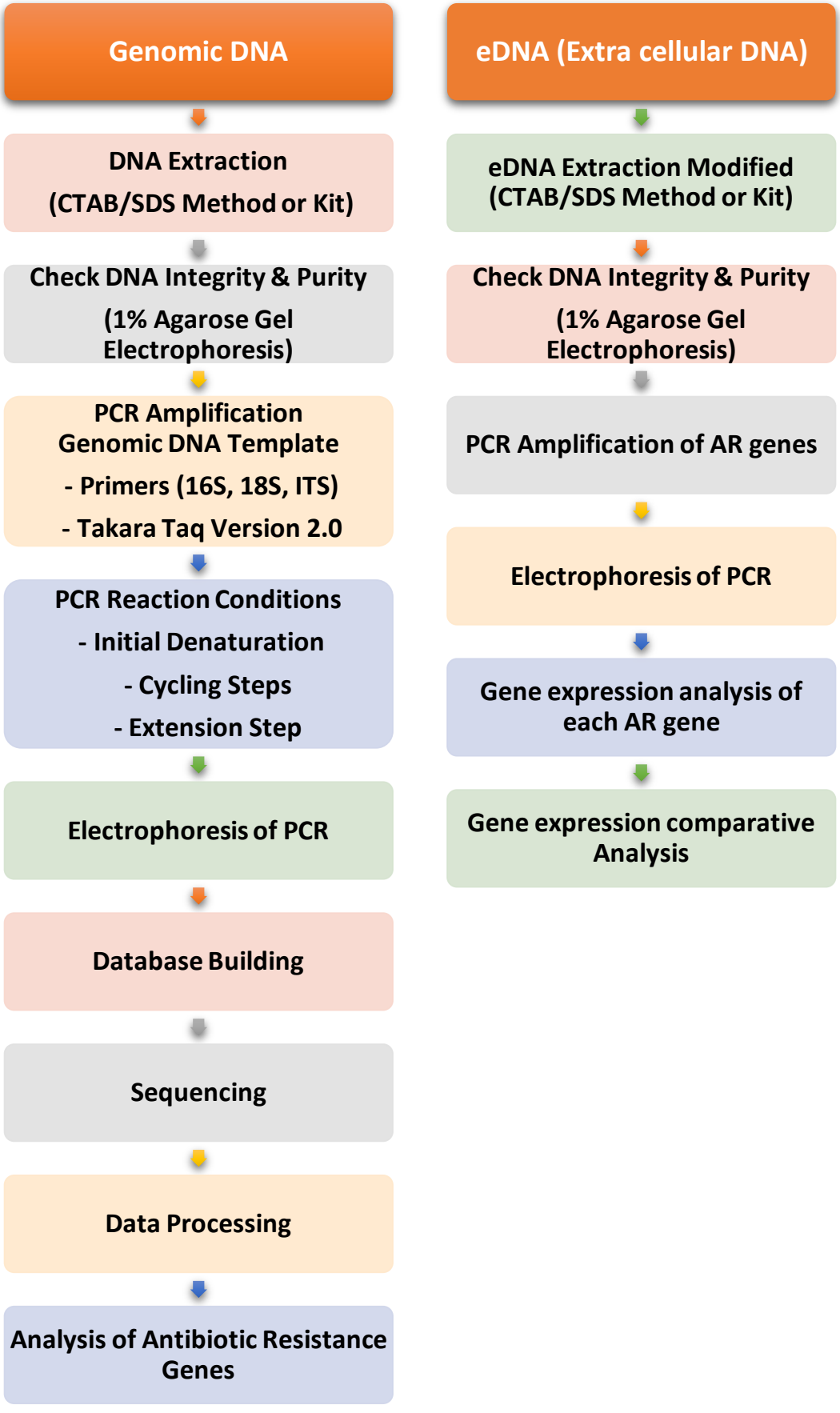

FIGURE 3.15: A flow chart showing extracellular DNA extraction and procedure for analysis

ramping for reliable and reproducible PCR amplification, was used to create the thermal cycling settings [158].

Electrophoresis Detection of PCR Products: One percent agarose-gel electrophoresis was used to measure the PCR product's size and concentration. The principal band's size was within the usual range for the particular PCR product, such as 16S v4,290-310 bp, and 16S v4-v5:400-450 bp, and it was in line with expected values.

The principal band's size was within the usual range for the particular PCR product, such as 16S v4,290-310 bp, and 16S v4-v5:400-450 bp, and it was in line with expected values. Future research can make use of this PCR product.

Pooling and Gel Cutting Purification: The concentration of each PCR product was determined using gene tools analysis software. Based on these concentrations, the volumes of each sample were adjusted to ensure equal amounts of DNA. The adjusted PCR products were then pooled.

Subsequently, the pooled the PCR-products were purified using the EZNA. PCR Gel-extraction Kit. Finally, the target DNA fragment was eluted with TE buffer. Database Building: The database was build up according to the standard process of nebnext ultra-DNA library preparation kit for Illumina.

Database Building: The database was build up according to the standard process of nebnext ultra-DNA library preparation kit for Illumina.

Sequencing: The amplify library was sequenced by PE-250 using Illumina Nova 6000-platform.

Analysis of Antibiotic Resistance Genes from Internal DNA: We used the Comprehensive Antibiotic Resistance Database (CARD) to find and measure antibiotic resistance genes (ARGs) in our samples after removing low-quality sequencing reads. We were able to identify the kinds and relative abundance of ARGs found in the microbial communities under investigation by comparing filtered sequences to CARD's large reference library. The resistome, or group of resistance genes found in a certain environment, is better understood thanks to this analysis.

3.9 Antibiotic Resistance Gene Expression of External DNA

Antibiotic Resistance Gene Expression of External DNA: All the consumables including pipettes, tips, microfuges tubes were autoclaved and dried. The instruments were contaminated free. The Pestle mortar were autoclaved, dried and prechilled at -20°C. The centrifuge were set at 4°C. The ice boxes was prepared because RNA is temperature sensitive [159].

eDNA Extraction: The external DNA that is bound to particulate matter was extracted. Dust particles from the filters were collected and 1 gram PM was added into 9 ml of 0.1m sodium phosphate buffer at pH 8.0 in falcon tube. Now 0.5 g of acid-washed PVP was added to the mixture. The speed of horizontal shaker was adjusted at 150 horizontal shakes per minute and samples were placed on the shaker for 1 minute. This mixing step was repeated three time for 1-minute break at each time. During the break of 1 minute the samples were placed on ice. Now a very small amount of Sodium dodecyl sulfate (SDS) at final concentration, 0.1percent was added, and the samples were shaken again for 10s. Low speed centrifugation at 500 × g for 10 minutes was performed. The temperature of the centrifuge was maintained at 4°C [160]. Following centrifugation, the supernatant was gathered and put into a sterile tube. Following two further rounds of washing, the pellet's supernatants were gathered. After combining the three supernatants, they were centrifuged at a high speed. This time, 10,000g for 20 minutes at 4°C was chosen as the centrifugation speed. To precipitate the DNA, one volume of a cetyltrimethylammonium bromide CTAB solution was added. After 30 minutes of incubation at 65°C, the samples were centrifuged once more at 5,000x g for 10 minutes at 4°C. The pellet was dissolved in TE buffer (10 mM Tris-HCl, 0.1 mM EDTA, 1 M NaCl; pH 8.0) after the supernatant was disposed of. The samples were then incubated on ice for an hour after we added 0.6 volume of cold isopropanol. At 4°C, high speed centrifugation was carried out for 15 minutes at 10,000 × g. The pellet was reconstituted in 10 mM Tris-HCl-0.1 mM EDTA at a final pH of 8.0. Each sample was then given an equal volume of phenol-chloroform-isoamyl alcohol in a 25:24:1 by volume ratio, and a 5-minute

high-speed centrifugation at 10,000 × g was carried out. After separating the supernatant, add an equal volume of chloroform-isoamyl alcohol in a 24:1 by volume ratio, and centrifuge once more for five minutes at 10,000 × g. After the supernatant was separated, 70% ethanol and sodium chloride were added at a final concentration of 0.2 M. Samples were incubated for 1 hour at 20°C [161]. Following the incubation period, samples were centrifuged once more for 15 minutes at 10,000 × g. After discarding the supernatant, the pellet was vacuum-dried and cleaned with ethanol. The particle was stored, and the supernatant was disposed of and allowed to air dry. The DNA pellet was kept at 4°C after being reconstituted in TE Buffer (Tris EDTA) [162].

Agarose Gel-Electrophoresis: One gram of agarose powder was dissolved in 100 milliliters of 1x TAE-buffer to create 1% agarose-gel. To guarantee that the agarose was completely dissolved, the solution was heated. To enable DNA visibility, 8 μL of ethidium bromide was then added to the gel solution. After that, the gel mixture was poured into wells for sample loading in a casting tray fitted with a comb. The gel was moved to an electrophoresis tank with 1X TAE buffer once it had solidified, and the comb was gently taken out. [163]. 2 μL of 6X bromophenol blue loading dye was mixed with a 7 μL aliquot of isolated DNA before loaded onto the gel wells. For 60 minutes, the electrophoresis was run at 75 volts and 500 mA. A UV transilluminator was then used to visualize the gel [164]. The gel electrophoresis results presented below illustrate DNA fragments visualized against a 1 kb DNA ladder as depicted in figure 3.16.

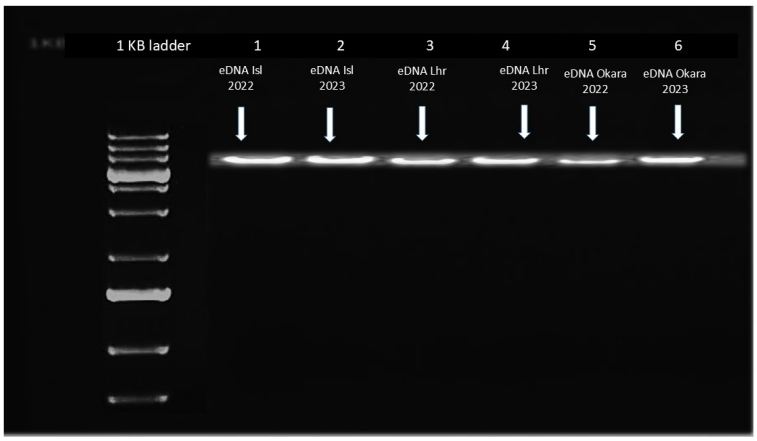

FIGURE 3.16: A pictorial view of agarose gel-electrophoresis: Ladder of 1KB was loaded in first well with DNA samples in next wells

Table 3.2: Primer Details for Antibiotic Resistance and *16S rRNA* Genes

Sr#	**Primer Name**	**Gene Name**	**Forward Seq**	**Reverse Seq**	**Tm**
1	Sulfonamide	*sul1*	CGCACCGGAAACATCGCTGCAC	TGAAGTTCCGCCGCAAGGCT CG	F-67.7°C, R-67.7°C
2	β-Lactamase1	*blaTEM*	TTCCTGTTTTTGCTCACCCAG	CTCAAGGATCTTACCGCTGT TG	F-67.7°C, R-67.7°C
3	β-Lactamase2	*blaCTX-M-32*	CGTCACGCTGTTGTTAGGAA	CGCTCATCAGCACGATAAAG	F-59.4°C, R-62.1°C
4	β-Lactamase3	*blaNDM-1*	TTGGCCTTGCTGTCCTTG	ACACCAGTGACAATATCACC G	F-56.1°C, R-59.4°C
5	Vancomycin-1	*vanA*	AAAAGGCTCTGAAAACGCAGTTAT	CGGCCGTTATCTTGTAAAAA CAT	F-60.1°C, R-59.3°C
6	Vancomycin-3	*vanRA*	CCCTTACTCCCACCGAGTTTT	TTCGTCGCCCCATATCTCAT	F-60.3°C, R-58.4°C
7	Transposase	*tnpA*	AATTGATGCGGACGGCTTAA	TCACCAAACTGTTTATGGAG TCGTT	F-56.4°C, R-62.5°C
8	Integrase	*intI1*	CGAACGAGTGGCGGAGGGTG	TACCCGAGAGCTTGGCACCC A	F-66.6°C, R-65.2°C
9	*blaTEM_F*	*blaTEM_F*	ATCTCAACAGCGGTAAGATC	GAGAATAGTGTATGCGGCG	F-56.4°C, R-57.3°C
10	*16S rRNA*	*16S rRNA*	GGGTTGCGCTCGTTGC	ATGGYTGTCGTCAGCTCGTG	F-55.8°C, R-61.5°C

Polymerase Chain Reaction (PCR): Polymerase Chain Reaction (PCR) is a laboratory technique used to multiply specific segments of DNA [165].
Following chemicals were used and in table all used and concentrations are mentioned below in table 3.3.

TABLE 3.3: Chemicals used for PCR and concentrations

S.No	PCR Reagents	Stock Conc.	Working Conc.	Vol/Rec	Vol. x (26)
1	taq Polymerase	5U/ μL	1.5 U	0.3 μL	7.8μL
2	PR	10 μM	0.2 μM	0.2 μL	5.2μL
3	PF	10 μM	0.2 μM	0.2 μL	5.2μL
4	PCR H2O			6.1 μL	158.6μL
5	MgCl2	25 mM	2.5 Mm	1 μL	26μL
6	eDNA template	-	-	1 μL	
7	dNTPs	10 mM	0.2 mM	0.2 μL	5.2μL
8	Buffer	10X	1X	1 μL	26μL
9	**Final Volume**			10 μL	

Where "n" would be any number for which you are making master mix.

Polymerase chain reactions were performed on a Galaxy XP Thermal Cycler (BIOER , PRC) [166]. optimized PCR conditions were shown in table 3.4.

TABLE 3.4: Optimized PCR conditions

#	Steps	Temp	Duration	Sub-cycles	No of PCR cycles
1	**Initial Denaturation**	95 °C	10min		1
2	**PCR Cycles**	95 °C	1min	Denaturation	40
3		—	1min	Primer annealing	
4		72 °C	1min	Primer extension	
5	**Final extension**	72 °C	10min		1
6	**Hold**	C, ∞	Indefinite: ∞		1

Gradient 1:16S Primer: By considering the Tm of primers, the first was run from 55°C to 65°C. In first row 16S amplified product was run with 1:10 dilution of

eDNA, while in Second row amplified products of 16S Primer with eDNA dilution of 1:100 as can be seen in figure 3.17. By analyzing the gel picture, there were desired amplified product, most suitable Tm was selected for qPCR was 58.65°C with 1:10 eDNA dilution [167].

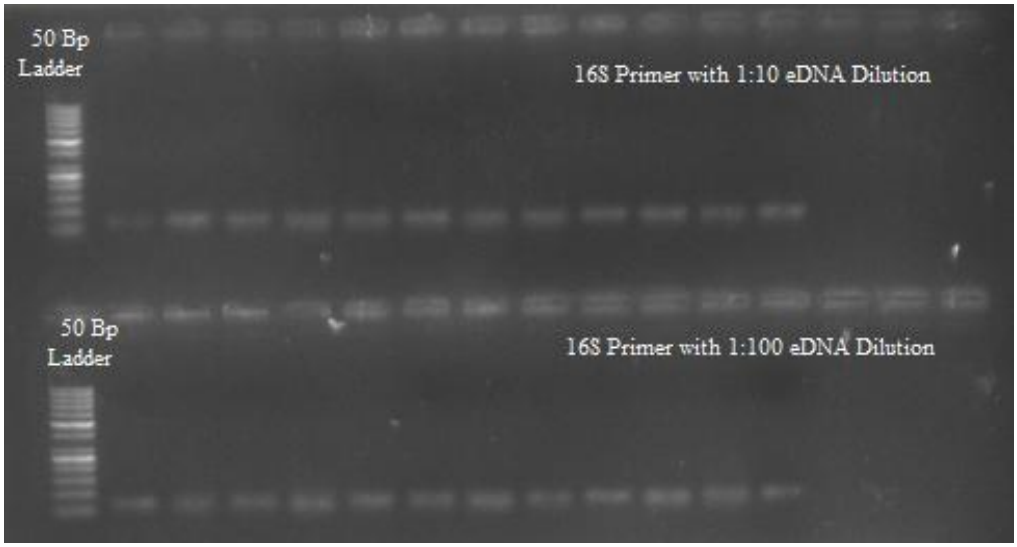

FIGURE 3.17: 16S amplified product run with 1:10 eDNA dilution in the first row and 1:100 eDNA dilution in the second row

Gradient 2: Primer Sulfonamide: The second gradient was conducted from 50°C to 60°C while taking the primer's Tm into account. Primer Sulfonamide amplified products were run in Figure 3.18.

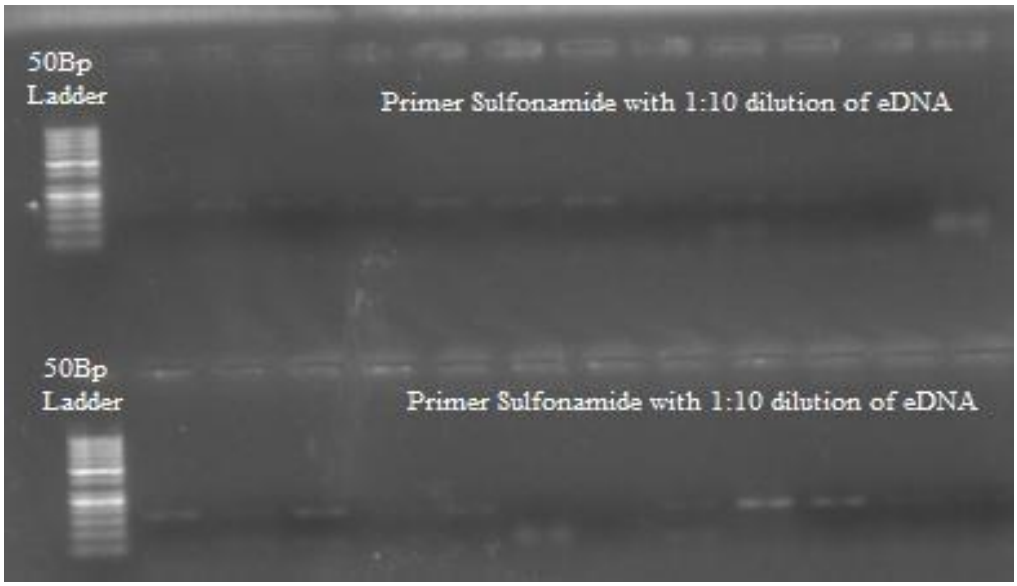

FIGURE 3.18: Primer sulfonamide run with 1:10 eDNA dilution in the first row and 1:10 eDNA dilution in the second row

Gradient 3: β-Lactamase-2 and β-Lactamase-3 Optimization: The gradient was conducted from 55°C to 67°C while taking the primers' Tm into account. Figure 3.19 shows the results of β-Lactamase-2 amplified products. Figure 3.20 shows the amplified products of the primer β-lactamase-3. [169]. The gel image analysis revealed the presence of unused eDNA bands, nonspecific binding, and the intended amplified product. With a 1:100 eDNA dilution, the Tm selected for β-lactamase-2 was 59.3°C, and the Tm selected for β-lactamase-3 for qRT-PCR was 62.4°C.

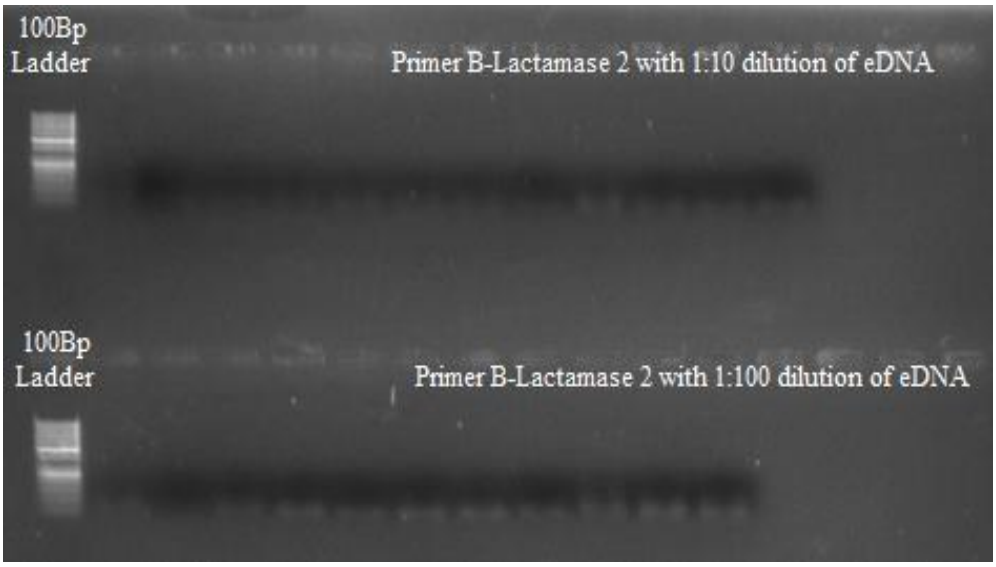

FIGURE 3.19: Primer β-lactamase 2 runs with 1:10 eDNA dilution in the first row and 1:100 eDNA dilution in the second row

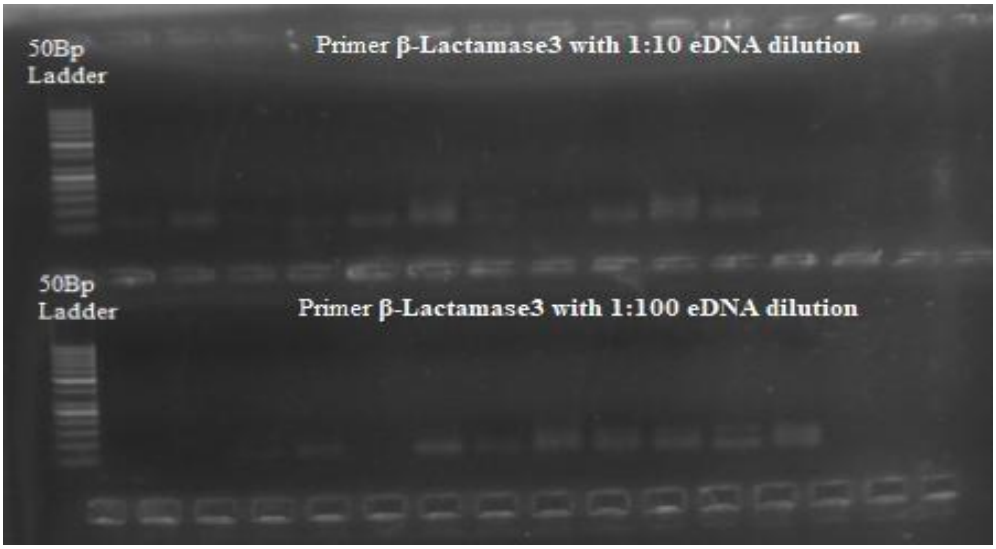

FIGURE 3.20: Primer β-lactamase 3 runs with 1:10 eDNA dilution in the first row and 1:100 eDNA dilution in the second row

Gradient 4: β-Lactamase-1 Optimization: A gradient was conducted from 59°C to 69°C while taking the primer's Tm into account. Figure 3.21 shows the results of β-Lactamase-1 amplified products.

The gel image analysis revealed the presence of unused eDNA bands, nonspecific binding, and the intended amplified product. The temperature at which β-lactamase-1 was selected was 64.3°C and the eDNA dilution was 1:100. [170].

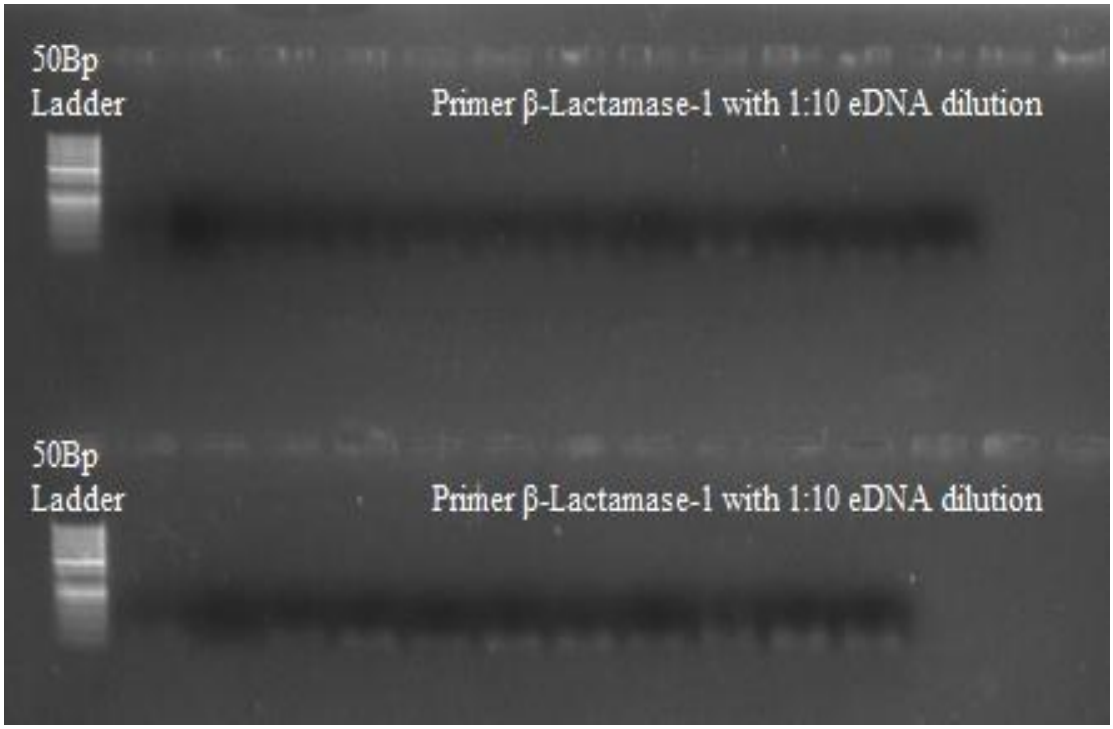

FIGURE 3.21: Primer β-lactamase 1 runs with 1:10 eDNA dilution in the first row and 1:10 eDNA dilution in the second row

Gradient 5: Vancomycin-1 and Vancomycin-3 Optimization.

A gradient was conducted from 56°C to 66°C while taking the primers' Tm into account. Vancomycin-1 amplified products were run in figure 3.22.

Figure 3.23 shows the amplified products of the Vancomycin-3 primer. The gel image analysis revealed the presence of unused eDNA bands, nonspecific binding, and the intended amplified product.

Vancomycin-1 Tm was chosen at 57.3°C with a 1:10 eDNA dilution, whereas Vancomycin-3 Tm was chosen for qRT-PCR at 56.9°C with a 1:10 eDNA dilution [171].

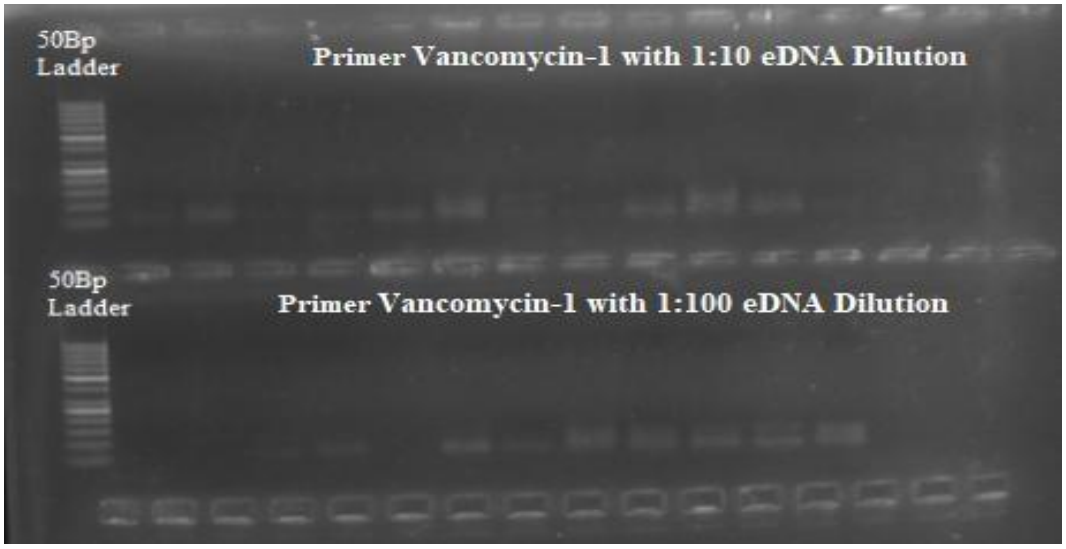

FIGURE 3.22: Primer Vancomycin 1 runs with 1:10 eDNA dilution in the first row and 1:100 eDNA dilution in the second row

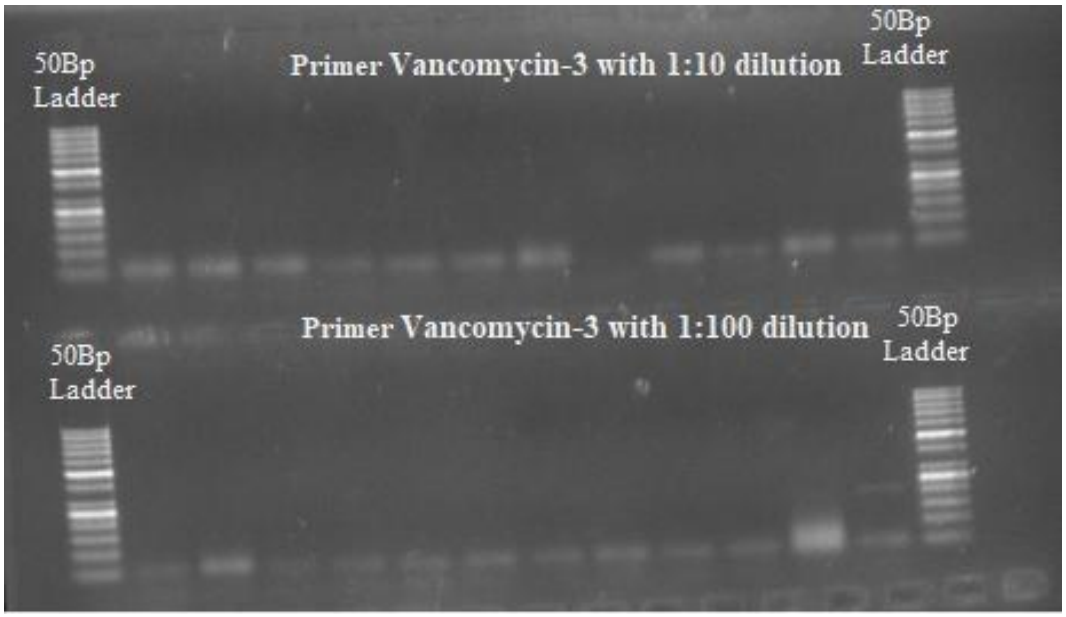

FIGURE 3.23: Primer Vancomycin 3 runs with 1:10 eDNA dilution in the first row and 1:100 eDNA dilution in the second row

Gradient 6: Transposase Optimization.

A gradient was conducted from 53°C to 63°C while taking the primer's Tm into account. Transposase amplified products were run in the first two rows, as seen in figure 3.24. The gel image analysis revealed the presence of unused eDNA bands, nonspecific binding, and the intended amplified product. Transposase was selected at 57.3°C with a 1:100 eDNA dilution. [172].

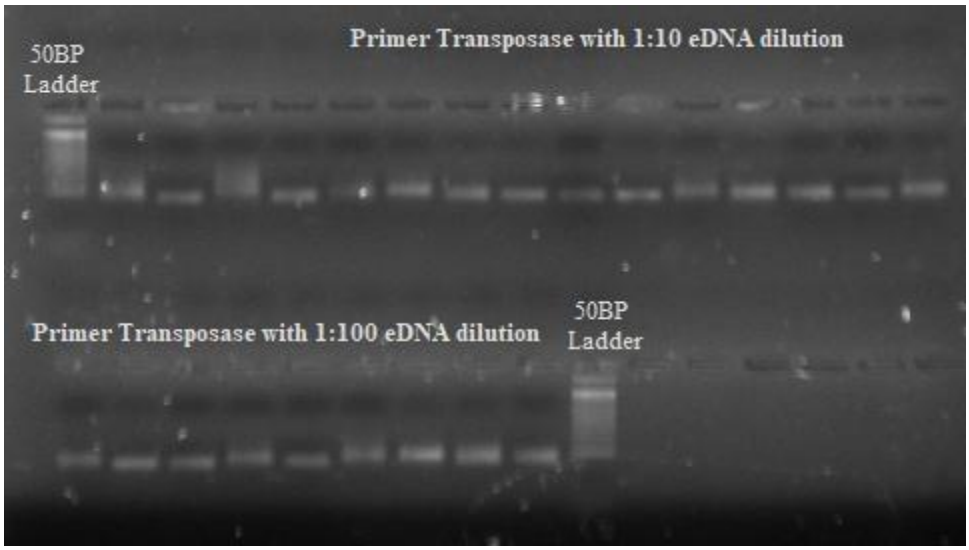

FIGURE 3.24: Primer Transposase runs with 1:10 eDNA dilution in the first row and 1:100 eDNA dilution in the second row

Gradient 7: Integrase Optimization.

A gradient was performed from 58°C to 68°C while taking the primer's Tm into account. Integrase amplified products were run in figure 3.25. The gel image analysis revealed the presence of unused eDNA bands, nonspecific binding, and the intended amplified product. Tm used for Integrase was 1:100 eDNA dilution at 63.3°C. [173].

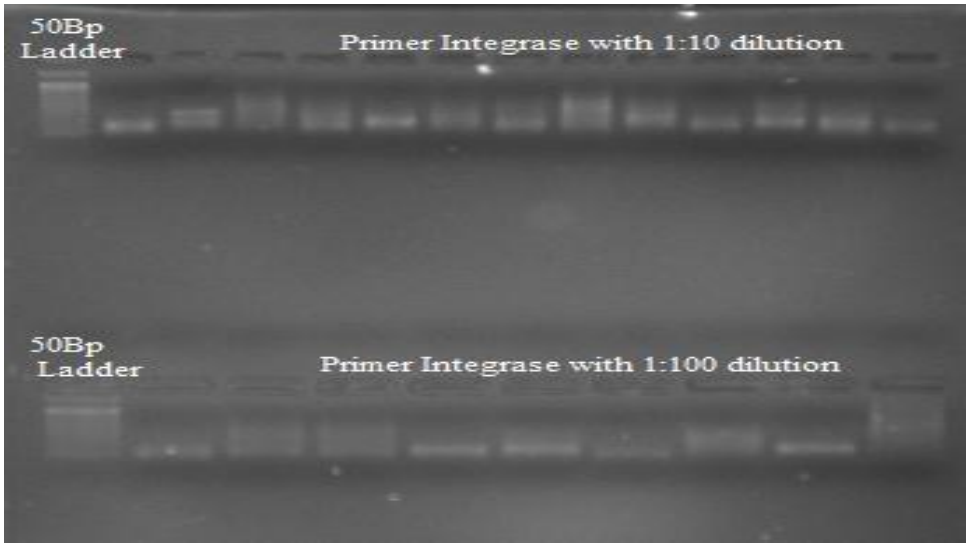

FIGURE 3.25: Primer Integrase runs with 1:10 eDNA dilution in the first row and 1:100 eDNA dilution in the second row

Gradient 8: *blaTEM F* Optimization

A gradient was performed from 55°C to 65°C while taking the primer's Tm into account. Figure 3.26 illustrates the amplified results of *blaTEM F* that were run in the first two rows. The gel image analysis revealed the presence of unused eDNA bands, nonspecific binding, and the intended amplified product. The temperature chosen for *blaTEM* was 62°C, and the eDNA dilution was 1:100 [174].

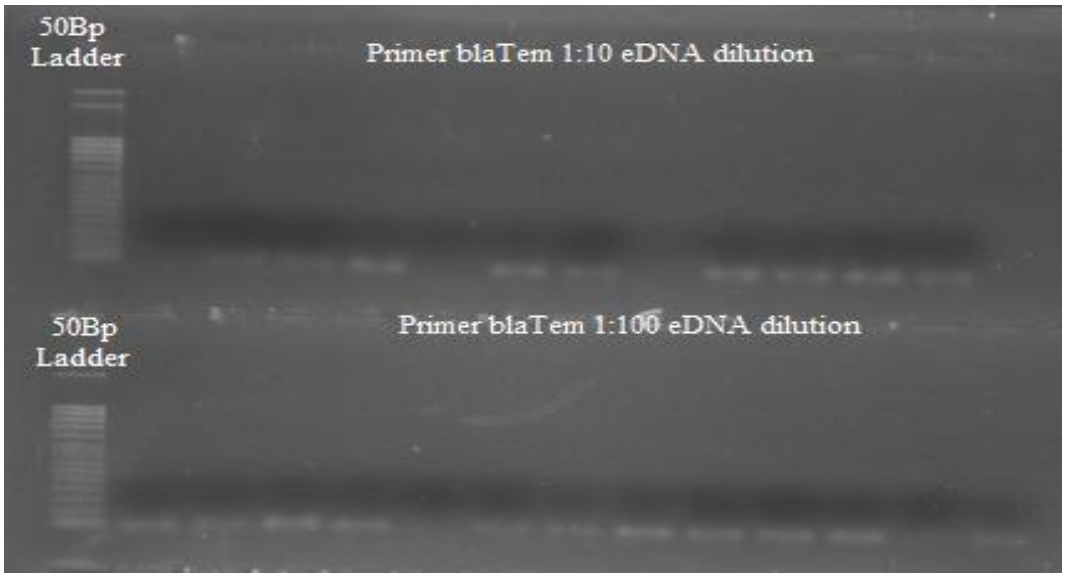

FIGURE 3.26: Primer *blaTEM* runs with 1:10 eDNA dilution in the first row and 1:100 eDNA dilution in the second row

Real-time polymerase chain reaction(RT-PCR) is a laboratory technique that amplifies and simultaneously quantifies specific DNA sequences. It involves a thermal cycler that heats and cools samples, and a fluorescence detection system that measures the amount of fluorescently labeled DNA product produced during every cycle. The following chemicals were used:

All the optimized concentrations are shown in table 3.5 & 3.6.

TABLE 3.5: Chemicals and concentrations for RT-PCR

S.No	**PCR Reagents**	**Stock Conc.**	**Working Conc.**	**Vol/Rec**	**Vol. x (n)**
1	SYBR Green	2X	1X	5 μL	360 μL
2	PR	10 μM	0.2 μM	0.2 μL	14.4 μL
3	PF	10 μM	0.2 μM	0.2 μL	14.4 μL
4	PCR H2O			3.6μL	259.2 μL
5	eDNA template	-	1:10	1 μL	
Final Volume				10 μL	

Where "n" can be any number that you are creating a master mix for.

Real time polymerase chain reactions were performed on Mic PCR (Bio Molecular System) [175].

TABLE 3.6: Optimized PCR conditions

Sr.	Steps	Conditions	Duration	Sub-cycles	PCR cycles
1	**Initial Denaturation**	95 °C	12min		1
2	**PCR Cycles**	95 °C	15 sec	Denaturation	40
3		—	20 Sec	Primer annealing	
4		72 °C	20 Sec	Primer extension	
5	**Hold**	95°C	15 sec		

Representative Graphs of Real Time PCR

Cycling Graph

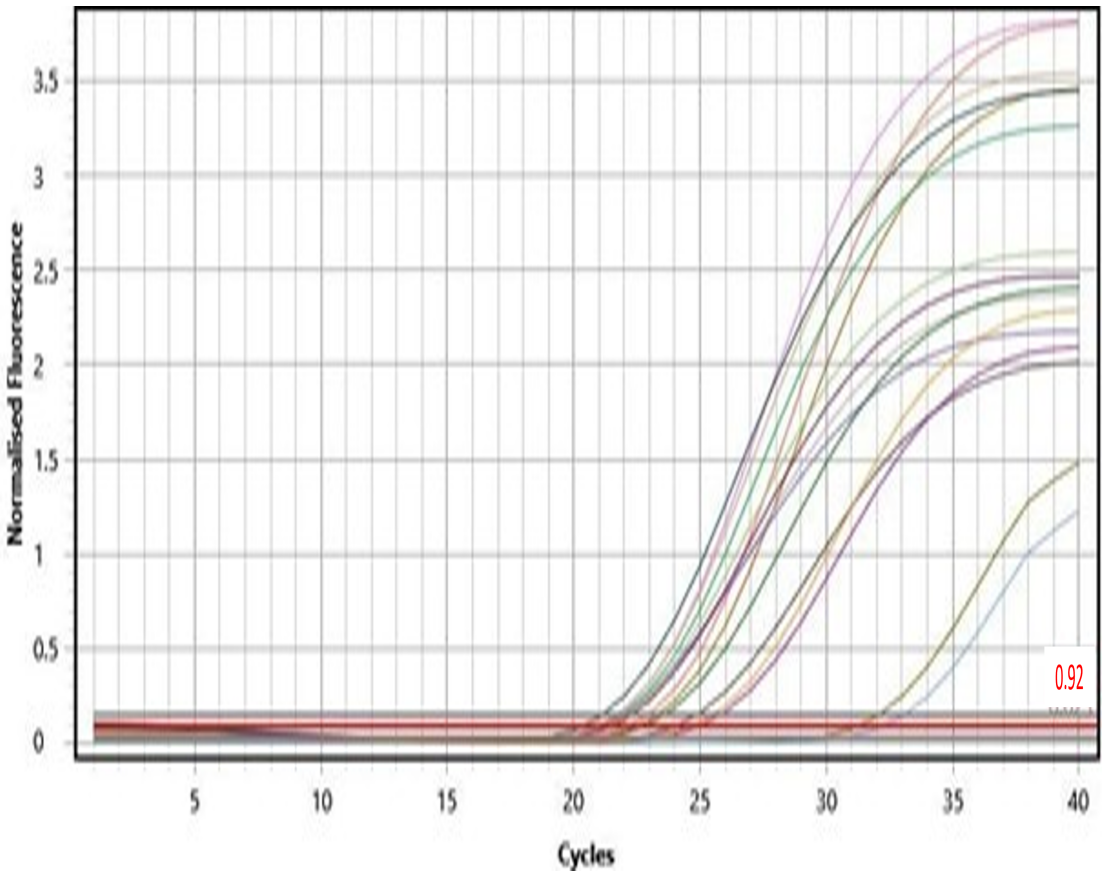

FIGURE 3.27: Image showing the cycling graph

Cycles (Cq) at the X axis and normalized fluorescence on the Y axis are displayed in real-time cycling graphs. Various colored peaks indicate distinct samples versus the threshold as depicted in Figure 3.27.

Melt Curve Graph

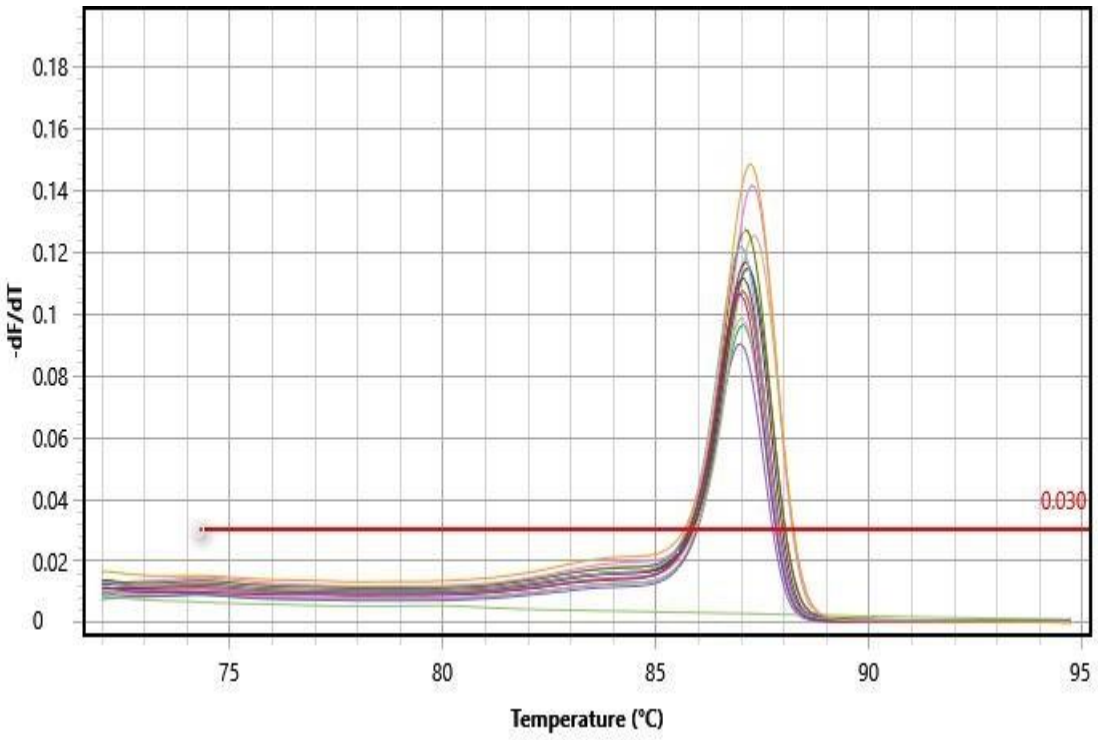

FIGURE 3.28: Image showing the Melt curve graph

Plotting the first derivative curve as F/T (y-axis) against temperature (^{o}C, x-axis) only shows the desired result being amplified. There are two peaks in the temperature range of 75°C to 80°C when dimer formation occurs as depicted in figure 3.28.

Chapter 4

Results

4.1 Results and Findings of Experiments on Animal Model Studies

To assess the effects of smog exposure on locomotor activity of animals (rats), an open field test was employed. This test measures the movement and exploratory behavior of rats within a confined space. The rats were grouped as control and test groups as in figure 4.1. As depicted in Figure 4.2, the results revealed a significant decrease in locomotor activity during the 5-minute duration of the 60 x 60 cm open field test.

FIGURE 4.1: Animal groups for the behavioral studies i.e. Control groups

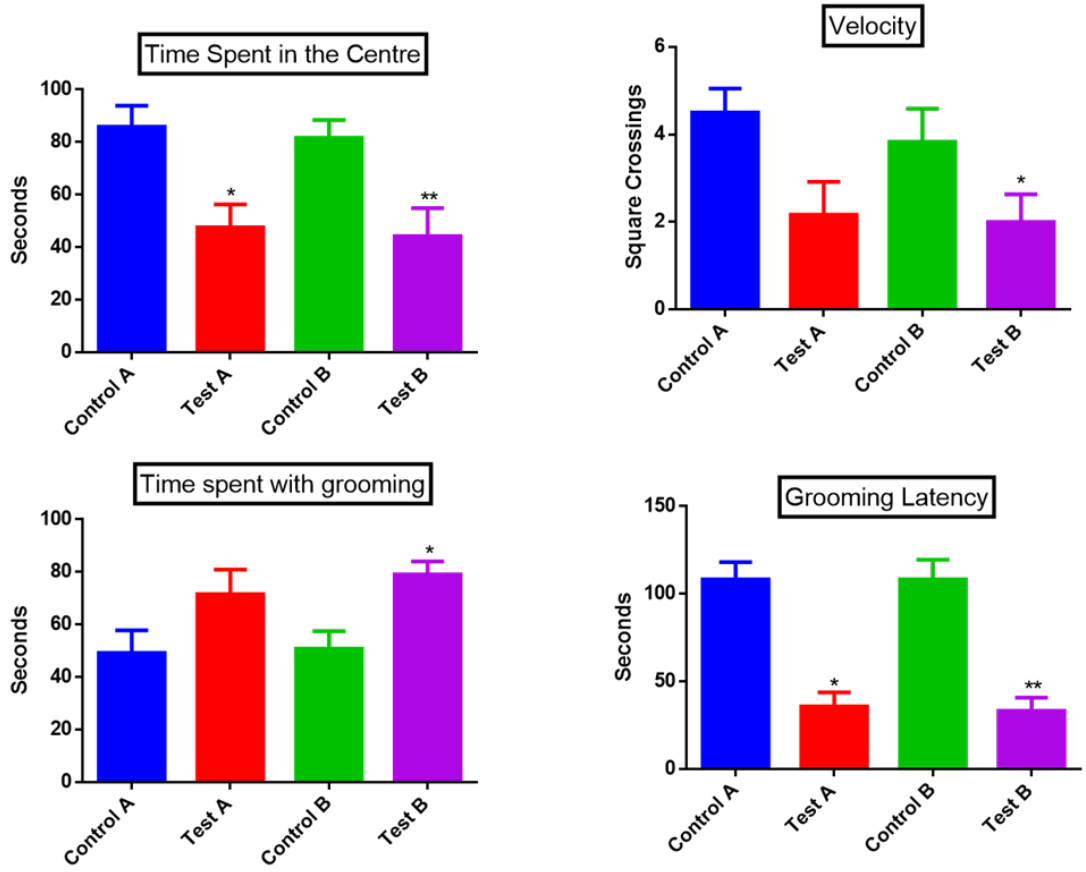

FIGURE 4.2: Effect of smog-laden environment on locomotor activity of rats in the open field test. Data are presented as mean ± SEM (standard error of the mean; n = 6 rats per group). Symbols denote statistical significance: * $p < 0.05$, ** $p < 0.01$ (Control A) Control Islamabad (Test A) Test Islamabad (Control B) Control Lahore (Test B) Test Lahore

4.2 Behavioral Studies on Rat's Model

Behavioral studies show that smog exposed rats spent minimum time as compare to control in the center also decrese velocity and grooming latency and increase the time spent with grooming. These findings suggested that exposure to a smog environment has a statistically significant inhibitory effect on locomotor activity in tested Sprague Dawley rats, as compared to control groups as shown in figure 4.2.

The Y maze test conclude that smog expose rats increase its alternative behavior. The results indicated that exposure to smog may impact the animals' memory functions. Data presented in Figure 4.3, analyzed using mean ± standard error of

the mean (SEM) with a sample size of 6, reveals significant changes in alteration behavior.

These findings suggested that smog exposure may compromise spatial memory or cognitive flexibility in the studied animals.

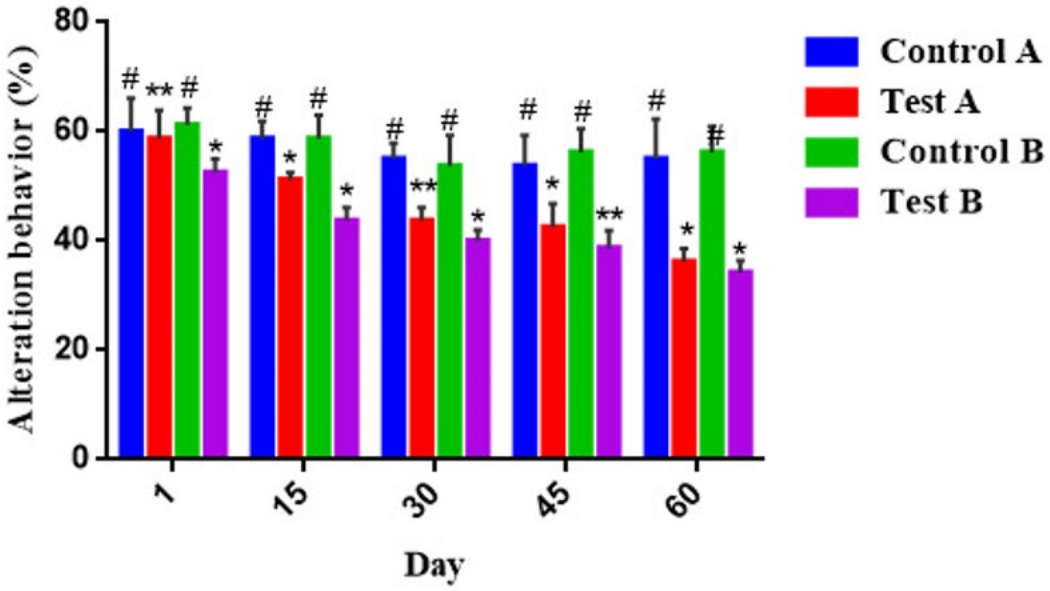

FIGURE 4.3: Effect of smog laden environment on rat's memory in Y-maze test. % alteration in animal behavior is shown. Data were analyzed by Mean ± SEM with (n = 6). Symbols denote statistical significance: * $p < 0.05$, ** $p < 0.01$. (Control A) Control Islamabad (Test A) Test Islamabad (Control B) Control Lahore (Test B) Test Lahore

4.3 Histopathological Findings

After sacrifice animal lung tissues were collected as shown in figure 4.4, the figure 4.5 displayed histological images of animal lung tissue, providing a microscopic view of the tissue's structure and cell types. The labeled groups likely represent different experimental conditions, such as exposure to varying levels of smog.

The labeled groups likely represent different experimental conditions, such as exposure to varying levels of smog. By comparing the control and experimental groups, the figure may reveal potential alterations in lung tissue morphology, offering clues about the effects of smog on lung cell integrity.

FIGURE 4.4: Image shows the collection of lungs tissue from the scarified animal

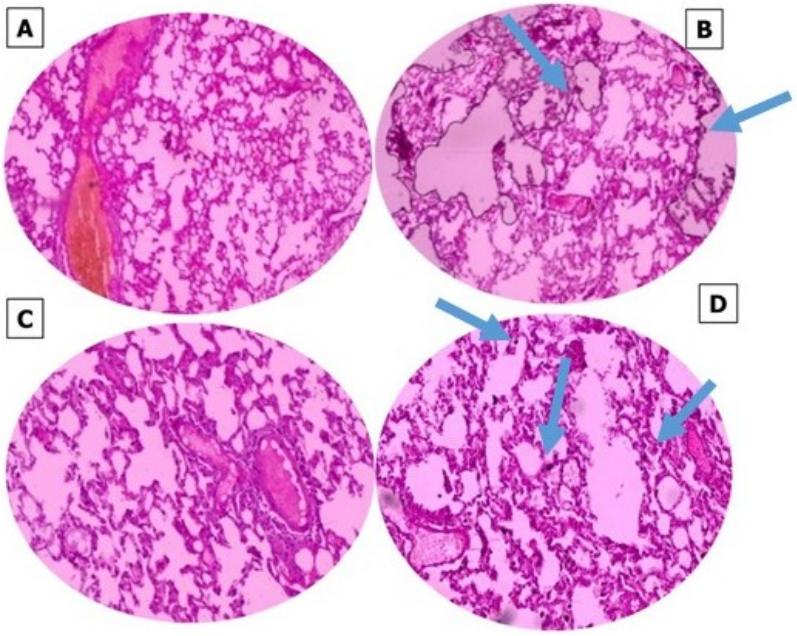

FIGURE 4.5: The histological examination of rat's lungs tissues, Arrows indicting the injury and carbon deposition the alveoli and smog exposed groups. (Control A) Control Islamabad (Test A) Test Islamabad (Control B) Control Lahore (Test B) Test Lahore

4.4 Immunological Assay Results

Data on CD4+ and CD8+ T cell populations in different samples that may have been exposed to pollution are shown in Table 4.1. The number of CD4+ and CD8+ T cells varies throughout samples. These observed alterations in T cell populations would suggest that the animals under study's immune systems may

be impacted by smog exposure. Using flow cytometry, the CD4+ and CD8+ T cell populations in the experimental and control animal groups are quantitatively analyzed in Figures 4.6 and 4.7. Flow cytometry is a method that combines fluorescent markers and lasers to detect and measure cell types according to their surface markers. This approach allowed for detailed analysis of immune cell types, including CD4+ and CD8+ T cells. The comparison of T cell levels between the control and experimental groups provides insights into potential immunological changes induced by the experimental conditions, which may involve exposure to a smog environment.

TABLE 4.1: Percentage of CD4+ and CD8+ cells in control and test animal groups. (n=3) (Mean ± SEM)

Sample	**CD8 Absolute Count**	**CD8 % (Mean ± SEM)**	**CD4 Absolute Count**	**CD4 % (Mean ± SEM)**
C-A Control	1941 ± 10	19.41 ± 0.07	2618 ± 15	26.18 ± 0.09
T-A Test	2234 ± 08	22.34 ± 0.03	3121 ± 10	31.21 ± 0.07
C-B Control	1567 ± 06	15.67 ± 0.06	2510 ± 19	25.10 ± 0.10
T-B Test	2881 ± 11	28.81 ± 0.08	3704 ± 13	37.04 ± 0.05

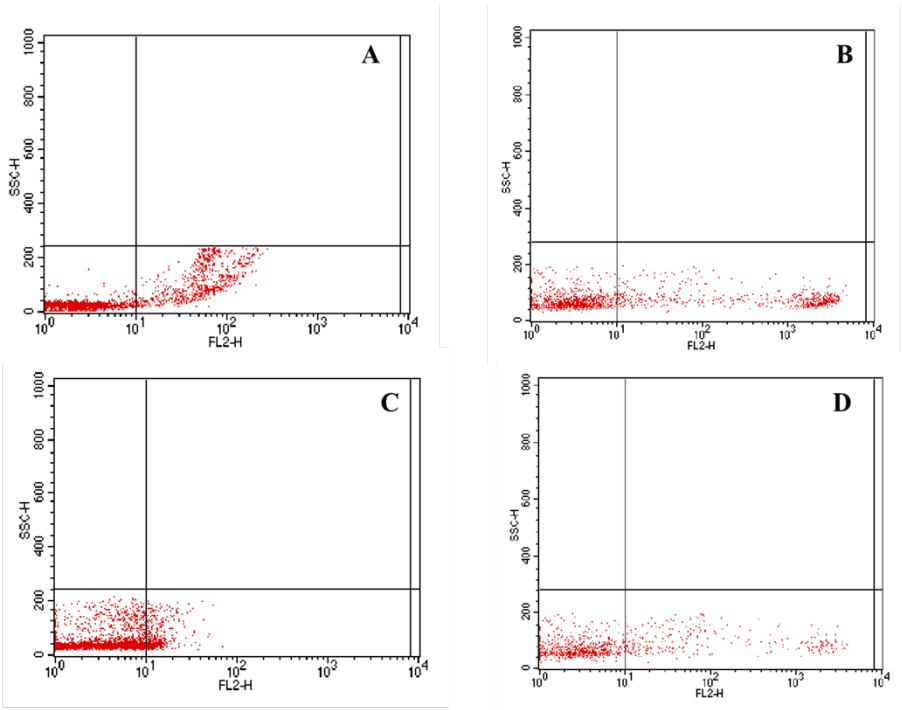

FIGURE 4.6: $CD4^+$ and $CD8^+$ T cell's quantification by flow cytometry in control and test groups of animals. (Control A) Control Islamabad (Test A) Test Islamabad (Control B) Control Lahore (Test B) Test Lahore

The observed variations in T cell populations between control and test groups suggest that exposure to a smog-laden environment may modulate immune function in the animals.

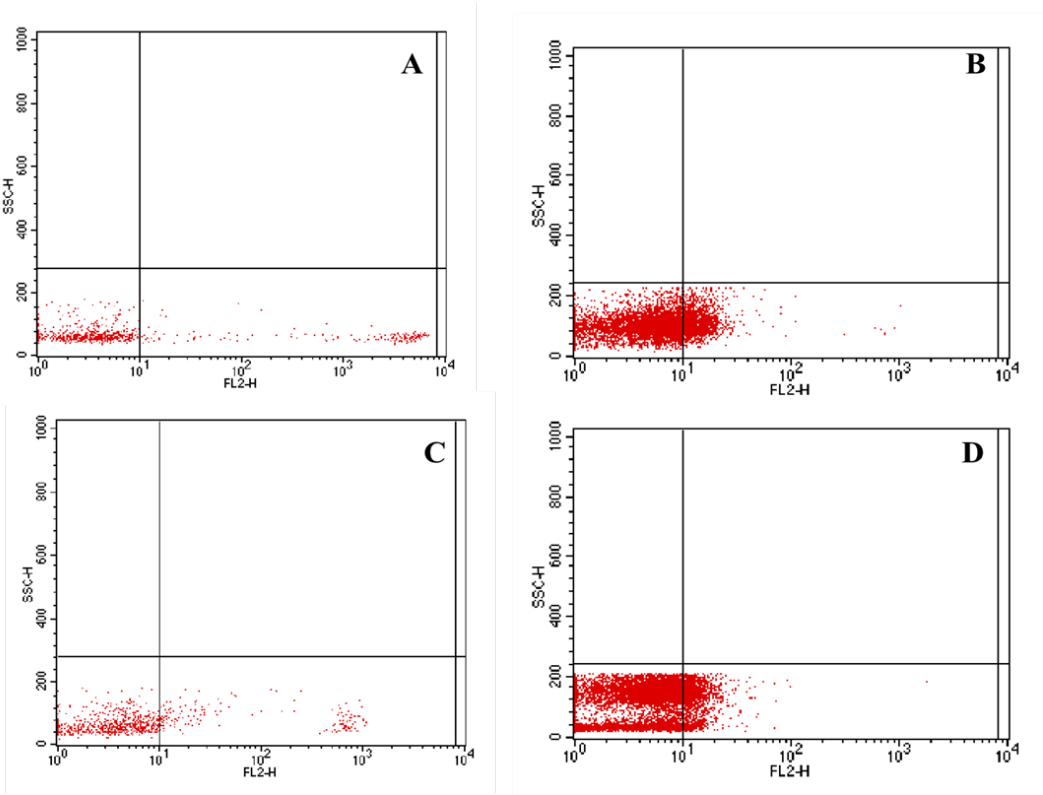

FIGURE 4.7: CD8+ T cells quantification by flow cytometry in control and test groups of animals. (Control A) Control Islamabad (Test A) Test Islamabad (Control B) Control Lahore (Test B) Test Lahore

4.5 Metagenomics' Analysis of Rat Lungs

Rat lung tissues exposed to smog showed a diversified microbial community, according to our metagenomic study using Kraken 2. Notably, the CARD database indicates that the existence of antibiotic-resistant genes, particularly those associated with Mycobacterium and Staphylococcus, raises questions regarding possible health consequences. Figure 4.8 displays the alpha diversity findings from the microbial sequence data of animal lung tissues.

Furthermore, figure 4.9 and figure 4.10 depict the relative abundance of the bacterial genera and bacterial species identified by metagenomic analysis of sequencing of rat's lung tissues.

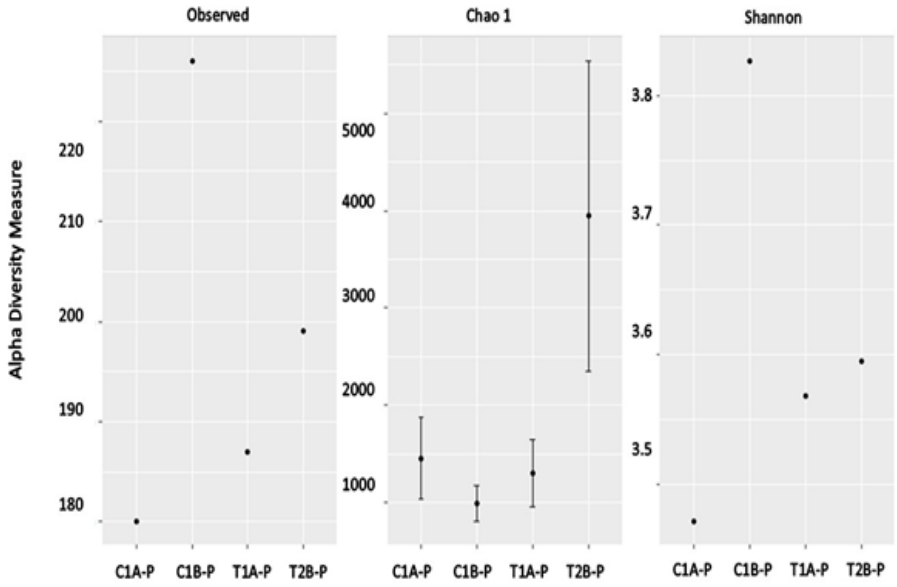

FIGURE 4.8: The image shows the alpha diversity results of the microbial sequence data of animal lung tissues. (C1A-P) Control Islamabad (T1A-P) Test Islamabad (C1A-P) Control Lahore (T1B-P) Test Lahore

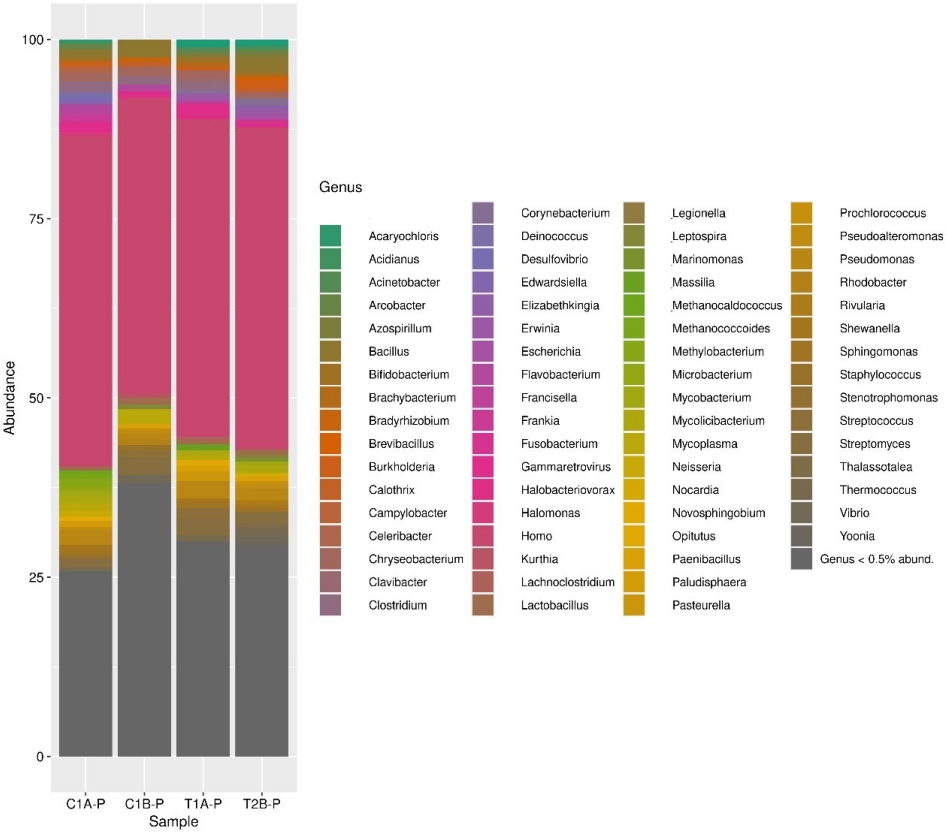

FIGURE 4.9: The (%) relative abundance of the bacterial genera identified by metagenomic analysis of sequencing of rat's lung tissues. (C1A-P) Control Islamabad (T1A-P) Test Islamabad (C1A-P) Control Lahore (T1B-P) Test Lahore

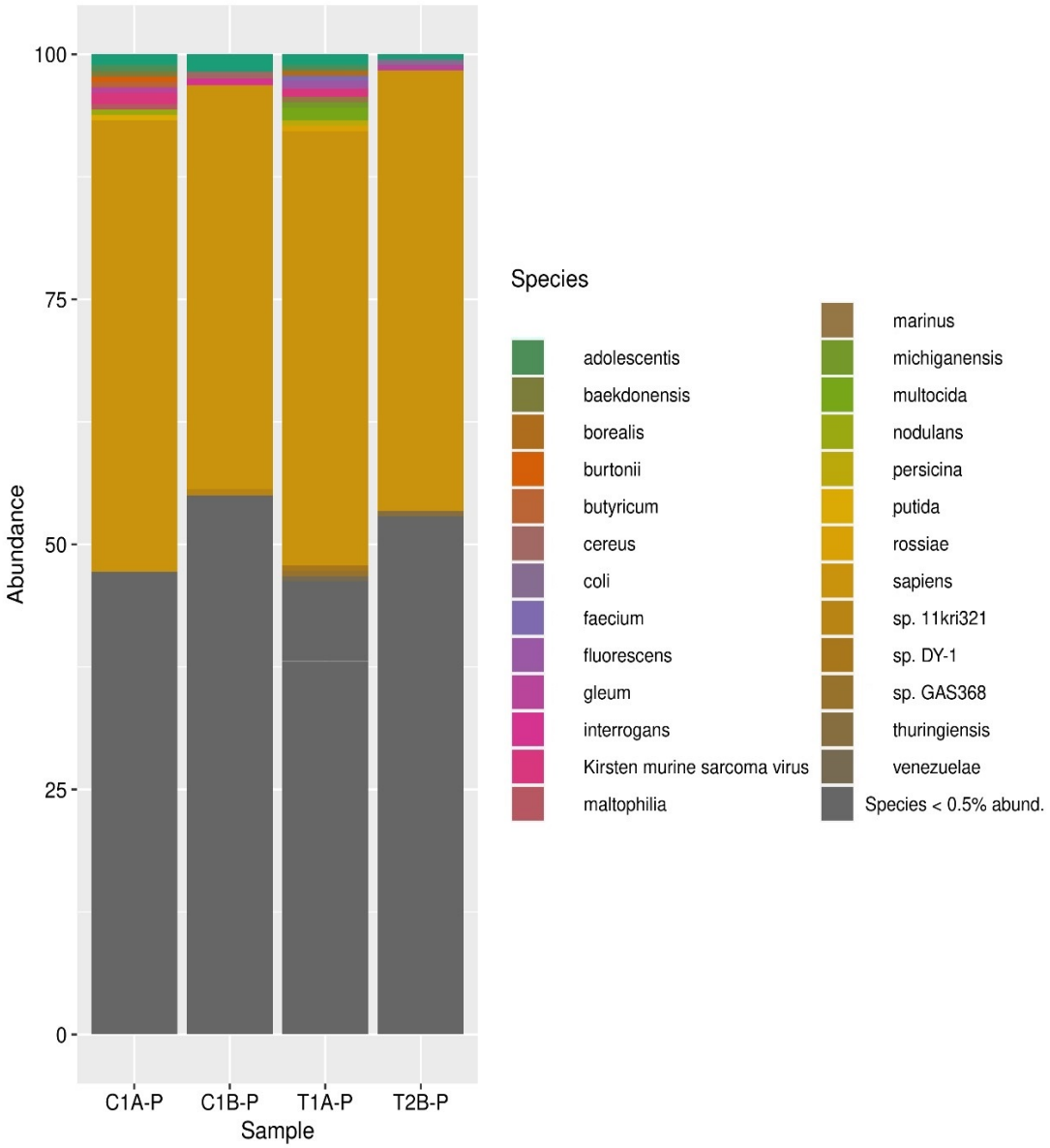

FIGURE 4.10: The (%) Relative abundance of the bacterial species identified by metagenomic analysis of sequencing of rat's lung tissues. (C1A-P) Control Islamabad (T1A-P) Test Islamabad (C1A-P) Control Lahore (T1B-P) Test Lahore

The microbial diversity and composition in rat lung tissues across control and treatment groups are shown in association in Figures 4.8, 4.9 and 4.10. Reduced biodiversity and uniformity of species in treatment groups are indicated by alpha diversity analysis (Figure 4.8), which points to microbial imbalance. While species-level analysis (Figure 4.10) shows decreased diversity and an increase in unidentified or low-abundance species, genus-level data (Figure 4.9) shows significant changes in dominant bacterial genera in treated samples. These findings

collectively imply that exposure to the environment may disturb the lung microbiome, resulting in a change in microbial composition and an imbalance in diversity.

4.5.1 Antibiotic Resistance Genes and Common Pathways in Islamabad Exposed Rats

The ARGs in the lung samples of test and control rats from Islamabad are displayed in Table 4.2. *BRO-1*, which is found in Test Sample 1, Control Sample 1, and Control Sample 2, indicates that beta-lactam antibiotic resistance is widespread. *OXA-168*, which is present in both Test Sample 1 and Control Sample 1, points to a common mechanism of resistance to beta-lactam antibiotics.

TABLE 4.2: ARG, s in Control and Test Rats lungs Samples of Islamabad.

S.No	T1A	T2A	C1A	C2A
1	*vanT* gene in *vanN* cluster		*sgm*	*vatB*
2	*vanP*		*mphJ*	*opcM*
3	*Staphylococcus aureus mupA* conferring resistance to mupirocin	*dfrA3b*	*Staphylococcus aureus mupA* conferring resistance to mupirocin	*bacA*
4	*qacB*	*vanXY* gene in *vanG* cluster	*mexY*	*norC*
5	*poxtA*	*tet(X4)*	*dfrA23*	*mphM*
6	*pmrA*	*tet(36)*	*cmeB*	*mgrA*
7	*OXA-737*	*catIII*	*Salmonella enterica cmlA*	*SHD-1*
8	*OXA-648*	*QnrB41*	*OXA-794*	*PDC-79*
9	*OXA-534*	*QepA1*	*OXA-766*	*OXA-92*
10	*OXA-168*	*PSV-1*	*OXA-512*	*OXA-258*
11	*OXA-134*	*PEDO-3*	*OXA-18*	*MCR-1.29*
12	*OKP-D-1*	*OXY-2-8*	*MYX-1*	*LRA-10*
13	*MexC*	*MexF*	*MCR-3.9*	*IMP-37*

continued on next page

S.No	T1A	T2A	C1A	C2A
14	*MCR-3.15*	*LUS-1*	*L1 beta-lactamase*	*GPC-1*
15	*MCR-3.11*	*FosB6*	*Erm(41)*	*FLC-1*
16	*Klebsiella pneumoniae KpnF*	*EAM-1*	*ESP-1*	*Erm(49)*
17	*FAR-1*	*CTX-M-230*	*CRP(cAMP receptor protein)*	*Erm(43)*
18	*CGB-1*	*CME-1*	*CME-2*	*Clostridium butyricum catB*
19	*BRO-1*	*Acinetobacter baumannii AbaF*	*APH(9)-Ia*	*BRO-1*
20	*abcA*	*tet(32)*	*aadA4*	*bcrA*
21	*AAC(3)-Iva*	*AAC(6')-Ir*	*AAC(6')-Ib-cr9*	*APH(3')-IIIa*
22			*vanR* gene in *vanO* cluster	
23			*vanX* gene in *vanO* cluster	
24			*vgaB*	

Table 4.3 lists possible population-wide resistance mechanisms that are backed by shared resistance genes. However, the existence of distinct resistance genes in every sample points to a variety of resistance tactics, which may be impacted by different bacterial populations or environmental exposures in rat lungs.

TABLE 4.3: Shared Resistance Genes in Control and test samples of Islamabad

S.No	Similar Resistance Genes	T1A	T2A	C1A	C2A
1	*vanXY* gene in *vanG* cluster		✓		
2	*tet(X4)*		✓		
3	*tet(36)*		✓		
4	*tet(32)*		✓		
5	*Staphylococcus aureus mupA* conferring resistance to mupirocin	✓		✓	
6	*OXA-92*				✓

continued on next page

S.No	Similar Resistance Genes	T1A	T2A	C1A	C2A
7	*OXA-258*				✓
8	*OXA-168*	✓		✓	
9	*MexF*		✓		
10	*MCR-3.15*	✓			
11	*MCR-3.11*	✓			
12	*FosB6*		✓		
13	*Erm(49)*				✓
14	*Erm(43)*				✓
15	*dfrA3b*		✓		
16	*CTX-M-230*		✓		
17	*BRO-1*	✓		✓	✓
18	*APH(3')-IIIa*				✓
19	*AAC(6')-Ib-cr9*			✓	

4.5.2 Antibiotic Resistance and Shared Genes in Lahore Expose Rats

Antibiotic resistance genes (ARGs) from Lahore samples are compared in Tables 4.4 and 4.5 across several datasets (C1B, C2B, T1B, and T2B). This comparison aids in locating possible similarities in the mechanisms underlying antibiotic resistance. Only dataset C1B contained the gene *OXA-168*, indicating that this sample has a distinct resistance profile. On the other hand, datasets C1B, C2B, and T1B all contained the gene *OpmB*, suggesting that these samples shared a resistance mechanism.

Table 4.4: ARG, s in Control and Test Rats lung Samples of Lahore

S.No	T1B	T2B	C1B	C2B
1	*AAC(6')-Ib8*	*AER-1*	*ECM-1*	*AAC(3)-VIa*
2	*AAC(6')-Ij*	*CTX-M-214*	*LRA-7*	*MCR-3.14*
3	*Acinetobacter baumannii AbaQ*	*EAM-1*	*MIR-19*	*OXA-18*
4	*Enterobacter cloacae acrA*	*EC-8*	*MexB*	*OXA-397*
5	*MexD*	*ECV-1*	*MexH*	*OXA-942*
6	*OXA-294*	*MAB*	*MexK*	*OXY-1-3*

continued on next page

S.No	T1B	T2B	C1B	C2B
7	*OprA*	*MexF*	*OXA-168*	*OpmB*
8	*PEDO-2*	*OXA-192*	*OmpA*	*SHV-167*
9	*evgS*	*OXA-732*	*OpmB*	*VAM-1*
10	*mdtO*	*facT*	*RSA2-1*	*mdtM*
11	*mphL*	*tet(38)*	*aacA43*	*tet(T)*
12	*myrA*	*vanD*	*cmlA9*	*vanF*
13	*tet(O/M/O)*		*dfr22*	
14	*tet(O/W)*		*lnuF*	
15			*mecD*	
16			*tcr3*	
17			*vanK* gene in *vanI* cluster	

TABLE 4.5: Shared Resistance Genes in Control and test samples of Lahore

S.No	Similar Genes	T1B	T2B	C1B	C2B
1	*vanF*		✓		
2	*VAM-1*	✓			
3	*tet(T)*		✓		
4	*OXY-1-3*				✓
5	*OXA-397*				✓
6	*OXA-18*				✓
7	*OXA-168*			✓	
8	*OpmB*	✓		✓	✓
9	*mdtM*		✓		
10	*MCR-3.14*				✓
11	*AAC(3)-VIa*			✓	

4.5.3 Significant Disease Associated with Resistance Genes

Developing focused tactics to counter this escalating threat requires a thorough understanding of both common and distinct antibiotic resistance genes. We can track resistance tendencies and customize treatment plans for particular populations and their distinct resistance profiles by keeping an eye on these genes. This all-encompassing strategy is necessary to address the constantly changing nature of antibiotic resistance and maximize therapeutic results, as shown in Table 4.6.

TABLE 4.6: Significant Disease-Associated Resistance Genes

S.No	Resistance gene associated	Significance
1	*vanXY* gene in *vanG* cluster	Vancomycin resistance gene
2	*tet(32)*, *tet(36)*, *tet(X4)*	Tetracycline resistance
3	*Staphylococcus aureus mupA* conferring resistance to mupirocin	Resistance to mupirocin
4	*OXA-168*, *OXA-134*, *OXA-534*, *OXA-648*, *OXA-737*	Beta-lactamase resistance
5	*MexF*	Resistance gene in Pseudomonas
6	*MCR-3.11*, *MCR-3.14*, *MCR-3.15*	Colistin resistance
7	*FosB6*	Resistance to fosfomycin
8	*CTX-M-230*	beta-lactamase
9	*Acinetobacter baumannii AbaF*n, AbaQ	Acinetobacter infections
10	*AAC(3)-Iva*	Aminoglycoside resistance

4.6 Air Quality Index and Climate Data Across Cities

The provided air quality data as shown in table 4.7 highlights the variations in air pollution levels, as measured by AQI-US and $PM_{2.5}$ concentrations, across three cities—Lahore, Islamabad, and Okara—during specified months from November 2022 to December 2022 and November 2023 to December 2023.

TABLE 4.7: Air Quality Index, $PM_{2.5}$ Concenration and climate data among different cities in 2022 and 2023.

City	**Month / Year**	**AQI-US (Mean ± SD)**	**$PM_{2.5}$ ($\mu g/m^3$) (Mean ± SD)**	**Temp (^oC) (Mean ± SD)**	**Humidity (%) (Mean ± SD)**
Lahore	Nov 2022	189.1 ± 35.4	134.2 ± 25.6	20.0 ± 2.3	62.7 ± 5.1
Lahore	Dec 2022	272.2 ± 40.2	276.1 ± 28.7	12.7 ± 1.1	77.8 ± 6.3
Lahore	Nov 2023	272 ± 38.5	251 ± 22.9	20.0 ± 2.6	68.4 ± 6.1
Lahore	Dec 2023	289.3 ± 42.7	276.6 ± 27.4	17.0 ± 2.7	63.2 ± 5.2
Islamabad	Nov 2022	143.8 ± 18.6	72.9 ± 11.4	16.9 ± 2.3	40.9 ± 6.7
Islamabad	Dec 2022	185.1 ± 22.1	110.9 ± 12.8	13.6 ± 1.9	35.6 ± 7.5

continued on next page

Table 4.7 continued from previous page

City	Month / Year	AQI-US (Mean ± SD)	$PM_{2.5}$ ($\mu g/m^3$) (Mean ± SD)	Temp (^oC) (Mean ± SD)	Humidity (%) (Mean ± SD)
Islamabad	Nov 2023	149.6 ± 19.4	80.0 ± 13.6	17.7 ± 2.5	35.9 ± 5.9
Islamabad	Dec 2023	184.4 ± 20.7	71.5 ± 14.2	18.9 ± 3.1	27.8 ± 6.8
Okara	Nov 2022	191.6 ± 24.6	67.5 ± 18.2	23.2 ± 2.7	29.8 ± 7.3
Okara	Dec 2022	205.6 ± 28.1	97.9 ± 21.5	17.4 ± 3.2	35.1 ± 6.4
Okara	Nov 2023	172.1 ± 26.4	74.3 ± 19.1	31.2 ± 8.1	31.8 ± 8.1
Okara	Dec 2023	214.5 ± 27.8	99.5 ± 23.1	17.8 ± 6.2	34.6 ± 7.9

4.7 Genomic DNA Analysis of Antibiotic Resistance Genes

The following tables represent the findings of AMR genes identified in environmental samples from three cities—Islamabad, Lahore, and Okara—across two years (2022 and 2023). These genes confer resistance to various antibiotics through different mechanisms, including antibiotic efflux, target alteration, and antibiotic inactivation. Below is a detailed discussion based on the gene data from each location and year.

4.7.1 Antibiotic Resistance Profiles in Isla*mab*ad Environmental Isolates (2022-2023)

In Islamabad, a comparative analysis of environmental isolates from 2022 and 2023 reveals consistent resistance patterns, particularly in glycopeptide resistance genes (*vanT*, *vanY*, *vanW*, *vanH*) and efflux pump genes (*adeF*, *qacG*, *qacJ*). These findings indicate an ongoing resistance to fluoroquinolones, tetracyclines, and disinfectants. The presence of *RbpA* continues to highlight rifamycin resistance within the isolates. Overall, the profile has remained largely stable over the two years, suggesting persistence or growing resistance in the environment. This consistency in gene types indicates stable selection pressures that maintain these

resistant bacterial populations, emphasizing a significant concern for public health regarding treatment outcomes for serious bacterial infections in the region (table 4.8 & 4.9).

TABLE 4.8: Resistance gene profiles of Islamabad environmental isolates (2022)

S.No	**Gene Name**	**Gene Cluster/-Family**	**Resistance Mechanism**	**Drug Class**
1	*vanY*	*vanB*, *vanA*, *vanM*, *vanF* clusters	Antibiotic target alteration	Glycopeptide antibiotic
2	*vanW*	*vanI* cluster	Antibiotic target alteration	Glycopeptide antibiotic
3	*vanT*	*vanG* cluster	Antibiotic target alteration	Glycopeptide antibiotic
4	*vanH*	*vanF* cluster	Antibiotic target alteration	Glycopeptide antibiotic
5	*RbpA*	*RbpA* family	Antibiotic target protection	Rifamycin antibiotic
6	*qacJ*	SMR efflux pump	Antibiotic efflux	Disinfecting agents, Antiseptics
7	*qacG*	SMR (Small multidrug resistance) efflux pump	Antibiotic efflux	Disinfecting agents
8	*adeF*	RND (Resistance-nodulation-division) efflux pump	Antibiotic efflux	Fluoroquinolone, Tetracycline antibiotics

TABLE 4.9: Resistance gene profiles of Islamabad environmental isolates (2023)

S.No	**Gene Name**	**Gene Cluster/-Family**	**Resistance Mechanism**	**Drug Class**
1	*vanY*	*vanA* cluster	Antibiotic target alteration	Glycopeptide antibiotic
2	*vanW*	*vanI* cluster	Antibiotic target alteration	Glycopeptide antibiotic
3	*vanT*	*vanG* cluster	Antibiotic target alteration	Glycopeptide antibiotic

continued on next page

S.No	Gene Name	Gene Cluster/-Family	Resistance Mechanism	Drug Class
4	*vanH*	*vanB* cluster	Antibiotic target alteration	Glycopeptide antibiotic
5	*RbpA*	RNA polymerase-binding protein	Antibiotic target protection	Rifamycin antibiotic
6	*qacJ*	Small multidrug resistance (SMR)	Antibiotic efflux	Disinfecting agents
7	*qacG*	Small multidrug resistance (SMR)	Antibiotic efflux	Disinfecting agents
8	*adeF*	Resistance nodulation division	Antibiotic efflux	Fluoroquinolone, tetracycline

4.7.2 Antibiotic Resistance Profiles in Lahore Environmental Isolates (2022-2023)

The Lahore 1 (2022) environmental isolates revealed several key antibiotic resistance genes, including *adeF*, a Resistance-Nodulation-Division (RND) efflux pump that provides resistance to fluoroquinolones and tetracyclines through drug efflux. Additionally, various glycopeptide resistance genes (*vanY*, *vanW*, and *vanH*) from clusters like *vanG*, *vanD*, and *vanM* modify bacterial targets, reducing the efficacy of glycopeptide antibiotics such as vancomycin. The *qacG* and *qacJ* genes, both Small Multidrug Resistance (SMR) efflux pumps, increase resistance to disinfectants and antiseptics by actively removing these agents from bacterial cells. Furthermore, *RbpA*, an RNA polymerase-binding protein, prevents rifamycin binding to its target, and *nimB*, a nitroimidazole reductase, enzymatically inactivates nitroimidazole antibiotics. These mechanisms — including efflux pumps (*adeF*, *qacG*, *qacJ*), target alteration (glycopeptide resistance genes), and antibiotic inactivation (*nimB*) — collectively reduce the effectiveness of critical antibiotics, posing challenges for treating infections caused by resistant organisms.

In 2023, key findings from Lahore's environmental isolates highlight an increased presence of resistance genes such as *adeF* and various glycopeptide resistance genes (*vanT*, *vanY*, *vanH*, *vanW*), which play prominent roles in antibiotic resistance.

Additionally, the detection of *OXA-50* indicates resistance to beta-lactam antibiotics, a primary drug class for bacterial infections, while the newly identified *vanR* gene contributes to glycopeptide resistance through regulatory functions. Compared to 2022, the AMR profile in 2023 shows an increase in the diversity of resistance genes, especially with the emergence of beta-lactam resistance, suggesting an evolving resistance trend (Appendix-A & Appendix-B).

4.7.3 Antibiotic Resistance Profiles in Okara Environmental Isolates (2022-2023)

In Okara, an analysis of environmental isolates from 2022 and 2023 reveals the persistence of significant antimicrobial resistance (AMR) genes. Key genes identified include efflux pumps, such as *adeF* and *rsmA*, which confer resistance to fluoroquinolones, tetracyclines, and other drug classes, as well as glycopeptide resistance genes (*vanH*, *vanY*, *vanT*) present in multiple clusters, indicating resistance to vancomycin. The efflux pumps *qacJ* and *qacG* also persist, conferring resistance to disinfectants and antiseptics, while the gene *poxtA* is associated with resistance through target alteration.

In 2023, the presence of *adeF* and *qacJ*/*qacG* remains strong, demonstrating continuous resistance to fluoroquinolones, tetracyclines, and disinfectants, alongside high resistance levels to glycopeptides from *vanT*, *vanH*, *vanY*, and *vanW*. The persistence of *RbpA* indicates ongoing resistance to rifamycin. Overall, the AMR gene profile in Okara remains stable over the two-year period, highlighting a concerning level of multidrug resistance in the environment and the potential impact on treatment options for bacterial infections (Table 4.10 & 4.11).

TABLE 4.10: Resistance gene profiles of Okara environmental isolates (2022)

#	Gene Name	Gene Cluster/Family	Drug Class	Resistance Mechanism
1	*vanY*	*vanB* cluster	Glycopeptide antibiotic	Antibiotic target alteration

continued on next page

#	Gene Name	Gene Cluster/-Family	Drug Class	Resistance Mechanism
2	*vanT*	*vanG* cluster	Glycopeptide antibiotic	Antibiotic target alteration
3	*vanH*	*vanB* cluster	Glycopeptide antibiotic	Antibiotic target alteration
4	*vanH*	*vanD* cluster	Glycopeptide antibiotic	Antibiotic target alteration
5	*rsmA*	RND	Fluoroquinolone antibiotic, Diaminopyrimidine, Phenicol	Antibiotic efflux
6	*qacJ*	SMR (Small Multidrug Resistance)	Disinfecting agents and antiseptics	Antibiotic efflux
7	*qacG*	SMR	Disinfecting agents and antiseptics	Antibiotic efflux
8	*poxtA*	Miscellaneous	Antibiotic	Antibiotic target alteration
9	*adeF*	RND (Resistance-Nodulation-Cell Division)	Fluoroquinolone antibiotic, Tetracycline	Antibiotic efflux
10	*adeF*	RND	Fluoroquinolone antibiotic, Tetracycline	Antibiotic efflux

TABLE 4.11: Resistance gene profiles of Okara environmental isolates (2023)

#	Gene Name	Gene Cluster/Family	Drug Class	Resistance Mechanism
1	*vanY*	Glycopeptide resistance gene cluster	Glycopeptide	Antibiotic target alteration
2	*vanW*	Glycopeptide resistance gene cluster	Glycopeptide	Antibiotic target alteration
3	*vanT*	Glycopeptide resistance gene cluster, *vanT*	Glycopeptide	Antibiotic target alteration

continued on next page

#	Gene Name	Gene Cluster/-Family	Drug Class	Resistance Mechanism
4	*vanH*	Glycopeptide resistance gene cluster	Glycopeptide	Antibiotic target alteration
5	*RbpA*	*RbpA* bacterial RNA polymerase-binding protein	Rifamycin	Antibiotic target protection
6	*qacJ*	SMR antibiotic efflux pump	Disinfecting agents, Antiseptics	Antibiotic efflux
7	*qacG*	SMR antibiotic efflux pump	Disinfecting agents, Antiseptics	Antibiotic efflux
8	*adeF*	RND antibiotic efflux pump	Fluoroquinolone, Tetracycline	Antibiotic efflux

4.8 Antibiotic Resistance Gene Expression Analysis of External DNA

4.8.1 Sulfonamide Resistance Gene

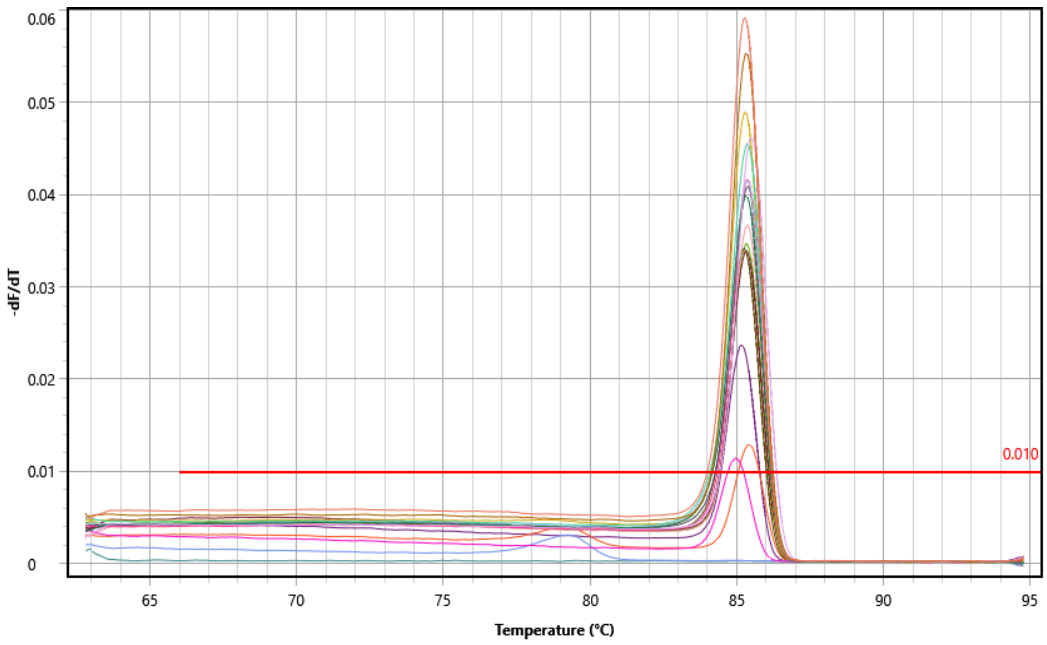

FIGURE 4.11: Real time melt curve graph sulfonamide resistance gene *sul1*

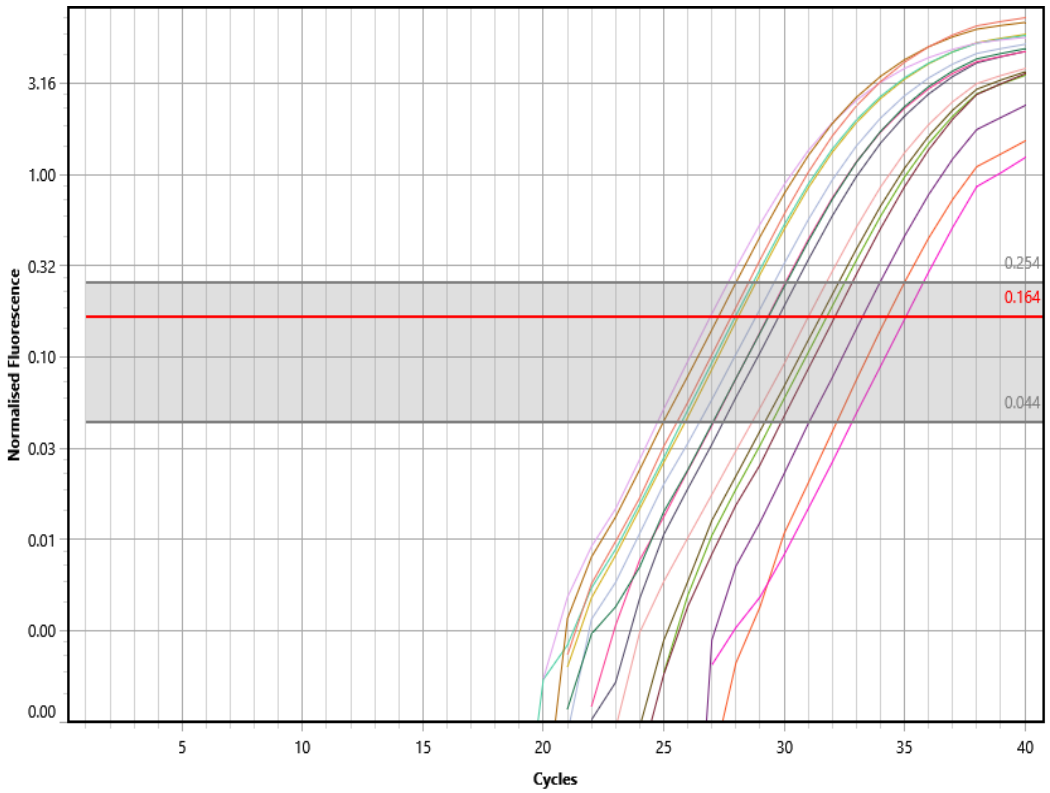

FIGURE 4.12: Real time cycling graph sulfonamide *sul1* resistance gene

The gene expression analysis for the ***sul1*** resistance gene reveals significant findings across the three cities as can be seen in table 4.12.

TABLE 4.12: Gene Expression Analysis Sulfonamide

Sample ID	**16S Cq Values**	**Target Gene Cq Values**	**Delta CT**	**Delta Delta CT**	**Fold Expression**	**Regulation Status**
Isl 2a	21.9739	27.1988	5.2248	-0.0346	1.0243	No significant change
Lahore 1	22.6663	33.8437	11.1774	5.9179	0.0165	Downregulated
Lahore 1a	22.4493	33.1749	10.7256	5.4662	0.0226	Downregulated
Lahore 2	22.2449	31.4193	9.1744	3.9149	0.0663	Downregulated
Lahore 2a	22.3782	30.9785	8.6003	3.3409	0.0987	Downregulated
Okara 1	20.9312	35.0241	14.0929	8.8335	0.0022	Downregulated
Okara 1a	21.9960	32.0652	10.0692	4.8097	0.0357	Downregulated
Okara 2	22.0804	28.0549	5.9745	0.7150	0.6092	Downregulated
Okara 2a	21.5711	29.6931	8.1220	2.8626	0.1375	Downregulated

The sulfonamide resistance gene (*sul1*) expression across Lahore, Islamabad, and Okara demonstrates a clear correlation with $PM_{2.5}$ levels and environmental conditions.

High $PM_{2.5}$ concentrations, particularly in Lahore, correspond to downregulated *sul1* expression, with colder, humid conditions amplifying this effect.

In contrast, Islamabad's moderate pollution and balanced climate resulted in relatively stable gene expression, suggesting that lower $PM_{2.5}$ and stable environmental conditions may help maintain ARG levels.

Okara, with warmer temperatures and lower humidity but moderate $PM_{2.5}$, also showed downregulation but less severe than Lahore's, indicating that both high $PM_{2.5}$ and specific climate factors collectively impact ARG expression stability.

4.8.2 Gene Expression Analysis of β-Lactamase 1

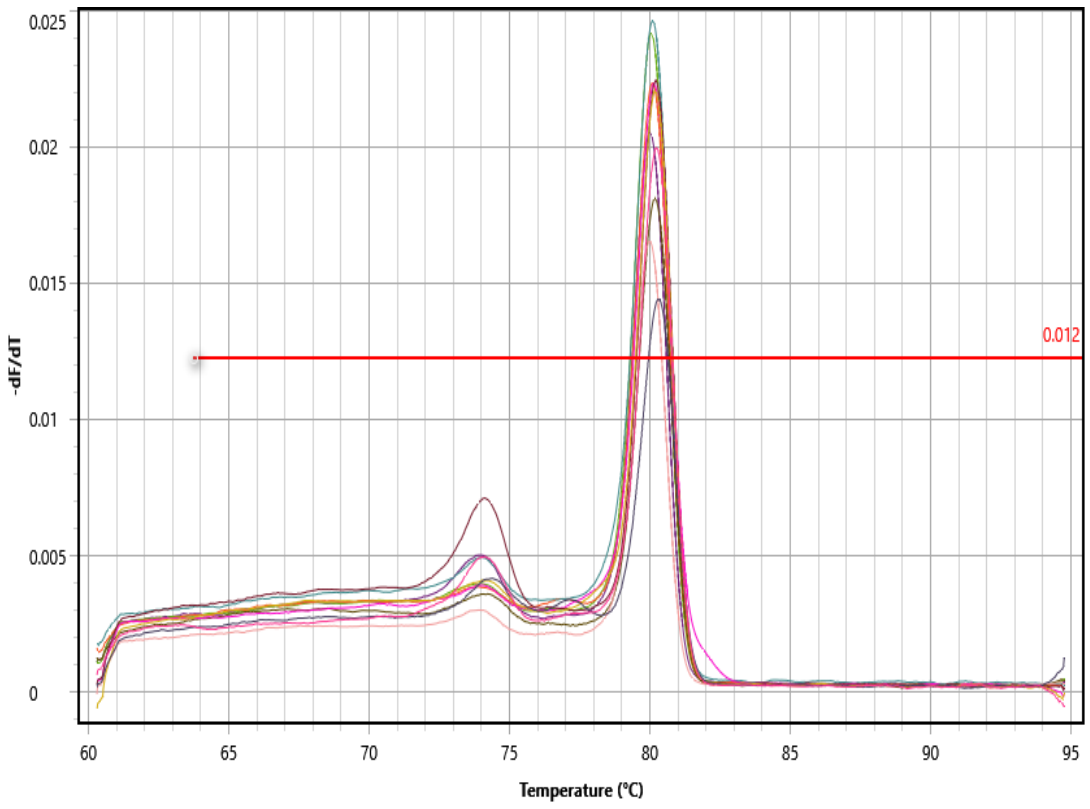

FIGURE 4.13: Real time melt curve graph b-lactamase1 *blaTEM* resistance gene

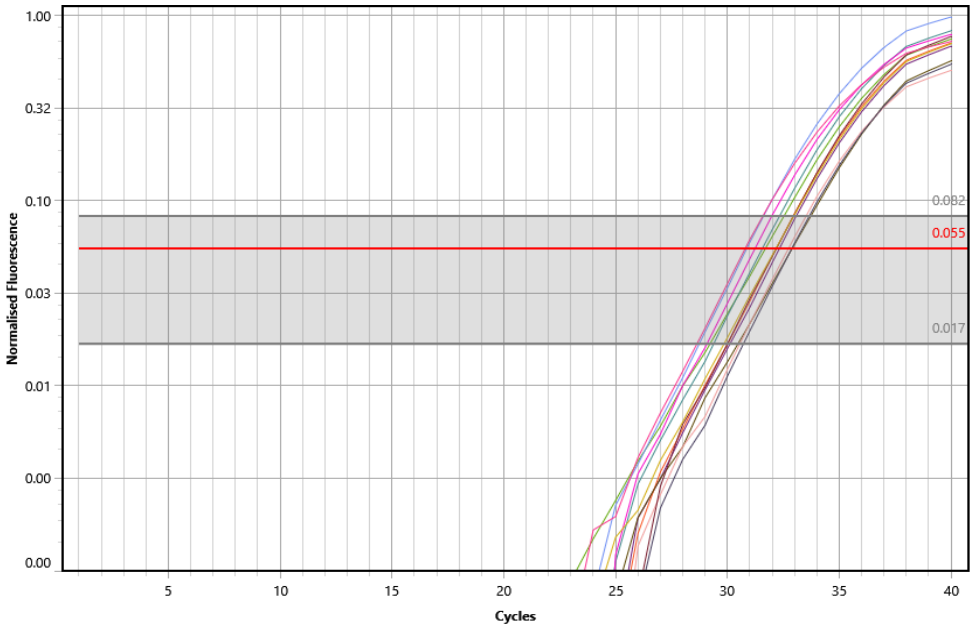

FIGURE 4.14: Real time cycling graph b-lactamase1 *blaTEM* resistance gene

The analysis of *blaTEM* gene expression across the samples shows varying regulation patterns, indicating complex interactions between environmental factors and antibiotic resistance as can be seen in table 4.13.

TABLE 4.13: β-lactamase 1 Analysis of Gene Expression

Sample ID	**ΔCt (Target - Ref)**	**ΔΔCt**	**Fold Expression**	**Regulation Type**
Isl 1	8.0155	-1.6318	**3.0991**	Upregulated
Isl 1a	9.5046	-0.1427	**1.1040**	Slightly Upregulated
Isl 2	10.1947	0.5475	0.6842	Downregulated
Isl 2a	10.8743	1.2270	0.4272	Downregulated
Lahore 1	10.7226	1.0753	0.4746	Downregulated
Lahore 1a	9.9930	0.3457	0.7869	Downregulated
Lahore 2	9.8743	0.2270	0.8544	Downregulated
Lahore 2a	9.6846	0.0373	0.9745	Slightly Downregulated
Okara 1	11.3373	1.6900	0.3099	Strongly Downregulated
Okara 1a	9.6502	0.0029	**0.9980**	No significant change
Okara 2	9.9165	0.2692	0.8298	Downregulated
Okara 2a	11.3004	1.6531	0.3179	Strongly Downregulated

The expression of the *blaTEM* gene reveals distinct regulatory patterns across cities, influenced by environmental conditions. In Islamabad, where $PM_{2.5}$ levels

were relatively moderate, *blaTEM* expression was largely upregulated, especially in sample Isl 1, indicating potential resilience in gene expression under milder pollution.

In Lahore, where $PM_{2.5}$ was highest, most samples showed downregulation, reflecting a suppression effect likely due to intense pollution combined with colder, humid conditions.

Okara showed strong downregulation in samples Okara 1 and Okara 2a, despite moderate $PM_{2.5}$ levels, suggesting that local climate factors (warmer but variable humidity) may also play a role in suppressing *blaTEM* expression.

This analysis underscores how high pollution and specific environmental factors collectively impact ARG regulation.

4.8.3 Gene Expression Analysis of β-Lactamase 2

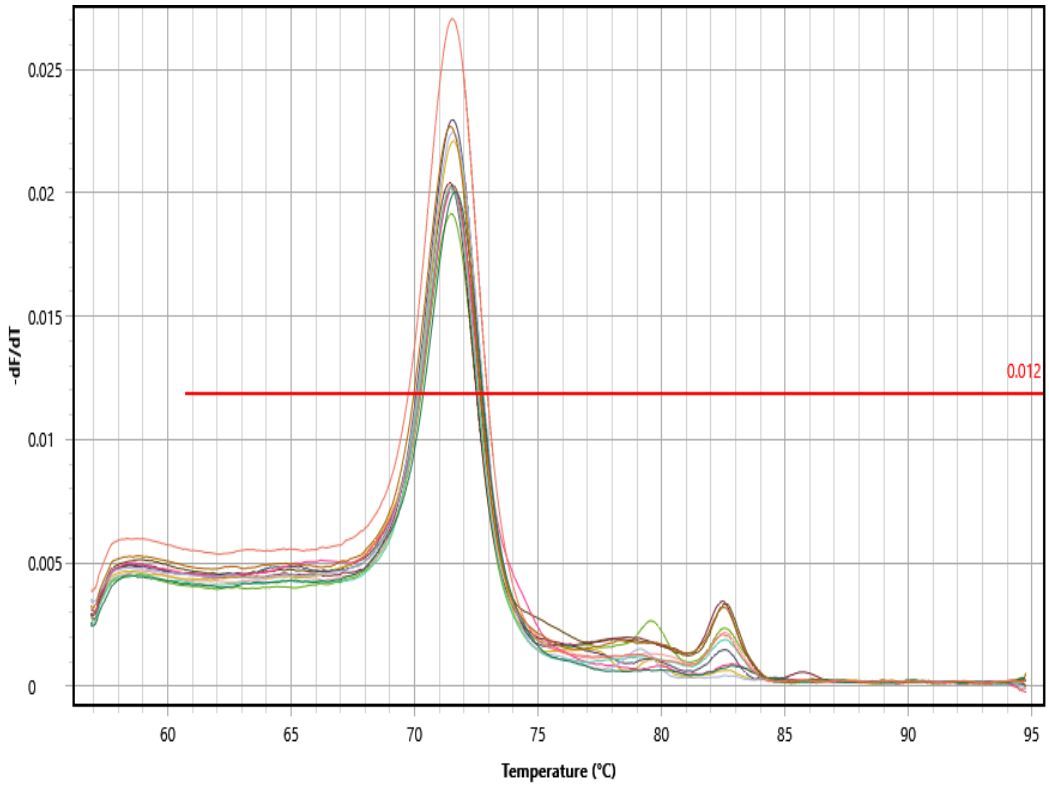

FIGURE 4.15: Real time melt curve graph β-Lactamase 2 *blaCTX-M-32* resistance gene

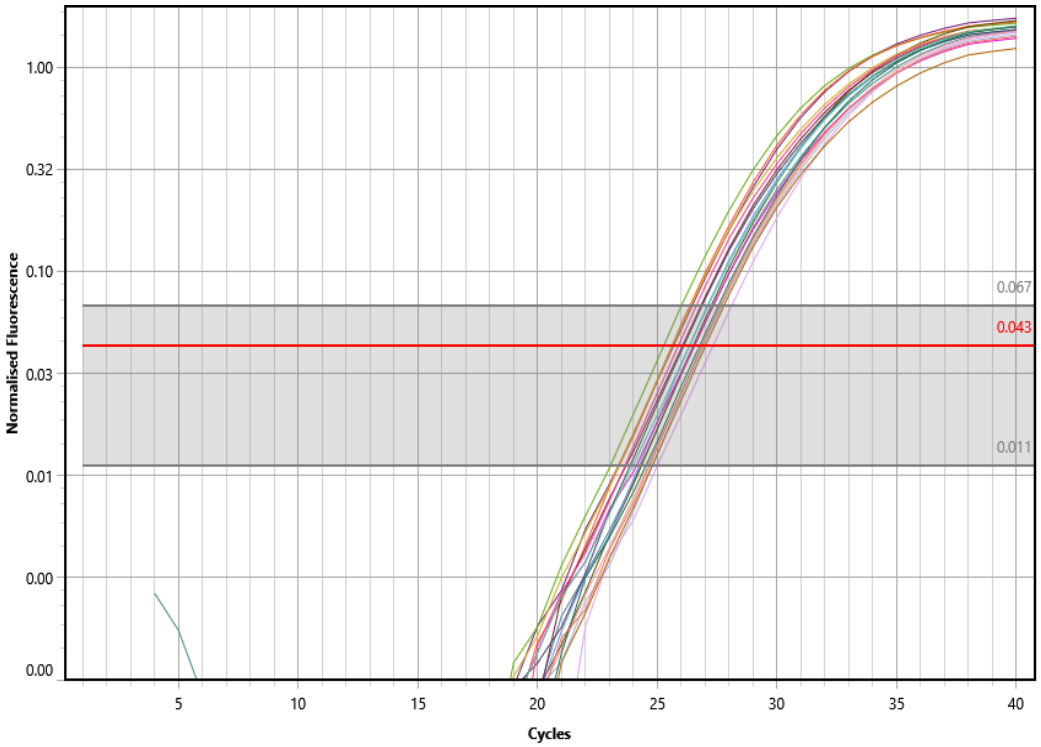

FIGURE 4.16: Real time cycling graph β-Lactamase 2 *blaCTX-M-32* resistance gene

The analysis of *blaCTX-M-32* gene expression reveals varying regulatory patterns across the samples from Islamabad, Lahore, and Okara, highlighting the complex interplay between environmental factors and antibiotic resistance as shown in table 4.14.

TABLE 4.14: βLactamase 2 - Analysis of gene expression in each sample

Sample ID	**ΔCt (Target - Ref)**	**ΔΔCt**	**Fold Expression**	**Regulation Type**
Isl 1	3.5110	-3.0441	**8.2485**	Upregulated
Isl 1a	7.2249	0.6697	0.6286	Downregulated
Isl 2	8.4163	1.8612	0.2753	Downregulated
Isl 2a	7.0684	0.5132	0.7007	Downregulated
Lahore 1	6.7607	0.2055	0.8672	Downregulated
Lahore 1a	7.4296	0.8745	0.5454	Downregulated
Lahore 2	6.5614	0.0063	0.9956	No significant change
Lahore 2a	7.0333	0.4782	0.7179	Downregulated
Okara 1	10.0110	3.4559	0.0911	Strongly Downregulated
Okara 1a	8.6382	2.0830	0.2360	Strongly Downregulated

continued on next page

Sample ID	ΔCt (Target - Ref)	ΔΔCt	Fold Expression	Regulation Type
Okara 2	11.2441	4.6889	0.0388	Strongly Downregulated
Okara 2a	10.6662	4.1111	0.0579	Strongly Downregulated

The *blaCTX-M-32* gene expression shows distinct regulatory trends across Islamabad, Lahore, and Okara, suggesting an impact from varying environmental conditions. In Islamabad, sample Isl 1 was upregulated, possibly due to moderate pollution levels that allowed higher *blaCTX-M-32* expression, while other samples from this city displayed downregulation. Lahore generally showed downregulation, with one sample (Lahore 2) indicating no significant change, which may be linked to high $PM_{2.5}$ levels that suppress expression. Okara displayed strong downregulation across all samples, likely driven by moderate $PM_{2.5}$ levels combined with higher temperatures and lower humidity, which may contribute to a suppression of *blaCTX-M-32* expression. These patterns highlight the influence of both pollution intensity and climate conditions on ARG expressions in each location.

4.8.4 Gene Expression Analysis of β-Lactamase 3

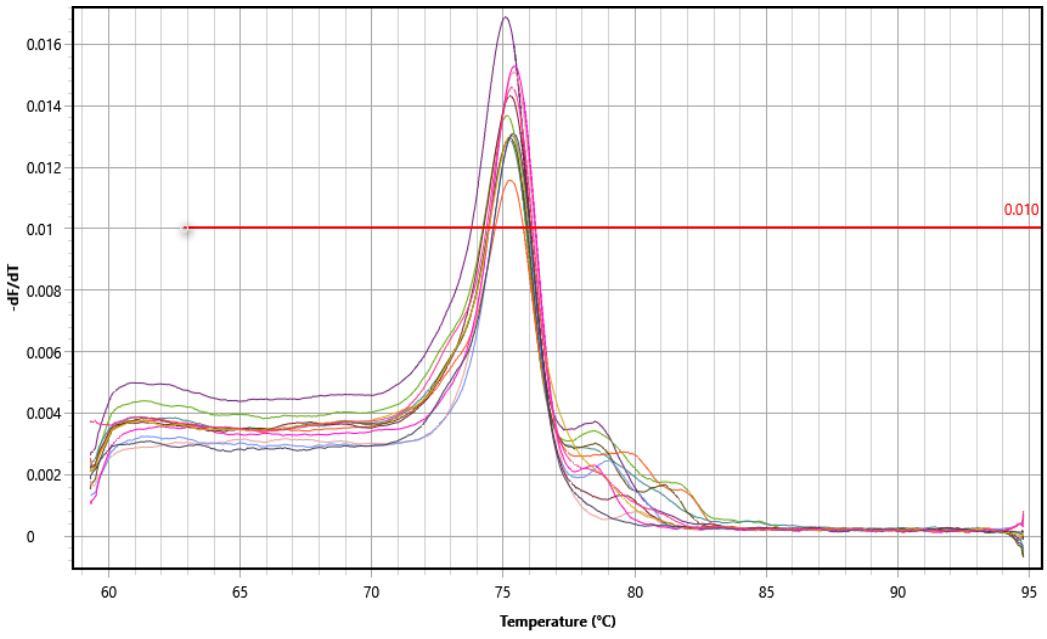

FIGURE 4.17: Real time melt curve graph B-Lactamase 3 *blaNDM-1* resistance gene

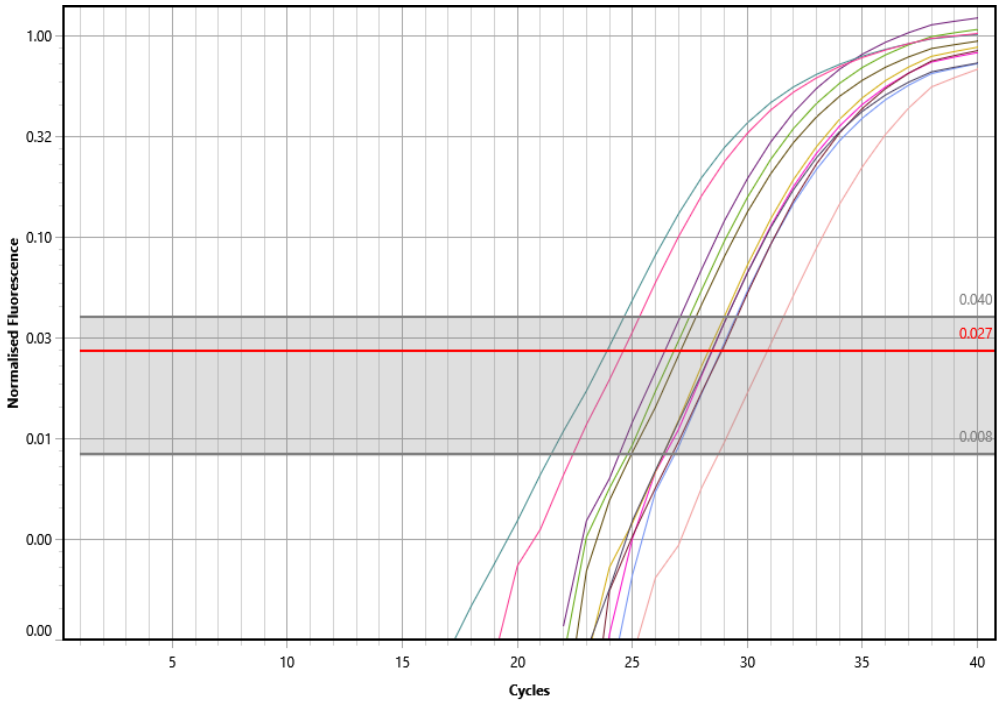

FIGURE 4.18: Real time cycling graph B-Lactamase 3 *blaNDM-1* resistance gene

The analysis of ***blaNDM-1*** gene expression across samples from Islamabad, Lahore, and Okara shows distinct regulatory patterns, reflecting the influence of environmental conditions on antibiotic resistance mechanisms as can be seen in table 4.15.

TABLE 4.15: Gene expression analysis of β-Lactamase 3

Sample ID	**16S Cq Values**	**B-Lactamase 3 Cq Values**	**Delta CT**	**Fold Expression**	**Regulation Status**
Isl 1	23.1747	28.8366	5.6619	0.6566	Downregulated
Isl 1a	22.6488	28.2359	5.5871	0.6916	Downregulated
Isl 2	21.9406	28.3632	6.4226	0.3876	Downregulated
Isl 2a	21.9739	24.5225	2.5486	5.6823	Upregulated
Lahore 1	22.6663	26.3283	3.6619	2.6264	Upregulated
Lahore 1a	22.4493	26.1398	3.6905	2.5749	Upregulated
Lahore 2	22.2449	26.1271	3.8822	2.2545	Upregulated
Lahore 2a	22.3782	25.9852	3.6070	2.7283	Upregulated
Okara 1	20.9312	27.0598	6.1285	0.4752	Downregulated
Okara 1a	21.9960	29.8178	7.8218	0.1469	Downregulated
Okara 2	22.0804	28.7797	6.6993	0.3199	Downregulated
Okara 2a	21.5711	28.3813	6.8102	0.2962	Downregulated

The *blaNDM-1* gene expression across samples from Islamabad, Lahore, and Okara reveals varied regulatory responses, likely influenced by local environmental factors.

In Islamabad, *blaNDM-1* was downregulated in most samples, except for sample Isl 2a, which showed upregulation, possibly due to a moderate pollution level and temperature.

In Lahore, all samples exhibited upregulation, potentially driven by high $PM_{2.5}$ concentrations, which may have induced ARG expression under increased stress conditions. Conversely, Okara showed consistent downregulation, suggesting that moderate $PM_{2.5}$ levels combined with warmer conditions may have suppressed *blaNDM-1* expression.

These findings highlight how different pollution levels and climatic conditions can modulate ARG expression in each city.

4.8.5 Gene Expression Analysis of Vancomycin 1

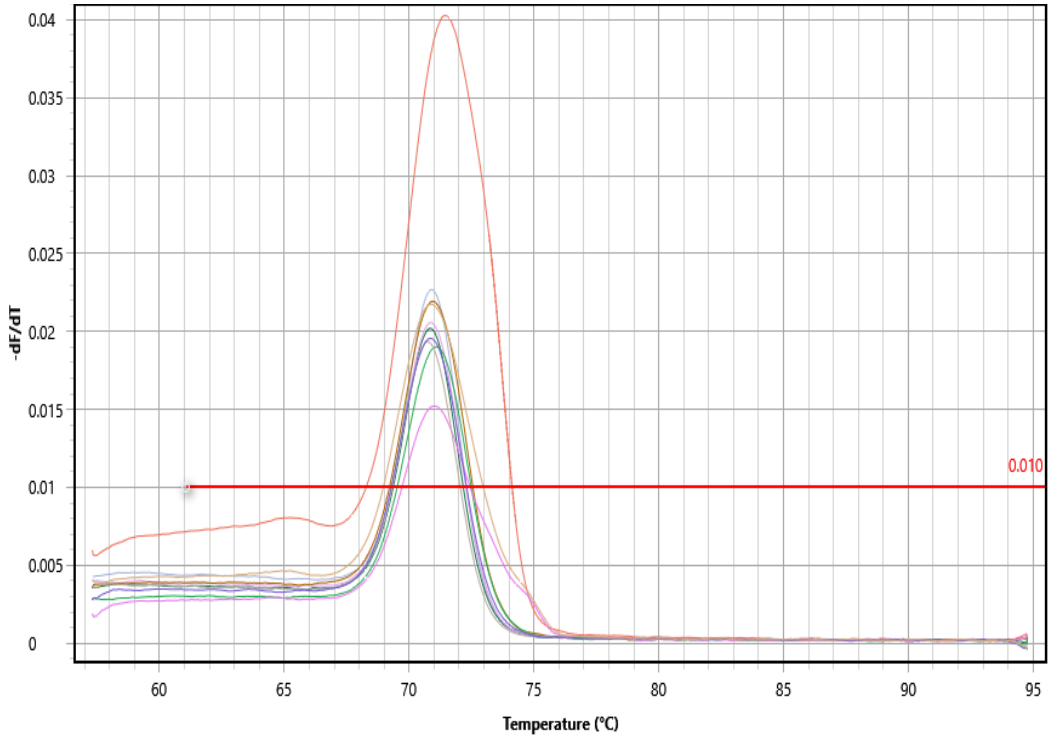

FIGURE 4.19: Real time melt curve graph Vancomycin-1 *vanA* resistance gene

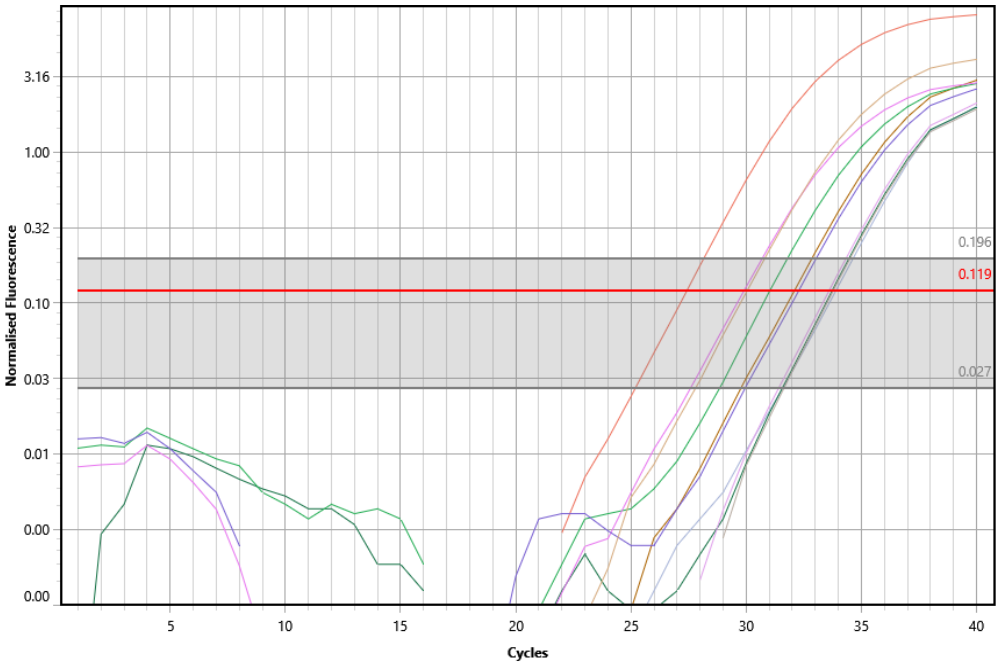

FIGURE 4.20: Real time cycling graph Vancomycin-1 *vanA* resistance gene

The expression analysis of the ***vanA*** gene, which confers resistance to vancomycin, reveals distinct regulatory patterns across the samples from Islamabad, Lahore, and Okara, indicating varying levels of selective pressure in different environments as can be seen in table 4.16.

TABLE 4.16: Gene expression analysis of vancomycin 1

Sample ID	**16S Cq Values**	**Vancomycin-1 Cq Values**	**Delta CT**	**Fold Expression**	**Regulation Status**
Isl 1	23.1747	32.6958	9.5211	1.3612	Upregulated
Isl 1a	22.6488	32.2069	9.5581	1.3267	Upregulated
Isl 2	21.9406	32.6787	10.7381	0.5856	Downregulated
Isl 2a	21.9739	32.0204	10.0465	0.9457	Downregulated
Lahore 1	22.6663	32.9469	10.2806	0.8041	Downregulated
Lahore 1a	22.4493	33.8406	11.3914	0.3723	Downregulated
Lahore 2	22.2449	33.6454	11.4005	0.3699	Downregulated
Lahore 2a	22.3782	33.5017	11.1235	0.4483	Downregulated
Okara 1	20.9312	30.0587	9.1275	1.7882	Upregulated
Okara 1a	21.9960	31.3333	9.3373	1.5461	Upregulated
Okara 2	22.0804	31.9077	9.8274	1.1008	Upregulated
Okara 2a	21.5711	30.8597	9.2886	1.5992	Upregulated

The *vanA* gene expression analysis shows clear differences across Islamabad, Lahore, and Okara, potentially reflecting environmental selection pressures.

In Islamabad, samples Isl 1 and Isl 1a showed upregulation, while the rest were downregulated, likely influenced by moderate $PM_{2.5}$ levels and stable climate conditions.

In Lahore, all samples exhibited downregulation, which may be linked to the city's high $PM_{2.5}$ and colder temperatures, potentially suppressing ARG expression.

In Okara, *vanA* was consistently upregulated across samples, possibly due to moderate pollution levels and warmer conditions that might favor gene expression. These results suggest that environmental factors, particularly air quality and temperature, play key roles in modulating ARG expression in each location.

4.8.6 Gene Expression Analysis of Vancomycin 2

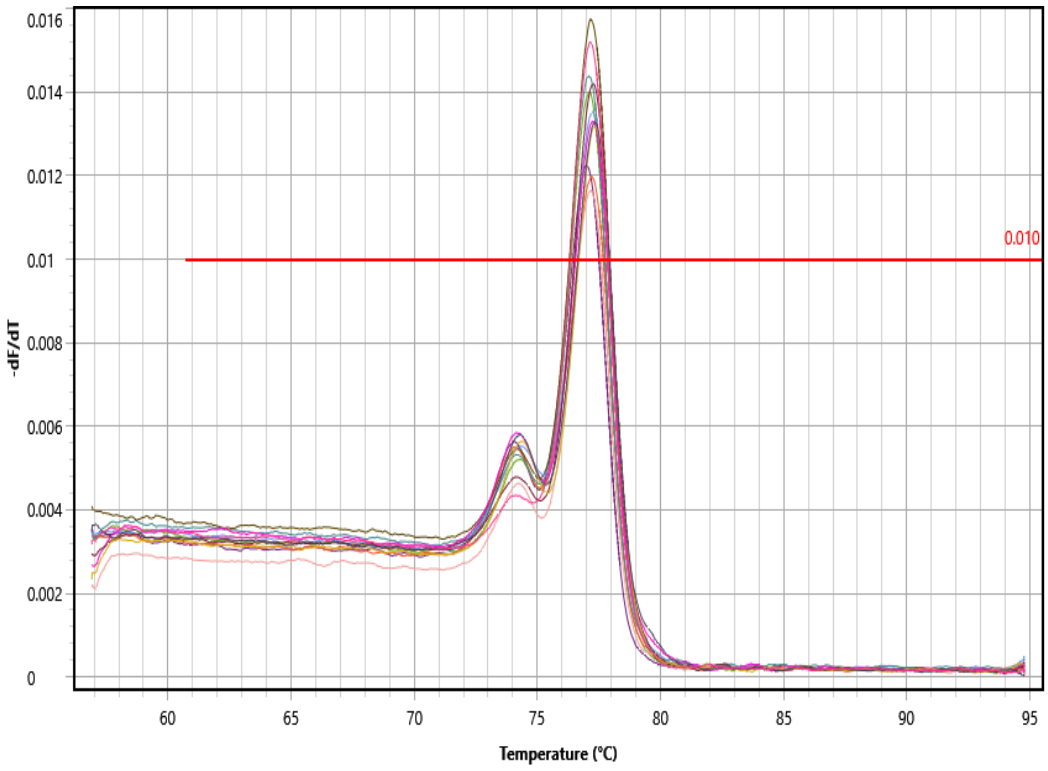

FIGURE 4.21: Real time melt curve graphs Vancomycin-3 *vanRA* resistance gene

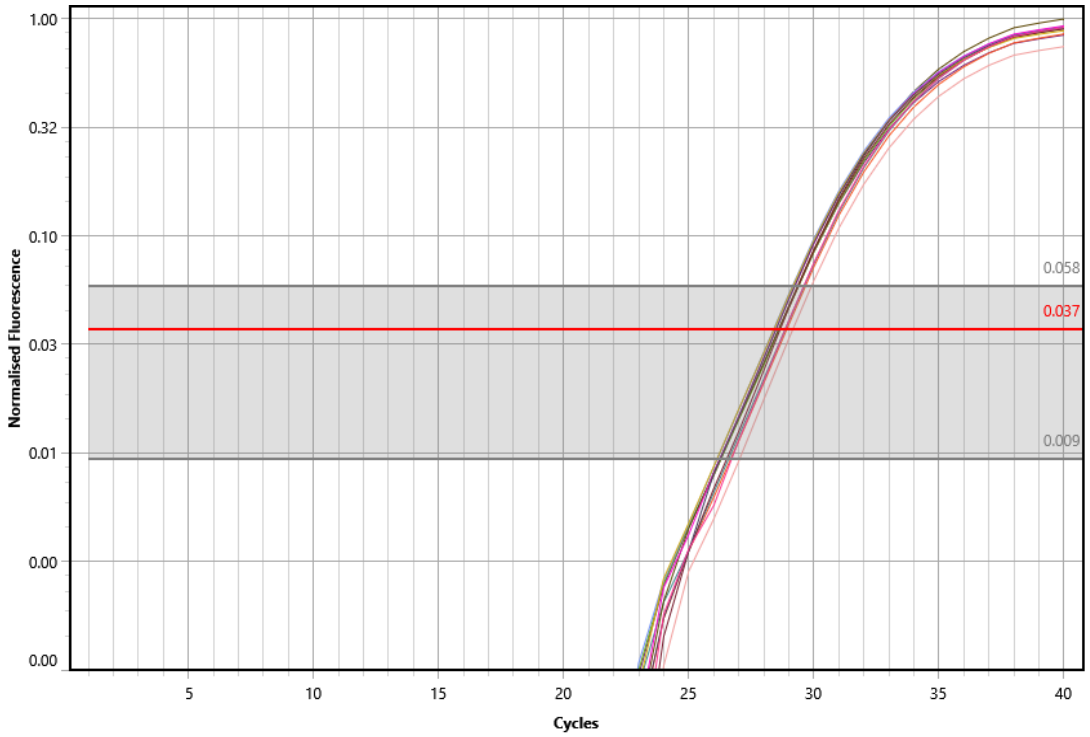

FIGURE 4.22: Real time cycling graph Vancomycin-3 *vanRA* resistance gene

The expression analysis of the ***vanRA*** gene, associated with vancomycin resistance, provides insights into the regulatory dynamics of antibiotic resistance across samples from Islamabad, Lahore, and Okara as can be seen in table 4.17.

TABLE 4.17: Gene expression analysis of vancomycin 2

Sample ID	**16S Cq Values**	**Vancomycin-3 Cq Values**	**Delta CT**	**Fold Expression**	**Regulation Status**
Isl 1	23.1747	28.5748	5.4000	1.6207	Upregulated
Isl 1a	22.6488	28.3340	5.6852	1.3300	Upregulated
Isl 2	21.9406	28.4059	6.4652	0.7745	Downregulated
Isl 2a	21.9739	28.8100	6.8360	0.5990	Downregulated
Lahore 1	22.6663	28.9524	6.2861	0.8769	Downregulated
Lahore 1a	22.4493	28.5504	6.1012	0.9969	Downregulated
Lahore 2	22.2449	28.8851	6.6402	0.6861	Downregulated
Lahore 2a	22.3782	28.8069	6.4288	0.7944	Downregulated
Okara 1	20.9312	28.5130	7.5818	0.3572	Downregulated
Okara 1a	21.9960	29.1196	7.1236	0.4907	Downregulated
Okara 2	22.0804	28.3203	6.2399	0.9054	Downregulated
Okara 2a	21.5711	28.8086	7.2375	0.4535	Downregulated

The *vanRA* gene expression analysis shows consistent downregulation across most samples from Islamabad, Lahore, and Okara, with limited upregulation observed only in Islamabad samples Isl 1 and Isl 1a.

These two samples' upregulation may be attributed to Islamabad's moderate $PM_{2.5}$ levels and stable climate, creating conditions favorable to ARG expression.

In Lahore, all samples showed downregulation, likely due to high $PM_{2.5}$ and colder, humid conditions that may inhibit gene expression.

Okara's samples were similarly downregulated, suggesting that moderate pollution levels and local environmental factors, like higher temperatures, could suppress *vanRA* expression. This analysis underscores the role of environmental conditions, particularly air quality and climate, in influencing ARG regulation across different regions.

4.8.7 Gene Expression Analysis of Transposase

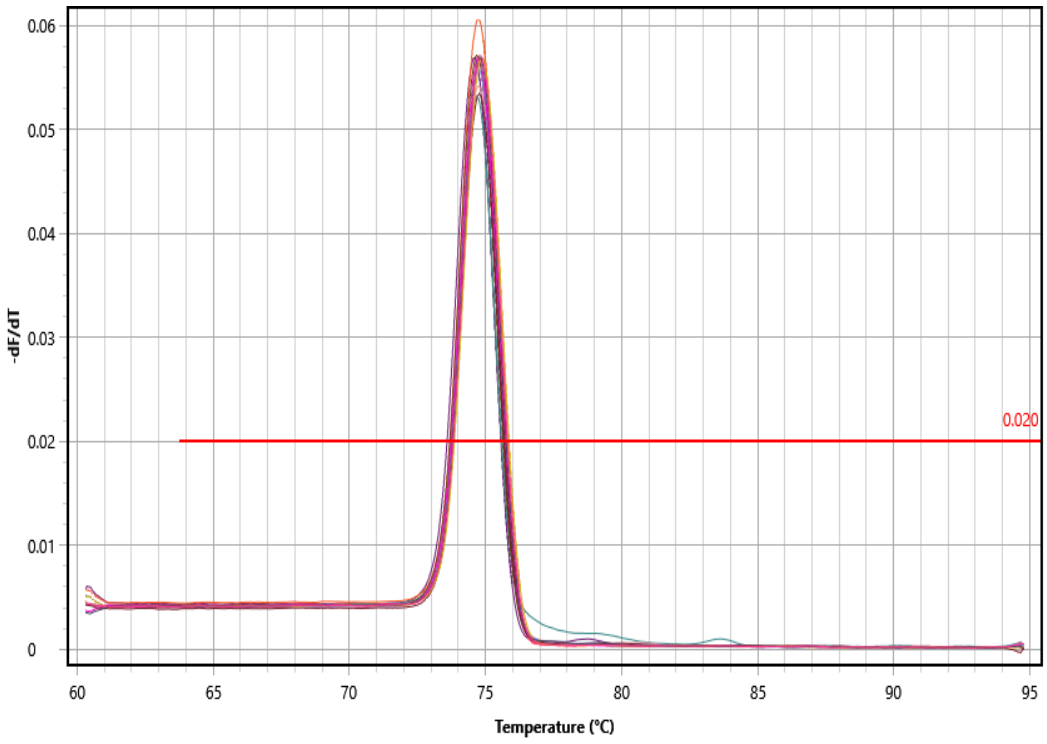

FIGURE 4.23: Real time melt curve graph Transposase *tnpA* resistance gene

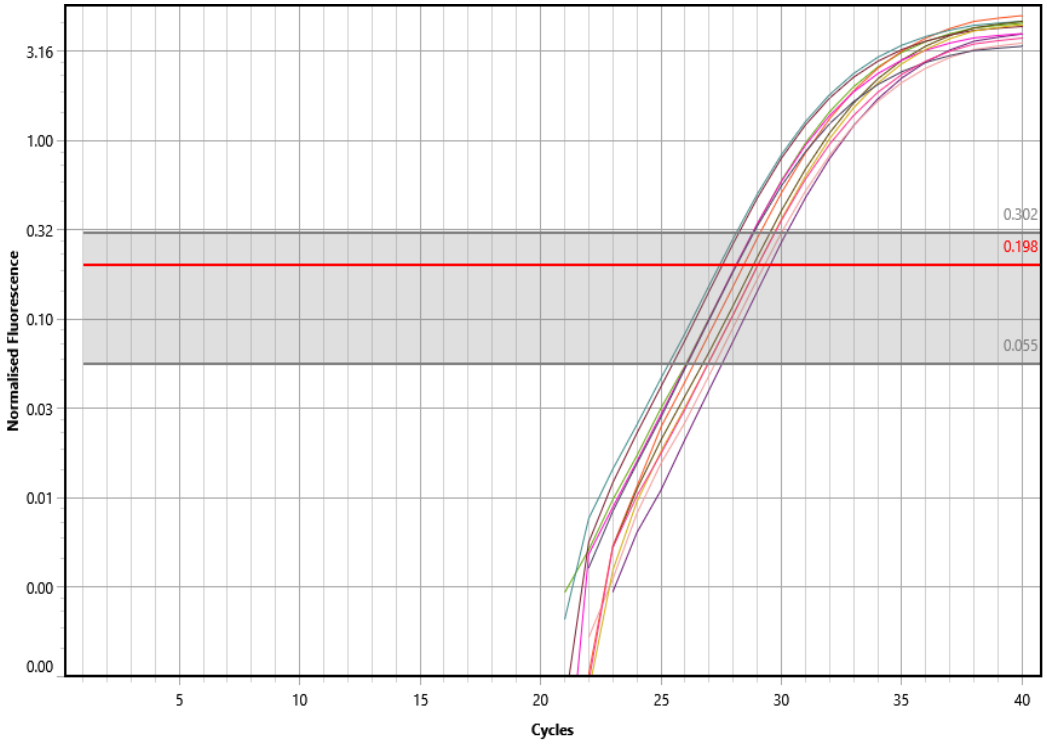

FIGURE 4.24: Real time cycling graph Transposase *tnpA* resistance gene

The analysis of the ***tnpA*** gene, which encodes transposase and plays a role in the mobility of antibiotic resistance genes, reveals distinct expression patterns across samples from Islamabad, Lahore, and Okara as can be seen in table 4.18.

TABLE 4.18: Gene expression analysis of Transposase

Sample ID	**16S Cq Values**	**Transposase Cq Values**	**Delta CT**	**Fold Expression**	**Regulation Status**
Isl 1	23.1747	27.4502	4.2755	3.1948	Upregulated
Isl 1a	22.6488	29.0025	6.3537	0.7566	Downregulated
Isl 2	21.9406	28.0904	6.1497	0.8715	Downregulated
Isl 2a	21.9739	28.9999	7.0260	0.4747	Downregulated
Lahore 1	22.6663	29.4359	6.7696	0.5671	Downregulated
Lahore 1a	22.4493	29.0792	6.6299	0.6247	Downregulated
Lahore 2	22.2449	28.3428	6.0979	0.9033	Downregulated
Lahore 2a	22.3782	29.3397	6.9615	0.4964	Downregulated
Okara 1	20.9312	28.7659	7.8347	0.2710	Downregulated
Okara 1a	21.9960	29.2227	7.2268	0.4131	Downregulated
Okara 2	22.0804	29.0774	6.9970	0.4844	Downregulated
Okara 2a	21.5711	28.0650	6.4939	0.6865	Downregulated

The *tnpA* gene expression analysis across samples from Islamabad, Lahore, and Okara shows varied regulatory responses.

In Islamabad, sample Isl 1 was notably upregulated, possibly due to moderate air quality that allowed for higher *tnpA* expression, while all other samples from Islamabad, Lahore, and Okara showed downregulation.

The consistent downregulation observed in Lahore and Okara samples may result from higher pollution levels, which could suppress gene mobility activity, particularly in colder, more humid conditions in Lahore and warmer temperatures in Okara.

These findings suggest that environmental factors such as air quality, temperature, and humidity have a strong influence on the regulation of *tnpA* across different cities.

4.8.8 Gene Expression Analysis of Integrase

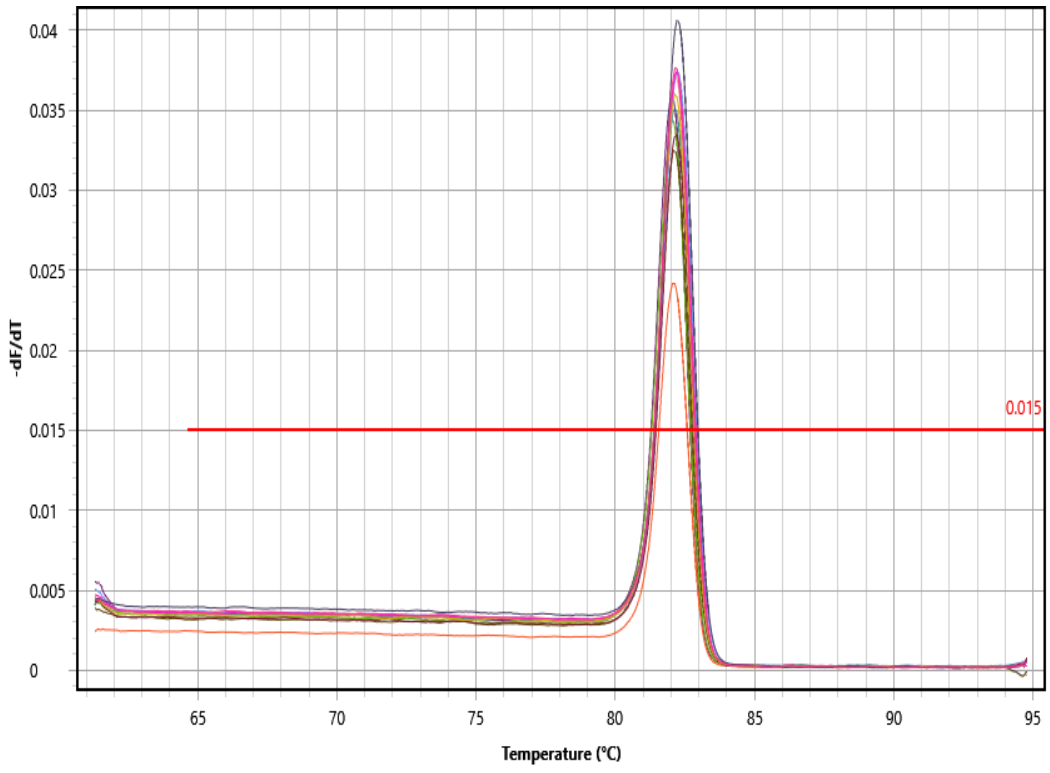

FIGURE 4.25: Real time melt curve graph Integrase *intI1* resistance gene

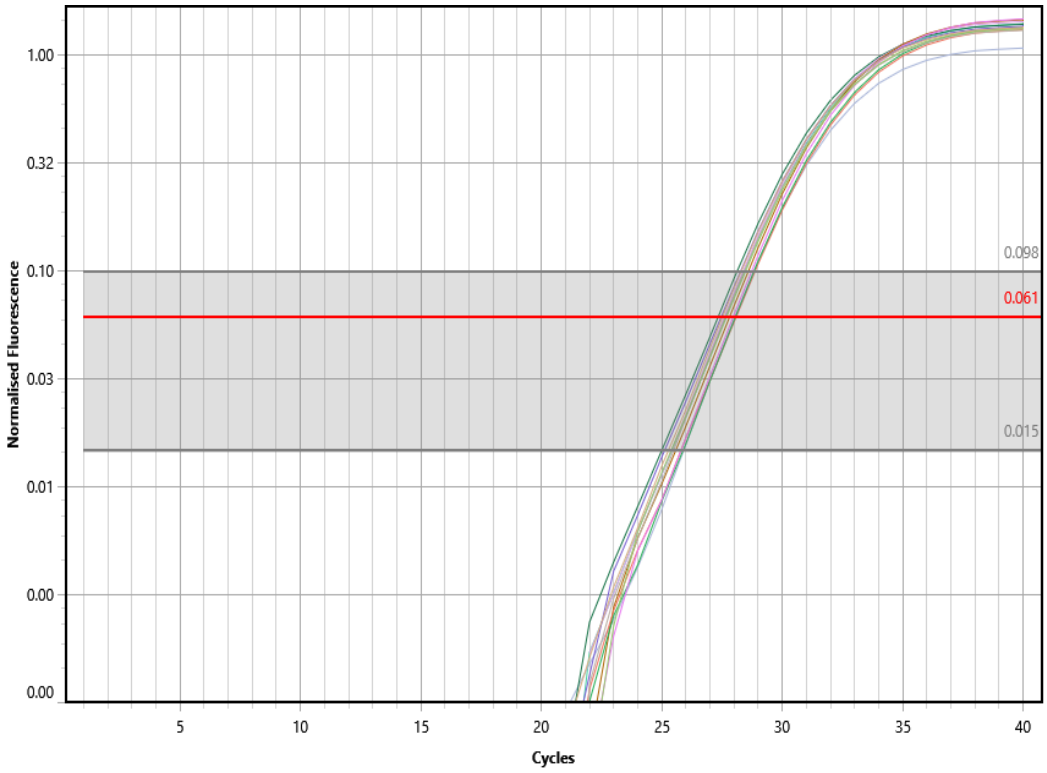

FIGURE 4.26: Real time cycling graph Integrase *intI1* resistance gene

The analysis of the ***intI1*** gene, which encodes integrase and is crucial for the incorporation of resistance genes into integrons, shows notable differences in expression across samples from Islamabad, Lahore, and Okara as can be seen in table 4.19.

TABLE 4.19: Gene expression analysis of Integrase

Sample ID	**16S Cq Values**	**Integrase Cq Values**	**Delta CT**	**Delta Delta CT**	**Fold Expression**	**Regulation Status**
Isl 1	23.1747	27.5594	4.3847	-0.9034	1.8704	Upregulated
Isl 1a	22.6488	27.9385	5.2897	0.0017	0.9988	Not significantly regulated
Isl 2	21.9406	27.9619	6.0212	0.7332	0.6016	Downregulated
Isl 2a	21.9739	27.4304	5.4565	0.1685	0.8898	Downregulated
Lahore 1	22.6663	28.5709	5.9046	0.6165	0.6522	Downregulated
Lahore 1a	22.4493	27.9218	5.4725	0.1845	0.8799	Downregulated

continued on next page

Sample ID	16S Cq Values	Integrase Cq Values	Delta CT	Delta Delta CT	Fold Expression	Regulation Status
Lahore 2	22.2449	28.1260	5.8812	0.5932	0.6629	Downregulated
Lahore 2a	22.3782	27.9130	5.5348	0.2468	0.8428	Downregulated
Okara 1	20.9312	27.7555	6.8243	1.5362	0.3448	Downregulated
Okara 1a	21.9960	28.0601	6.0641	0.7761	0.5840	Downregulated
Okara 2	22.0804	28.0371	5.9567	0.6687	0.6291	Downregulated
Okara 2a	21.5711	27.9401	6.3690	1.0809	0.4727	Downregulated

The gene expression analysis of the *intI1* gene, responsible for integrase and vital for integrating resistance genes into integrons, reveals significant variations across samples from Islamabad, Lahore, and Okara. In Islamabad, sample Isl 1 exhibited a notable upregulation, likely reflecting favorable environmental conditions for gene expression.

4.8.9 Gene Expression Analysis of *blaTEM_F*

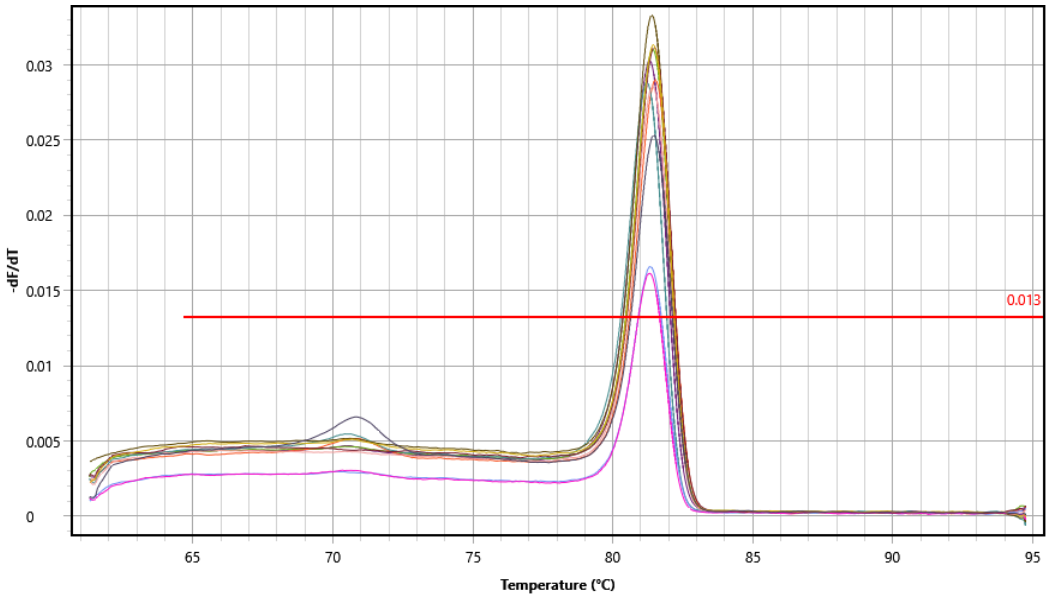

FIGURE 4.27: Real time melt curve graphs *blaTEM F* resistance gene

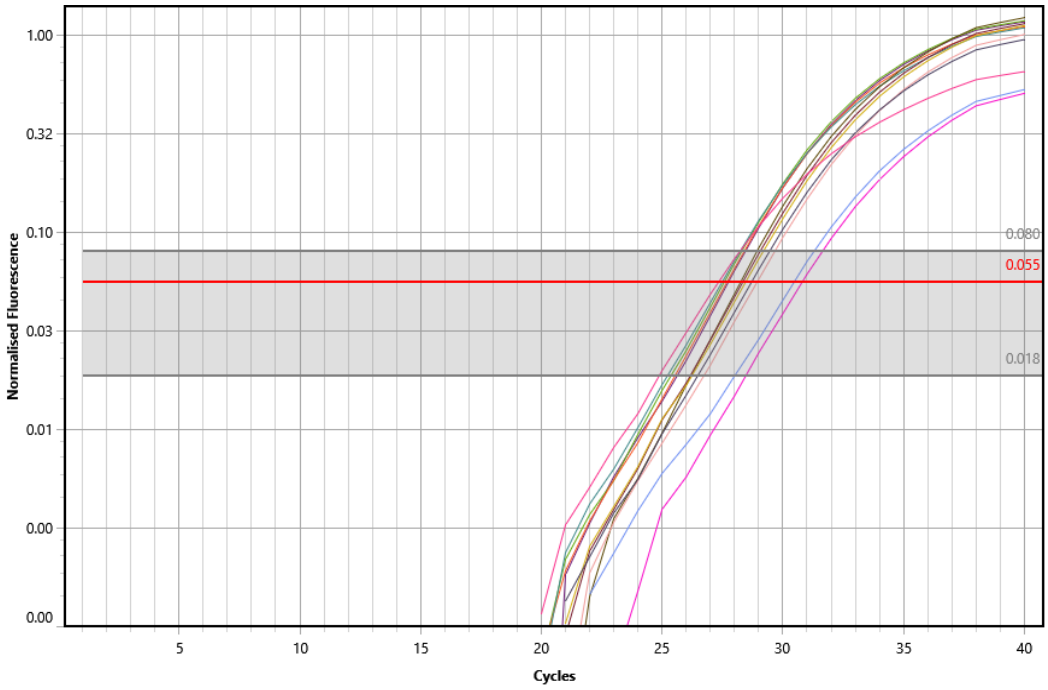

FIGURE 4.28: Real time cycling graph *blaTEM F* resistance gene

The analysis of the ***blaTEM_F*** gene, which encodes integrase and is crucial for the incorporation of resistance genes into integrons, shows notable differences in expression across samples from Islamabad, Lahore, and Okara as can be seen in table 4.20.

TABLE 4.20: Gene expression analysis of *blaTEM_F*

Sample ID	**16S Cq Values**	***blaTEM* Cq Values**	**Delta CT**	**Delta Delta CT**	**Fold Expression**	**Regulation Status**
Isl 1	23.1747	28.2745	5.0998	-0.2595	1.1970	No significant change
Isl 1a	22.6488	28.3846	5.7358	0.3766	0.7703	Downregulated
Isl 2	21.9406	27.2371	5.2965	-0.0628	1.0445	No significant change
Isl 2a	21.9739	27.2789	5.3049	-0.0543	1.0384	No significant change
Lahore 1	22.6663	27.6772	5.0109	-0.3484	1.2731	No significant change
Lahore 1a	22.4493	27.4971	5.0479	-0.3114	1.2409	No significant change

continued on next page

Sample ID	**16S Cq Values**	***blaTEM* Cq Values**	**Delta CT**	**Delta Delta CT**	**Fold Expression**	**Regulation Status**
Lahore 2	22.2449	27.2165	4.9716	-0.3876	1.3082	No significant change
Lahore 2a	22.3782	27.4144	5.0363	-0.3229	1.2509	No significant change
Okara 1	20.9312	28.1956	7.2644	1.9051	0.2670	Downregulated
Okara 1a	21.9960	28.9026	6.9066	1.5474	0.3421	Downregulated
Okara 2	22.0804	30.3974	8.3170	2.9578	0.1287	Downregulated
Okara 2a	21.5711	30.7462	9.1751	3.8159	0.0710	Downregulated

The analysis of the *blaTEM-F* gene expression across various samples reveals distinct regulatory patterns. In the Islamabad samples, Isl 1, Isl 2, and Isl 2a displayed no significant changes in expression levels, indicating stability in *blaTEM-F* regulation. However, sample Isl 1a showed downregulation. In Lahore, all samples (Lahore 1, Lahore 1a, Lahore 2, and Lahore 2a) exhibited no significant changes in expression. Conversely, samples from Okara (Okara 1, Okara 1a, Okara 2, and Okara 2a) showed a marked downregulation of *blaTEM-F* expression, with fold changes decreasing significantly. This pattern suggests that environmental factors, particularly in Okara, may exert a strong negative influence on *blaTEM-F* expression, potentially impacting antibiotic resistance dynamics in that region.

4.9 Comparative Study of Internal Genes and External AMR Gene Uptake

The comparison of internal resistome analysis with external DNA shows, there is no evidence of resistance gene uptake from external DNA by the internal genome data across Islamabad, Lahore, and Okara in both years. The internal genes present do not correspond with any of the external genes listed, indicating that no uptake has occurred in any of the regions analyzed (Table 4.21 & 4.22).

Table 4.21: Internal AMR Genes Summary

Region	**Year**	**AMR Genes**
Islamabad	2022	*vanY*, *vanT*, *vanW*, *qacG*, *adeF*, *RbpA*, *qacJ*, *vanH*
Islamabad	2023	*vanT*, *vanY*, *adeF*, *vanW*, *vanH*, *RbpA*, *qacG*, *qacJ*
Lahore	2022	*adeF*, *vanY* (*vanG* cluster), *vanY* (*vanD* cluster), *vanY* (vanM cluster), *vanW* (*vanI* cluster), *vanW* (*vanO* cluster), *vanW* (*vanF* cluster), *vanH* (*vanD* cluster), *vanH* (*vanO* cluster), *vanT* (*vanG* cluster), *qacG*, *qacJ*, *RbpA*, *nimB*
Lahore	2023	*vanT*, *vanY*, *adeF*, *vanW*, *qacJ*, *vanH*, *RbpA*, *OXA-50*, vanR
Okara	2022	*vanT*, *adeF*, *vanH*, *vanY*, *qacJ*, rsmA, *qacG*, *vanH* (duplicate), *adeF* (duplicate), *poxtA*
Okara	2023	*adeF*, *vanY*, *vanT*, *vanH*, *qacJ*, *RbpA*, *qacG*, *vanW*

Table 4.22: Comparative Analysis of Internal and External resistome DNA in Islamabad, Lahore, and Okara

External Gene	**Internal Gene (Islamabad 2022)**	**Internal Gene (Islamabad 2023)**	**Internal Gene (Lahore 2022)**	**Internal Gene (Lahore 2023)**	**Internal Gene (Okara 2022)**	**Internal Gene (Okara 2023)**	**Gene Uptake**
Sulfonamide (*sul1*)	-	-	-	-	-	-	No
	-	-	-	-	-	-	No
	-	-	-	-	-	-	No
	-	-	-	-	-	-	No
β-Lactamase 1 (*blaTEM*)	-	-	-	-	-	-	No
	-	-	-	-	-	-	No
	-	-	-	-	-	-	No
	-	-	-	-	-	-	No
β-Lactamase 2 (*blaCTX-M-32*)	-	-	-	-	-	-	No

continued on next page

External Gene	**Internal Gene**	**Internal Gene**	**Internal Gene**	**Internal Gene**	**Internal Gene**	**Internal Gene**	**Gene Uptake**
	-	-	-	-	-	-	No
	-	-	-	-	-	-	No
	-	-	-	-	-	-	No
β-Lactamase 3 (*blaNDM-1*)	-	-	-	-	-	-	No
	-	-	-	-	-	-	No
	-	-	-	-	-	-	No
	-	-	-	-	-	-	No
Vancomycin 1 (*vanA*)	-	-	-	-	-	-	No
	-	-	-	-	-	-	No
	-	-	-	-	-	-	No
	-	-	-	-	-	-	No
Vancomycin 3 (*vanRA*)	-	-	-	-	-	-	No
	-	-	-	-	-	-	No
	-	-	-	-	-	-	No
	-	-	-	-	-	-	No
Transposase (*tnpA*)	-	-	-	-	-	-	No
	-	-	-	-	-	-	No
	-	-	-	-	-	-	No
	-	-	-	-	-	-	No
Integrase (*intI1*)	-	-	-	-	-	-	No
	-	-	-	-	-	-	No
	-	-	-	-	-	-	No
	-	-	-	-	-	-	No
blaTEM-F	-	-	-	-	-	-	No
	-	-	-	-	-	-	No
	-	-	-	-	-	-	No
	-	-	-	-	-	-	No

Chapter 5

Discussion

Our study showed that the rats that were exposed to smog moved more slowly, spent less time in the open field, groomed more, and quicker compared to control rats. These findings point toward increased anxiety-like behavior and reduced exploratory drive. The open field test is widely used in behavioral neuroscience to assess both general locomotion and anxiety: animals that stay near the walls (avoid center) or move little are interpreted as showing anxiety or stress responses [176]. Similar patterns have been reported in rodents exposed to air pollution: for example, Kyi-Tha-Thu *et al.* (2022) found that early life exposure to traffic-related air pollutants led to increased anxiety-like behaviors in rats [177]. Also, Ji *et al.* (2024) demonstrated that real-world $PM_{2.5}$ exposure in mice disrupted dopamine signaling and induced anxiety- and depression-like behaviors consistent with reduced center exploration [178]. The grooming results in our study further support that interpretation; grooming is known to be a stress-sensitive behavior in rodents, and shorter grooming latency plus extended grooming duration often accompany elevated stress or arousal states under environmental or physiological insult [179]. Taken together, our open field data align well with recent literature showing that chronic particulate exposure can induce behavioral suppression and anxiety-like phenotypes through oxidative stress and neuroinflammation. Regarding memory, our Y-maze results showed that smog-exposed rats had a lower alternation percentage across the 60 days, pointing to impaired spatial working

memory or cognitive flexibility. Because the Y-maze alternation metric relies on successive arm entries, this deficit suggests that smog exposure interfered with the rats' ability to retain or update short-term spatial information. Several recent studies support this type of effect. Wei *et al.* (2024) showed that mice exposed to $PM_{2.5}$ had damage to hippocampal circuits and reduced Y-maze performance, implicating ferroptosis and oxidative stress pathways [180].

Moreover, Liu *et al.* (2024) demonstrated that $PM_{2.5}$ exposure accelerates tau aggregation and induces cognitive impairments, reinforcing how particulate pollutants can impair synaptic and memory function [181]. In developmental models, Zhang *et al.* (2023) reports that maternal exposure to concentrated ambient $PM_{2.5}$ leads to spatial memory defects in offspring, measured through maze paradigms [182]. While the lower locomotion can affect alternation rates, the result of our open filed study allow us to interpret that the Y-maze deficits more confidently as memory impairment rather than pure motor slowing. In addition, the combined behavioural data supports the conclusion that chronic smog exposure in rats leads to a phenotype anxiety-like suppression and measurable working memory impairment, reflecting pollutant-mediated neurotoxicity in circuits governing emotion and cognition.

our histological findings showed that prolonged smog exposure produced clear lung tissue damage in rats. Control groups had normal alveolar architecture with thin septa, were as the smog-exposed groups displayed alveolar wall thickening, partial detachment, enlarged air spaces suggestive of early emphysema, and heavy infiltration of macrophages and neutrophils. The carbon deposits were also visible in alveolar walls, that reflect direct particulate matter accumulation.

These changes indicate that smog inhalation induces oxidative stress and inflammatory injury. Similar findings have been reported in rats exposed to diesel exhaust, where alveolar thickening, inflammatory infiltration, and emphysema-like changes were observed [183]. Other work has shown that chronic $PM_{2.5}$ exposure causes alveolar destruction and fibrosis in mice [184]. The inflammatory infiltration we observed supports the view that particulates activate macrophages, leading to cytokine release and neutrophil recruitment [185]. Alveolar enlargement

is likely the result of oxidative damage and protease imbalance, consistent with mechanisms of pollution-induced emphysema [186]. The carbon deposition seen in our slides parallels human and animal studies where black carbon accumulation is considered a marker of particulate burden [187].

Continuing from the behavioral and histopathological observations, the immunological assays provided important evidence that smog exposure exerts systemic effects on adaptive immunity. Flow cytometry analysis showed a clear increase in both CD4+ and CD8+ T cell populations in test groups compared to their matched controls. In particular, CD4+ T cell proportions rose from 26.18% in the control group (C-A) to 31.21% in the exposed group (T-A), and from 25.10% (C-B) to 37.04% (T-B). Similarly, CD8+ T cells increased from 19.41% (C-A) to 22.34% (T-A), and from 15.67% (C-B) to 28.81% (T-B). These elevations suggest that smog exposure acts as an immunological stressor, promoting T cell activation and proliferation beyond basal levels.

Such findings are consistent with recent animal and human studies reporting pollution-induced immune dysregulation. For example, Hargrove *et al.* found that mice exposed to simulated smog atmospheres exhibited systemic immune activation and shifts in lymphocyte populations, supporting the idea that pollutants mobilize adaptive immunity [187]. Similarly, Soler-Segovia *et al.* demonstrated that diesel exhaust particles enhanced CD4+ T cell responses and drove a pro-inflammatory phenotype, in line with the elevated CD4+ frequencies seen in our study [188]. Jo *et al.* further reported that fine particulate matter exposure can alter the CD4:CD8 ratio, reflecting an imbalance in adaptive immune regulation similar to the trends observed here [189].

Mechanistically, these immune alterations may arise because inhaled particulate matter and gaseous components activate antigen-presenting cells in the lung, triggering downstream pathways such as NF-κB and MAPK that stimulate cytokine release and recruit T lymphocytes. Recent studies have shown that such activation promotes sustained T cell proliferation and systemic inflammation [190, 191]. While some investigations have also reported immune suppression under chronic or more severe exposure conditions [192], the robust increase in both CD4+ and

CD8+ subsets in our study suggests that the smog exposure period was sufficient to trigger immune activation rather than exhaustion.

Taken together, the observed increases in T cell subsets confirm that smog exposure does not only damage the lungs structurally but also provokes systemic immune modulation. This adaptive immune activation is likely to contribute to inflammatory cascades that may exacerbate tissue injury, behavioral changes, and long-term susceptibility to respiratory and systemic diseases.

Following the immunological results, the metagenomic analysis of rat lung tissues provides further evidence that smog exposure has a profound impact on the respiratory ecosystem. The alpha diversity results demonstrated a noticeable reduction in diversity indices—including Observed, Chao1, and Shannon—in smog-exposed rats compared to controls. This suggests that the exposed lungs harbored fewer unique bacterial taxa and displayed reduced overall complexity. Such a loss of microbial richness points toward dysbiosis, where a normally diverse and balanced microbial community becomes disrupted. A reduction in diversity is not only a marker of ecological instability but is also strongly associated with higher vulnerability to colonization by pathogenic and resistant microorganisms. Similar findings have been reported in human studies, where chronic exposure to $PM_{2.5}$ and ozone was associated with a decline in airway microbial diversity, correlating with inflammation and susceptibility to respiratory disease [193, 194].

At the genus level, the data revealed major compositional shifts between control and test groups. The control lungs contained a more even balance of commensal and environmental genera, whereas the smog-exposed lungs were dominated by opportunistic pathogens such as Pseudomonas, Acinetobacter, Mycoplasma, and Staphylococcus. These genera are clinically important because they are frequently implicated in chronic respiratory infections and are known to harbor multiple resistance determinants. For instance, Pseudomonas species are notorious for their adaptive resistance mechanisms, including efflux pumps and biofilm formation, which allow them to thrive under stress conditions such as pollution exposure. Enrichment of Mycoplasma and Staphylococcus further highlights the pathogenic risk associated with pollution-driven dysbiosis, as these taxa have been linked

with airway inflammation and persistent colonization in polluted environments [195, 196].

Interestingly, taxa that are typically rare in healthy lungs—such as Legionella, Burkholderia, and Stenotrophomonas—appeared more abundant or at least more detectable in the smog-exposed groups. These organisms are opportunistic pathogens that can cause severe infections under immune stress and are often associated with multidrug resistance. Their enrichment under polluted conditions is consistent with findings from Qin *et al.* [197], who showed that particulate matter fosters the survival of stress-tolerant bacterial taxa while suppressing more sensitive commensals. This suggests that smog not only reshapes microbial communities but also selectively favors those organisms best equipped to withstand oxidative and toxic stress, many of which are pathogenic.

Species-level analysis provided further resolution, showing that smog-exposed lungs contained higher proportions of Stenotrophomonas maltophilia, Pasteurella multocida, Chryseobacterium gleum, and Pseudomonas putida. Each of these species carries clinical significance. *S. maltophilia* is an emerging multidrug-resistant pathogen with intrinsic resistance to β-lactams and aminoglycosides due to chromosomally encoded efflux systems and β-lactamases [198].

P. multocida is associated with respiratory infections in both animals and humans, and its increased abundance reflects a compromised host environment. *C. gleum* is another opportunistic pathogen increasingly reported in immunocompromised patients, often with multidrug resistance. The high abundance of P. putida in both control and test groups suggests its role as a persistent colonizer of the respiratory tract, though its relative dominance under polluted conditions underscores its adaptability. Human studies in heavily polluted areas have similarly reported increased airway colonization by Stenotrophomonas and Pseudomonas, supporting the translational relevance of these results [199].

The collective pattern across alpha diversity, genera, and species indicates that smog exposure drives microbial imbalance in the lungs, characterized by a shift from diverse, balanced communities toward a narrower set of opportunistic and

resistant taxa. Reduced biodiversity undermines ecosystem resilience, while enrichment of pathogens increases the likelihood of respiratory inflammation, chronic colonization, and infection. Importantly, many of the dominant genera and species identified in the exposed groups are recognized carriers of antibiotic resistance genes, which ties directly into the ARG analysis described in the next section. Thus, the metagenomic evidence not only reveals ecological disruption but also signals a strong link between environmental pollution and the enrichment of clinically significant resistance traits.

The resistome analysis of rat lungs exposed to smog in Islamabad and Lahore provides strong evidence that environmental air pollution is not merely a respiratory toxicant but a dynamic vector for antimicrobial resistance (AMR) dissemination. The integration of metagenomic sequencing with functional annotation against the CARD database revealed a broad array of resistance determinants, including β-lactamases, colistin resistance genes, efflux pump components, and glycopeptide resistance clusters. Importantly, while both Islamabad and Lahore samples demonstrated enrichment of clinically significant ARGs, the profiles revealed unique differences that highlight the influence of local environmental conditions and microbial communities on resistance selection.

In Islamabad samples, several ARGs were consistently present across both test and control groups, suggesting a baseline background of resistance within the lung microbiota. BRO-1, detected in both test and control samples, indicated that β-lactamase activity is a widely distributed resistance trait. Similarly, the detection of OXA-168 in both exposed and control lungs points to a common β-lactam resistance mechanism, reflective of its global distribution in Enterobacteriaceae and non-fermenters [200]. The identification of mupA in Staphylococcus aureus across both groups was particularly noteworthy, as mupirocin resistance is generally associated with clinical use in topical treatments. Its presence in environmental samples highlights how ARGs traditionally linked to hospitals may circulate more widely in ambient microbiota [201].

However, the Islamabad test samples revealed additional, highly concerning determinants absent in controls. Among these were MCR-3.11 and MCR-3.15, two

colistin resistance variants. The emergence of MCR genes has been considered one of the most critical threats in AMR because colistin is often the final therapeutic option for infections caused by multidrug-resistant Gram-negative pathogens. Studies have shown that airborne particulate matter and polluted soils can harbor plasmid-borne mcr genes, facilitating horizontal transfer between environmental and pathogenic bacteria [202].

The exclusive appearance of these determinants in smog-exposed lungs strongly implicates environmental inhalation as a route of ARG acquisition. Other notable test-specific genes included pmrA, which regulates modifications of lipid A in bacterial membranes conferring polymyxin resistance, and poxtA, linked to resistance against oxazolidinones and phenicols, further broadening the resistance spectrum [203]. The enrichment of MexC and MexF, both efflux pump components of Pseudomonas aeruginosa, indicates adaptive mechanisms to expel multiple antibiotics simultaneously, conferring multidrug resistance [204].

In contrast, Lahore samples revealed a more heterogeneous and divergent resistome profile. Unlike Islamabad, where some ARGs were shared across test and control groups, Lahore lungs showed no universally conserved ARGs, highlighting greater variability and site-specific resistance evolution. OXA-168 was restricted to control C1B, while OpmB was consistently detected across C1B, C2B, and T1B, pointing to efflux-mediated resistance as a recurring adaptation. The test groups, T1B and T2B, displayed an extensive set of unique ARGs. These included β-lactamases such as OXA-192, OXA-294, OXA-732, and OXA-397, underscoring the dominance of β-lactam hydrolysis as a resistance mechanism in polluted lungs [205]. Tetracycline resistance determinants (tet(38), tet(O/M/O), tet(O/W)) were highly prevalent, while glycopeptide resistance genes (vanD, vanK, vanF) further emphasized the multidrug nature of the Lahore resistome. Particularly concerning was the presence of MCR-3.14 in T2B, highlighting colistin resistance as a recurring theme in both cities, and VAM-1, an ESBL, suggesting the horizontal acquisition of resistance to extended-spectrum cephalosporins [206].

The comparison of Islamabad and Lahore resistomes reveals both convergences and divergences. Convergences included the enrichment of OXA-type β-lactamases

and MCR-family colistin resistance genes in both cities, underscoring that smog exposure provides favorable conditions for the maintenance and amplification of last-line resistance mechanisms. This aligns with earlier findings that β-lactamases, particularly OXA variants, are widely distributed in airborne environments and capable of hydrolyzing penicillins, cephalosporins, and even carbapenems [207].

Similarly, the repeated detection of MCR alleles (MCR-3.11, MCR-3.15, MCR-3.14) echoes global studies showing that environmental pollution serves as a key reservoir and dissemination pathway for colistin resistance genes [208].

However, divergences between the two sites point to localized microbial and ecological influences. Islamabad samples revealed more overlap between test and control lungs, indicating that background resistomes may be broadly present even without smog exposure. Lahore samples, however, exhibited highly distinct ARG patterns across datasets, with each group harboring unique resistance determinants. This heterogeneity may reflect differences in local pollution composition, microbial seeding from industrial or vehicular sources, and stochastic colonization events in lung microbiota [209].

Functionally, the ARGs detected spanned multiple antibiotic classes, highlighting the evolution of multidrug-resistant (MDR) phenotypes. The tet gene family (tet(32), tet(36), tet(X4), tet(O/M/O), tet(O/W)) confers tetracycline resistance, limiting options for respiratory and gastrointestinal infections. The van gene clusters (vanK, vanD, vanF, vanXY) drive glycopeptide resistance, severely undermining vancomycin therapy against Gram-positive pathogens [210]. Aminoglycoside-modifying enzymes (AAC(6')-Ib8, AAC(6')-Ij, AAC(3)-VIa) render aminoglycosides such as amikacin and gentamicin ineffective, reducing ICU treatment options. Efflux pump determinants (MexB, MexD, MexF, OpmB, mdtM, mdtO, facT) facilitate broad-spectrum resistance, while porins such as OmpA and OprA modulate membrane permeability, reducing drug uptake [211].

The mupA gene in S. aureus is especially alarming, as it complicates the management of skin and respiratory infections already difficult to treat under MDR conditions [212].

Collectively, these findings integrate into a clear narrative: smog exposure drives the enrichment of a multiclass resistome in the lungs, spanning β-lactams, colistin, aminoglycosides, tetracyclines, macrolides, and glycopeptides. The clinical implication is that bacteria inhabiting polluted airways are potentially resistant to nearly all frontline antibiotic classes, leaving few therapeutic options in the event of infection. This echoes recent reports demonstrating that airborne particulate matter can carry clinically relevant ARGs across urban environments and that inhalation exposure may establish these determinants within human or animal hosts [213, 214].

In sum, the combined analysis of Islamabad and Lahore rat lungs underscores that urban smog exposure acts not only as a chemical and oxidative stressor but also as a genetic driver of antimicrobial resistance. The convergence of β-lactamase and colistin resistance with efflux- and glycopeptide-mediated mechanisms highlights a worrying overlap between environmental pollution and the global AMR crisis. These results demonstrate that the lung microbiome under smog exposure can evolve into a potent reservoir of multidrug resistance, emphasizing the urgent need for environmental interventions to curb both pollution and the spread of ARGs.

The results of the behavioural assays would clearly show that exposure to smog has a significant impact on neurological function in rats. In the open field test, the animals under polluted conditions showed a significant reduction in locomotor activity, involving decrease speed, reduced time spent in the central zone, and changes in grooming behaviors. Likewise, the Y-maze test also identified impaired cognitive reactions and maps, with exposed animals having a higher rate of alternation rate of interrupted memory processes. In combination, these behavioural alterations confirm that smog exposure impairs both motor and cognitive functions, likely reflecting particulate matter- and gaseous pollutant-induced neurotoxic stress.

Histopathological study of lung tissues support the physiological overload of smog inhalation. Smog-exposed rats showed significant morphological changes, such as thickened alveolar septa, partial alveolar wall detachment, inflammatory cell

infiltration, and widening of alveolar spaces, all indicative of early emphysematous change. These are typical of chronic lung damage, demonstrating that prolonged exposure to smog damages normal lung morphology and induces inflammatory and fibrotic reactions. Such structural damage aligns with the observed behavioral deficits, suggesting that respiratory dysfunction may also contribute to systemic stress and impaired neurological performance.

Immunological assays provided further evidence of systemic effects, as smog-exposed groups showed marked increases in both CD4+ and CD8+ T cell populations compared to controls. The elevated percentages of these lymphocyte subsets indicate that pollutant exposure triggers adaptive immune activation, possibly as a response to the constant antigenic load and tissue damage caused by inhaled particles. This immune stimulation reflects not only localized lung inflammation but also systemic immunomodulation, which could predispose organisms to chronic inflammatory conditions or alter their resilience to infections.

Atlast, metagenomic analysis was found to show that smog exposure changes the lung's microbiome by decreasing overall diversity with an enrichment of potentially pathogenic bacterial species. Notably, the Islamabad and Lahore samples had a wide ranging resistome with the identification of clinically important antibiotic resistance genes like OXA-type β-lactamases, colistin resistance determinants (MCR types), tetracycline resistance genes, and efflux pump systems. Whereas Islamabad samples reflected overlapping ARGs in the control and exposed groups, Lahore samples showed a more heterogeneous and diverse resistome profile, that implies site-specific pressure driving microbial resistance. Collectively, these observations underscore the double threat of smog exposure: direct physiological damage to the host and augmentation of a microbial community carrying multidrug resistance factors.

The findings from Islamabad environmental isolates in 2022 give a vital insight into how airborne microbial communities correlated with fine particulate matter ($PM_{2.5}$) support and spread antibiotic resistance genes (ARGs). The resistome profile for the recent year showed consistent detection of glycopeptide resistance genes such as vanT, vanY, vanW, and vanH. These genes make a core region of

the van cluster that modifies the terminal D-Ala-D-Ala residues in peptidoglycan precursors, thus decreasing the affinity of vancomycin and other antibiotics. Their presence in environmental DNA indicates that vancomycin-resistant Enterococci (VRE) or related species are not only clinical challenges but are also embedded in environmental reservoirs.

The persistence of these genes outside hospital environments suggests strong selective pressures, possibly reinforced by the interplay of pollution, antibiotic residues, and microbial exchange, maintaining these resistance determinants in the urban air of Islamabad [215].

The 2022 profile also highlighted efflux-mediated resistance. Genes such as qacJ and qacG—belonging to the small multidrug resistance (SMR) family—are well known for their role in extruding disinfectants and antiseptics, particularly quaternary ammonium compounds, which are widely used in households, healthcare, and agriculture. Their prevalence in air particulates suggests that environmental bacteria in Islamabad are continuously exposed to disinfectant residues and other co-contaminants, which may co-select for resistance traits.

In addition, adeF, a member of the resistance-nodulation-division (RND) family efflux pumps, was identified. adeF is strongly associated with Acinetobacter baumannii, a pathogen of considerable clinical concern due to its multidrug-resistant profile [216]. The repeated recovery of adeF in outdoor air samples emphasizes that particulate matter may provide an efficient medium for the survival and dissemination of Acinetobacter-like organisms or their resistance genes, thereby creating a potential pathway for hospital-origin resistance determinants to persist in the broader environment.

Another gene consistently identified in the 2022 dataset was RbpA, which provides rifamycin resistance by protecting RNA polymerase from antibiotic inhibition. This gene is particularly concerning in the South Asian context, where rifampicin remains the backbone of tuberculosis therapy. The finding that RbpA was detectable in Islamabad's $PM_{2.5}$-associated microbial communities points toward the presence of rifamycin-resistant bacteria in the air. Given that Pakistan is

among the high-burden countries for tuberculosis, such environmental reservoirs of rifamycin resistance could complicate disease control by facilitating transmission of resistant traits between environmental microbes and pathogenic mycobacteria [217].

The 2023 resistome profile of Islamabad demonstrated a remarkable level of stability relative to 2022. The same predominant resistance determinants—vanT, vanY, vanW, vanH, qacJ, qacG, adeF, and RbpA—were repeatedly found to be identified, with least confirmation of expansion or diversification. This indicates that instead of being a transitory characteristic, these genes are part of a consistent, established core resistome of the city's airborne microbiome. That is, the microbial communities found in the smog in Islamabad seem to be at a state of balance in which the prevalence of ARGs is continuously sustained. The persistence of the van cluster indicates that vancomycin resistance remains a fixed feature of the resistome, while the ongoing detection of efflux pumps and RbpA underscores the chronic environmental pressures that reinforce both multidrug resistance and rifamycin resistance [218].

When these resistome data are contextualized with the air quality results from the same periods, the relationship becomes clearer. In November and December 2022, the mean AQI values in Islamabad were 143.8 and 185.1, respectively, with $PM_{2.5}$ concentrations rising to 72.9 $\mu g/m^3$ and 110.9 $\mu g/m^3$. These levels are classified as "unhealthy" by WHO standards and imply sustained exposure to particulate matter pollution. In 2023, AQI levels remained similar (149.6 in November and 184.4 in December), while $PM_{2.5}$ concentrations showed slight variation, measuring 80.0 $\mu g/m^3$ in November and 71.5 $\mu g/m^3$ in December. Interestingly, despite the modest decline in $PM_{2.5}$ between December 2022 and December 2023, the resistome profile did not exhibit notable change. This suggests that once ARGs have become established in the airborne microbial community, their persistence does not necessarily depend on short-term fluctuations in pollution levels but may be maintained through chronic, long-term environmental pressures [219].

The stability of Islamabad's resistome contrasts with patterns seen in cities like Lahore, where more extreme $PM_{2.5}$ levels corresponded with more dynamic shifts

and the emergence of unique ARGs. In Islamabad, however, moderate but continuous pollution exposure seems to sustain an entrenched resistome rather than drive diversification. This highlights an important aspect of environmental antibiotic resistance: while very high particulate levels can accelerate the acquisition and spread of new ARGs, even moderately high but persistent pollution can entrench existing resistance traits into microbial populations. Such persistence presents a silent but significant risk, as it ensures that resistance genes remain continuously available in the environment as a reservoir for horizontal gene transfer.

Overall, the Islamabad data from 2022 and 2023 together paint a picture of a resilient and persistent airborne resistome, dominated by glycopeptide resistance (van genes), rifamycin resistance (RbpA), and efflux-mediated multidrug resistance (qacJ, qacG, adeF).

These results demonstrate that even in the absence of year-to-year diversification, the continuous presence of these genes poses a chronic public health risk. The combination of persistent ARGs with consistently elevated AQI and $PM_{2.5}$ levels suggests that air pollution in Islamabad functions as both a carrier and a stabilizer of antibiotic resistance, embedding critical resistance determinants into the city's microbial ecosystem.

The analysis of antibiotic resistance profiles in Lahore's environmental isolates between 2022 and 2023 shows important trends that align with increasing environmental antibiotic resistance challenges. In 2022, isolates displayed a wide range of resistance determinants, including glycopeptide resistance genes such as vanT, vanO, vanM, vanD, vanH, vanG, and vanF, which collectively indicate extensive vancomycin resistance in Enterococci. This multi-gene presence reflects the global concern of glycopeptide resistance spreading in community and hospital environments, where environmental contamination acts as a reservoir for resistance determinants [220]. The simultaneous detection of RbpA, associated with rifamycin resistance, further suggests environmental persistence of Mycobacterium-related resistance traits, while adeF, a Resistance-Nodulation-Division (RND) efflux pump, contributes to fluoroquinolone and tetracycline resistance. Additional efflux-related genes such as qacJ and qacG expand resistance to disinfectants and

antiseptics, highlighting an alarming trend of resistance not only to antibiotics but also to commonly used cleaning and sterilization agents [221].

The detection of nimB, responsible for nitroimidazole resistance, indicates anaerobic resistance pathways, often linked to gastrointestinal pathogens. Together, these findings point toward a complex, multi-layered resistance landscape in Lahore during 2022.

By 2023, the resistance profile revealed both continuity and new developments. Glycopeptide resistance genes remained prominent, with consistent detection of vanY, vanW, vanT, vanR, and vanH, indicating ongoing selective pressure from environmental contamination and human use of glycopeptides. The persistence and expansion of van gene clusters across consecutive years suggests an environmental stabilization of resistant Enterococci, which is especially concerning because these genes can be horizontally transferred between bacterial populations [222].

The RbpA gene continued to be detected, confirming sustained rifamycin resistance, while qacJ and adeF were again identified, demonstrating persistence of efflux-mediated multidrug resistance. Notably, in 2023 a new resistance marker, OXA-50, was identified, representing beta-lactam resistance commonly associated with Pseudomonas aeruginosa. The detection of OXA-50 in environmental samples marks a significant shift, as it suggests that resistance to frontline beta-lactam therapies is becoming more widespread in environmental reservoirs. This emergence likely reflects both clinical overuse and environmental dissemination of resistant Pseudomonas strains [223].

When comparing the two years, Lahore's data indicate that not only are the determinants of resistance continuing but they are also diversifying. The 2022 profiles indicated wider resistance diversity, and this included nitroimidazole resistance (nimB), which was not seen in 2023. Nevertheless, the 2023 isolates yielded beta-lactam resistance (OXA-50), which was not found in 2022, indicating an evolutionary trend toward clinically important resistance classes. This trade-off in beta-lactam resistance gain and loss of nitroimidazole resistance reflects the dynamic adaptability of environmental bacterial populations to alternating selective

pressures [224]. Notably, the occurrence of efflux pump genes in combination with glycopeptide and beta-lactam resistance reflects multi-drug resistance phenotypes that remarkably implicate therapeutic choices.

Environmental monitoring suggests that Lahore's consistently high $PM_{2.5}$ and AQI levels (as previously discussed) may provide a conducive environment for resistance selection and dissemination. Particulate matter can act as a carrier of resistant bacteria and mobile genetic elements, supporting the persistence of ARGs in ambient air [225].

The correlation between poor air quality and elevated resistance genes, particularly OXA-type beta-lactamases and glycopeptide clusters, suggests that air pollution not only affects respiratory health directly but also facilitates the environmental spread of antimicrobial resistance.

Taken together, Lahore's AMR gene profiling over 2022–2023 emphasizes both continuity in resistance determinants such as glycopeptides, rifamycin, and efflux-mediated pathways, as well as the alarming emergence of new resistance markers like OXA-50. This progression highlights the dual challenge of tackling persistent resistance genes while also monitoring for newly emerging ones, especially under sustained environmental stressors such as smog and high $PM_{2.5}$ levels.

The resistome of Okara's environmental isolates during 2022 revealed a complex but stable set of antimicrobial resistance genes (ARGs). Prominently, several glycopeptide resistance genes, including vanY, vanT, and vanH, were detected across different clusters. These genes encode mechanisms of target alteration, which prevent glycopeptide antibiotics such as vancomycin from binding effectively to bacterial cell wall precursors, thereby conferring high-level resistance.

The presence of multiple van cluster genes indicates that vancomycin resistance determinants are not only present in clinical environments but also embedded within airborne microbial communities of Okara [226]. The detection of poxtA further highlights ribosomal protection mechanisms, associated with resistance to phenicols, tetracyclines, and oxazolidinones, which broadens the threat profile of these isolates [227].

In addition to target-alteration genes, efflux systems were strongly represented in 2022. The RND efflux pump rsmA was identified, which can export structurally diverse antibiotics including fluoroquinolones and phenicols [228]. Similarly, the SMR efflux pumps qacJ and qacG were present, which confer resistance to disinfectants and antiseptics such as quaternary ammonium compounds—agents frequently used in healthcare and community settings [229]. The detection of adeF, another RND efflux gene conferring resistance to tetracyclines and fluoroquinolones, further supports the notion that Okara's environmental microbiota possess multidrug efflux capacity [230]. The co-occurrence of RND and SMR efflux pathways reflects strong environmental selection pressures that favor survival against multiple chemical stressors, including air pollutants and anthropogenic antimicrobials.

By 2023, the resistance pattern was still relatively constant. The stability of glycopeptide resistance genes (vanY, vanW, vanT, vanH) reflects ongoing selective pressure for vancomycin resistance. RbpA detection is also significant, imparting rifamycin resistance by protecting RNA polymerase against antibiotic binding [231]. The stability of efflux determinants—especially qacJ, qacG, and adeF—indicates ongoing multidrug resistance characteristics among Okara's airborne microbial communities. This year-to-year stability shows that, have been established, ARG reservoir may persist in local atmospheric microbiota under constant environmental pressures and anthropogenic activities [232].

In comparison between the two years, no additions of strange esistance classes were seen, as opposed to Lahore, where beta-lactam resistance spread in 2023. Rather, Okara's resistome supports a stable, established profile that is dominated by glycopeptide and efflux resistance determinants. This is suggestive of Okara's microbial community having already adapted to local conditions and persisting with its resistance extent over time. The repetitive finding of both efflux (RND and SMR) and vancomycin resistance determinants stresses the stability of this resistome [233].

The data correlation with air pollution also supports these results. Concentrations of Okara's $PM_{2.5}$ (67–99 $\mu g/m^3$) and AQI values (172–214) were in a relatively to extremely polluted level. Previous studies support the fact that particulate matter

can be used as carriers for ARGs and resistant bacteria, where their survival and spread to different environmental niches are made possible [234]. Efflux pump genes qacJ and qacG, which are resistant to disinfectants and antiseptics, have previously been shown to be co-selected under pollutant stress, which implies that environmental pollutants have a direct impact on ARG survival [235].

Therefore, although Okara's burden of pollution is low compared to Lahore, the ubiquitous resistome indicates that moderate but chronic air pollution is enough to provide a stable source of airborne microbial ARGs [236].

Together, the results suggest that Okara's environmental isolates possess a mature, multidrug-resistant resistome, with stable persistence of glycopeptide, efflux, and rifamycin resistance determinants. This raises possible hazards of horizontal gene transfer to clinically relevant pathogens, thus confounding future therapeutic effects and further establishing the need for urgent monitoring and decrease strategies [237].

The interplay between microbial adaptation and environmental pressures is reflected in the antibiotic resistance profiles of environmental isolates from Islamabad, Lahore, and Okara. These profiles show both commonalities and distinct city-specific variations.

In all three cities, glycopeptide resistance determinants from the van clusters (vanT, vanY, vanW, vanH) were found constantly. This suggests a region-wide existence of vancomycin resistance and how these determinants have become a part of environmental microbial communities. Likewise, efflux pump determinants like qacJ, qacG, and adeF were detected in all populations, suggesting that efflux-mediated resistance is an intrinsic survival mechanism in microbial communities within polluted environments. These similarities indicate that baseline resistance to glycopeptides and to several antibiotics is now an innate environmental attribute in urban Pakistan.

Despite these similarities, the trajectories of resistance evolution differ among the cities. In Islamabad, the resistome displayed relative stability across 2022

and 2023, with repeated detection of glycopeptide resistance genes, RbpA for rifamycin resistance, and efflux pumps. No major diversification into new classes of resistance was noted, suggesting that while pollution maintains entrenched resistance, the evolutionary pressures here are not driving rapid expansion of genetic diversity.

In contrast, Lahore exhibited the most dynamic and diverse resistome. In 2022, its profile already included multiple glycopeptide resistance genes, RbpA, nimB for nitroimidazole resistance, and efflux determinants. By 2023, new elements such as the regulatory gene vanR and OXA-50 beta-lactamase had emerged, broadening the resistance spectrum to include beta-lactam antibiotics. This indicates that Lahore's microbial populations are under stronger selection pressure, likely driven by its consistently extreme $PM_{2.5}$ concentrations and AQI values, which exceeded those of the other cities. This higher pollution burden may accelerate horizontal gene transfer and the emergence of multidrug-resistant determinants.

Okara, while similar to Islamabad in showing a relatively stable resistome, differed in maintaining a broad combination of efflux mechanisms. Both SMR (qacJ, qacG) and RND (adeF, rsmA) families were consistently detected, together providing resilience against antibiotics, disinfectants, and pollutants. The appearance of poxtA in 2022 and the persistence of RbpA in 2023 further illustrate how Okara's resistome, though not expanding like Lahore's, is robust and well-adapted to survive under chronic environmental pressures.

When compared directly, the three cities illustrate a spectrum of environmental resistance dynamics. Islamabad represents stability, where resistance determinants are entrenched but not diversifying. Lahore illustrate varieties, with the appearance over time of new and clinically relevant genes. Okara demonstrates strong persistence, where overspreading resistance mechanisms are sustained by multiple mechanisms to maintain a resistant resistome without significant change. Combined, these contrasts highlight how differences in air quality and local environmental stress may influence the direction and magnitude of antibiotic resistance evolution from region to region.

The examination of extracellular DNA (exDNA) from $PM_{2.5}$ samples yielded important information regarding the expression of ARGs in Islamabad, Lahore, and Okara. exDNA is also a dynamic reservoir of ARGs and is centrally involved in the environmental dissemination of antimicrobial resistance via horizontal gene transfer, so its study has special significance in contaminated urban areas [238].

Expression profiles showed that city-specific and gene-specific differences existed, which reflected how local pollution levels and microbial community dynamics regulate ARGs.

The blaCTX-M-32 gene had mixed patterns of expression in Islamabad, with both upregulation and downregulation being reported, suggesting fluctuating selective pressures on ESBL-producing bacteria. Samples from Lahore had primarily downregulated expression, while Okara had robust downregulation, demonstrating inhibited activity of this clinically relevant gene. Earlier research emphasizes the stability of blaCTX-M variants in both clinical and environmental environments, which underscores the ability of environmental reservoirs to facilitate ESBL spread even beyond the healthcare system [239, 240]. Reduced activity in Okara and Lahore can be indicative of greater environmental pressures repressing ESBL stability at these locations.

The blaNDM-1 gene, which provides resistance to carbapenems, was found to be largely downregulated in Islamabad and Okara but relatively more expressed in Lahore. This is of clinical concern since blaNDM-1 is associated with multidrug-resistant Enterobacteriaceae [241]. The increased activity in Lahore could be due to its higher pollution load, as it has a consistently higher AQI and $PM_{2.5}$ levels, which can generate selective pressures that favor the carriage of carbapenem resistance genes [242]. In contrast, the downregulation in Islamabad and Okara could be an indication of reduced ecological support for blaNDM-1 activity under such conditions.

The blaTEM gene had predominantly upregulated expression in Islamabad, moderate downregulation in Lahore, and extreme downregulation in Okara. These results indicate that Islamabad's air microbiome is more supportive of persistence

of penicillin and early cephalosporin resistance genes, whereas Okara's environment is less supportive. The blaTEM-F variant was minimally or not significantly altered in Islamabad and Lahore but was highly downregulated in Okara. These results concur with reports implicating blaTEM persistence in more active in urban settings [243, 244].

The intI1 gene, a horizontal gene transfer marker, was upregulated in Islamabad but downregulated in Lahore and Okara. This is notable since intI1 has been used as a reference for ARG mobility [245].

Its upregulation in Islamabad reveals higher potential for horizontal transfer of resistance genes, whereas downregulation in Lahore and Okara reveals lower transfer potential. Likewise, sul1, which tends to occur in combination with intI1, did not significantly alter in Islamabad but was greatly downregulated in Lahore and Okara, indicating reduced sulfonamide resistance in these environments [246].

The tnpA transposase gene was moderately upregulated in Islamabad but uniformly downregulated in Lahore and Okara, indicating that Islamabad continues to promote transposon-mediated ARG, while the other two cities fail to do so. This is in agreement with earlier reports that environmental stress factors drive transposon activity [247].

The vanA gene was upregulated in Islamabad and Okara but downregulated in Lahore, whereas vanRA was upregulated in Islamabad but significantly downregulated in Lahore and Okara. These van genes confer glycopeptide resistance, notably vancomycin resistance, and their survival in Islamabad and Okara indicates a disconcerting environmental reservoir of resistance to antibiotics [248].

Taken together, the comparative analysis reveals distinct expression dynamics across the three cities. Islamabad showed mixed expression patterns, including upregulation of blaTEM, intI1, vanA, and vanRA, suggesting a higher adaptive capacity for ARG persistence and transfer under fluctuating pollution pressures. Lahore exhibited broad downregulation of most ARGs, though blaNDM-1 remained relatively active, indicating selective dominance of carbapenem resistance

under severe pollution conditions. Okara displayed consistent strong downregulation across most genes, suggesting reduced overall ARG activity, although vanA remained upregulated, highlighting persistence of glycopeptide resistance. These results confirm that exDNA in $PM_{2.5}$ not only harbors resistance determinants but also exhibits environment-dependent expression, which is shaped by urbanization, pollution stress, and local microbial communities [249].

The combined analysis of internal and external DNA provides a clear picture of antibiotic resistance dynamics across the three cities. Internal DNA, obtained through metagenomics, shows the reservoir of resistance genes present in $PM_{2.5}$, while external DNA, analyzed through real-time PCR, reflects which of these genes are actively regulated. Together, they reveal not only the presence of resistance determinants but also their potential functional activity in polluted air.

In Islamabad, a stable resistome was observed, with key glycopeptide resistance genes (vanH, vanT, vanW, vanY), efflux pumps (adeF, qacJ, qacG), and rifamycin resistance genes consistently present. External DNA results further showed upregulation of genes such as blaTEM, intI1, vanA, and vanRA, indicating that several of these genes are not just present but actively expressed. This suggests a high potential for horizontal gene transfer and ongoing resistance activity in the air microbiome.

Lahore, which consistently had the highest AQI and $PM_{2.5}$ values, displayed the broadest diversity of resistance genes in internal DNA, including glycopeptide, beta-lactamase, and efflux-associated genes. However, external DNA analysis showed that many of these genes were downregulated, with the exception of blaNDM-1, which remained actively expressed. This suggests that while Lahore's environment supports a wide range of resistance genes, only the most clinically significant ones are maintained at high expression levels under extreme pollution stress.

In Okara, resistance genes such as glycopeptide clusters, efflux pumps, and poxtA were consistently detected across both years, showing stability in genetic reservoirs. Yet, external DNA expression analysis revealed strong downregulation for

most genes, with only vanA showing clear upregulation. This indicates that although the genetic potential for resistance exists in Okara, the functional expression of these genes is comparatively suppressed.

Overall, Islamabad shows both gene richness and active expression, Lahore harbors the most diverse resistome but with selective expression, and Okara demonstrates gene presence with widespread suppression of activity. These patterns align with air quality data, suggesting that pollution levels strongly influence not only the presence but also the activity of airborne resistance genes.

Taken together, the animal exposure study, along with the internal and external DNA analysis of $PM_{2.5}$, highlights the serious implications of air pollution in driving antimicrobial resistance. The animal model confirmed that inhalation of polluted air alters respiratory microbiota and promotes antibiotic-resistant bacteria, reflecting real biological impacts. Internal DNA analysis established that $PM_{2.5}$ carries a wide array of resistance genes, serving as reservoirs of antimicrobial resistance in the environment. External DNA results further revealed that many of these genes are not only present but actively expressed, with city-specific differences in regulation. Islamabad showed strong expression activity, Lahore exhibited broad genetic diversity with selective expression of clinically significant genes, and Okara demonstrated suppressed activity despite gene presence. Together, these findings emphasize that polluted air is not just a carrier of resistance genes but an active driver of their transmission and regulation, posing a dual threat to environmental and public health.

Chapter 6

Conclusion and Future Prospects

The long-term exposure of rats to smog uncovered deep and multi-faceted health effects, supporting the multidimensional risks of extended air pollution. Behavioral tests showed predominant neurological damage, with exposed rats showing decreased locomotor activity, depressed exploratory drive, and adverse memory performance. These alterations indicate that airborne contaminants directly impair cognitive and motor function, most likely acting through neuroinflammatory mechanisms. Immunologic profiling also supported this association, with increased CD4+ helper and CD8+ cytotoxic T-cell counts. Such chronic immune activation is indicative of a pro-inflammatory state, which not only seeks to counteract pollutant-induced tissue damage but also has the potential to worsen immune-mediated injury to host tissues. Histopathological analysis of lung tissues supported these observations, with alveolar wall thickening, congestion, heightened mucus secretion, and dense inflammatory cell infiltrates. These pathological changes confirm that smog exposure disturbs pulmonary architecture, impairs gas exchange, and renders the respiratory system more vulnerable to secondary infection. Accompanying these pathological and physiological alterations, lung metagenomic sequencing revealed a dramatic reduction in microbial diversity and a significant shift in community structure. Of particular interest, smog exposure promoted the growth of opportunistic pathogens like Pseudomonas, Acinetobacter,

and Stenotrophomonas, while at the same time enriching the abundance and expression of antibiotic resistance genes. This biphenotypic phenomenon—microbial dysbiosis and resistome expansion—emphasizes smog's ability not only to impair host defenses but also to create a microenvironment that facilitates antibiotic-resistant infections. Together, these results highlight that chronic exposure to smog in animal models causes integrated disturbances of the neurological, immunological, histological, and microbiological levels. Through triggering behavioral impairment, systemic inflammation, lung damage, and disruption of microbiota, smog acts as an all-around health risk factor. Such a rat model therefore offers important mechanistic information on how urban air pollution decays health and highlights the necessity for swift interventions directed at mitigating both direct and indirect effects of exposure to smog.

The comparative analysis of internal and external DNA across the regions of Islamabad, Lahore, and Okara reveals critical insights into the dynamics of antibiotic resistance mechanisms. Notably, there is no evidence of resistance gene uptake from external DNA into the internal genomes across all samples from Islamabad, indicating a lack of horizontal gene transfer in this region. This pattern is consistent across various resistance markers, including multiple β-lactamases and vancomycin resistance genes, suggesting that the internal resistance capabilities are intrinsic to the bacterial populations present. The internal gene summary highlights the presence of diverse antibiotic resistance genes (AMR genes) in different regions and years, with Islamabad consistently showing a core set of resistance genes in both 2022 and 2023. Lahore stands out with its rich diversity of AMR genes, particularly in 2022, where various clusters of vancomycin resistance genes are identified, indicating a complex resistance landscape. Although the variety of AMR genes is somewhat reduced in 2023, the presence of significant resistance determinants persists. Okara's AMR profile is consistent across both years, featuring similar resistance genes such as vanY and vanH, albeit with less diversity than Lahore. Overall, while the internal AMR gene profiles reflect substantial resistance capabilities, the absence of external gene uptake suggests that these resistance traits are largely inherent to the local bacterial strains rather than acquired from external sources. This finding underscores the necessity for ongoing

surveillance and research to better understand the mechanisms of antibiotic resistance in these regions, as well as to inform strategies for managing and mitigating antibiotic resistance effectively [227].

The findings of this study reveal a significant gap in the overlap between internal and external antimicrobial resistance (AMR) genes, highlighting an often-overlooked area in AMR research: the role of environmental DNA as a distinct reservoir for resistance genes. Many studies focus only on internal DNA, missing the broader context provided by environmental DNA, which holds diverse ARGs that can potentially spread into clinical populations [228]. Environmental sources such as soil, water, and air act as reservoirs where antimicrobial resistance genes circulate and may later transfer to pathogenic populations. Recognizing this dimension is essential for a comprehensive understanding of how ARGs evolve and proliferate, especially given the selective pressures present in environments like agriculture and wastewater systems [229]. The results of this study may not be as broadly helpful as they could be due to the small sample size and limited seasonality coverage. Direct clinical significance is further limited by the use of rat models and the lack of data on human exposure. For wider applicability, these factors should be covered in future research.

This study effectively fulfilled the stated research objectives by demonstrating the diverse health impacts of smog exposure in rats. Behavioral assessment showed significant lethargy and reduced responsiveness. Histopathological analysis of lung tissue revealed alveolar thickening, congestion, and inflammatory infiltration, indicating clear respiratory damage. Immunologically, smog exposure triggered a marked rise in CD4+ and CD8+ lymphocyte percentages—CD4+ increased up to 37.04% and CD8+ up to 28.81%—signaling immune system activation and po-tential systemic inflammation. Metagenomic profiling revealed the presence of high-risk antibiotic resistance genes (ARGs) in both rat lung tissues and airborne particulate matter during smog events. Detected ARGs included MCR, CTX-M, van clusters, mecA, blaIMP, and efflux pump genes (MexF, acrA), many of which were associated with pathogens like *Acinetobacter baumannii, Staphylococcus aureus* and *Enterobacter cloacae*. Together, these findings highlight the

dual biological hazard of smog—causing direct physiological damage and serving as a vector for antimicrobial resistance. The absence of external DNA analysis in many AMR studies limits the effectiveness of AMR surveillance, intervention strategies, and predictive models. Environmental DNA can reveal patterns and hotspots of ARGs that may later affect human health. Expanding AMR surveillance to include external DNA sources would allow public health agencies to track and mitigate ARGs more effectively. Additionally, incorporating this data into predic-tive models would yield a more accurate picture of AMR transmission dynamics, informing proactive policies that reduce ARG transfer risks. This study advocates a shift in AMR research to incorporate both internal and external DNA analysis, offering a more holistic approach to understanding and combating antimicrobial resistance across ecosystems. The study draws attention to the need it is of including ARG monitoring into cities air quality management and environmental surveillance. Stronger antibiotic regulations and planning techniques to lower threats to the public's health are supported by these findings. These findings also highlight the need for immediate attention to policy creation and enforcement in nations such as Pakistan, where appropriate monitoring and implementation measures are missing.

6.1 Future Prospects

Our latest findings, which demonstrated the substantial effects of pollution on the physiology and immunology of animals in Lahore and Islamabad, indicate the pressing need for additional molecular-level research. These results highlight the importance of smog as a major environmental issue on a global scale and call for a better understanding of its consequences in order to create focused solu- tions. Investigating the molecular processes that underlie the negative impacts of pollution on human health can lead to fresh discoveries and creative solutions. According to the results, it is advised that qPCR-based ARG tracking be used in conjunction with monthly air sampling in smog-affected areas in order to follow resistance trends. Assessment of human exposure and seasonal sampling should be part of

future research to investigate long-term impacts. The health hazards associated with airborne antibiotic resistance should be addressed by promoting the use of metagenomic analysis in environmental surveillance, raising public awareness, and applying policies. Funding this research is essential for developing environmental and public health solutions globally, since smog continues to be a major health hazard. Given that environmental sources are important reservoirs for antimicrobial resistance genes, this study emphasizes the need of integrating external DNA analysis into AMR research. Based on the rising air pollution, smog and the re-lated health implications. There is an urgent need to work on the implementation of policies effectively. The existing policies have already been made based on the 133 practicability and feasibility. A more comprehensive knowledge of AMR dynam-ics is made possible by considering both internal and external DNA. This helps to improve surveillance, intervention tactics, and predictive models for fighting resistance in a variety of ecosystems.

Bibliography

[1] S. Abdul Jabbar, L. Tul Qadar, S. Ghafoor, L. Rasheed, Z. Sarfraz, A. Sarfraz, M. Sarfraz, M. Felix, and I. Cherrez-Ojeda, "Air quality, pollution and sustainability trends in south asia: a population-based study," *International Journal of Environmental Research and Public Health*, vol. 19, no. 12, p. 7534, 2022.

[2] U. Asghar, S. Rafiq, A. Anwar, T. Iqbal, A. Ahmed, F. Jamil, M. S. Khurram, M. M. Akbar, A. Farooq, N. S. Shah, *et al.*, "Review on the progress in emission control technologies for the abatement of co2, sox and nox from fuel combustion," *Journal of Environmental Chemical Engineering*, vol. 9, no. 5, p. 106064, 2021.

[3] P. Srinamphon, S. Chernbumroong, and K. Y. Tippayawong, "The effect of small particulate matter on tourism and related smes in chiang mai, thailand," *Sustainability*, vol. 14, no. 13, p. 8147, 2022.

[4] Y. Xue, L. Wang, Y. Zhang, Y. Zhao, and Y. Liu, "Air pollution: A culprit of lung cancer," *Journal of hazardous materials*, vol. 434, p. 128937, 2022.

[5] M. Li, M. Hu, L. Jiang, J. Pei, and C. Zhu, "Trends in cancer incidence and potential associated factors in china," *JAMA Network Open*, vol. 7, no. 10, pp. e2440381–e2440381, 2024.

[6] W. H. Organization, "Review of evidence on health aspects of air pollution: Revihaap project: technical report," report, World Health Organization. Regional Office for Europe, 2021.

[7] G. O. Ofremu, B. Y. Raimi, S. O. Yusuf, B. A. Dziwornu, S. G. Nnabuife, A. M. Eze, and C. A. Nnajiofor, "Exploring the relationship between climate change, air pollutants and human health: impacts, adaptation, and mitigation strategies," *Green Energy and Resources*, p. 100074, 2024.

[8] F. Wang, L. Xiang, K. S.-Y. Leung, M. Elsner, Y. Zhang, Y. Guo, B. Pan, H. Sun, T. An, G. Ying, *et al.*, "Emerging contaminants: a one health perspective," *The Innovation*, vol. 5, no. 4, 2024.

[9] M. S. B. Pena and A. Rollins, "Environmental exposures and cardiovascular disease: a challenge for health and development in low-and middle-income countries," *Cardiology clinics*, vol. 35, no. 1, pp. 71–86, 2017.

[10] J. Saini, M. Dutta, and G. Marques, "Indoor air quality monitoring systems based on internet of things: A systematic review," *International journal of environmental research and public health*, vol. 17, no. 14, p. 4942, 2020.

[11] I. Parajuli, H. Lee, and K. R. Shrestha, "Indoor air quality and ventilation assessment of rural mountainous households of nepal," *International journal of sustainable built environment*, vol. 5, no. 2, pp. 301–311, 2016.

[12] Q. Zhang, X. Meng, S. Shi, L. Kan, R. Chen, and H. Kan, "Overview of particulate air pollution and human health in china: Evidence, challenges, and opportunities," *The Innovation*, vol. 3, no. 6, 2022.

[13] R. Dar, S. Tanvir-ul Hassan Dar, and H. Dar, "the impacts of environmental iot-based models for: Sustainable environmental," *IoT-based Models for: Sustainable Environmental Management*, vol. 227, p. 15, 2024.

[14] J. Xie, L. Jin, T. He, B. Chen, X. Luo, B. Feng, W. Huang, J. Li, P. Fu, and X. Li, "Bacteria and antibiotic resistance genes (args) in pm2. 5 from china: implications for human exposure," *Environmental science and technology*, vol. 53, no. 2, pp. 963–972, 2018.

[15] A. Kaun and J. Uldam, "Digital activism: After the hype," *New Media and Society*, vol. 20, no. 6, pp. 2099–2106, 2018.

[16] W. Thomas and A. M. M. Daud, "Impact of meteorological conditions on airborne particulates (pm2.5 and pm10) concentration on universiti tun hussein onn malaysia (uthm) ambient: Humidity: Humidity," *Journal of Advancement in Environmental Solution and Resource Recovery*, vol. 2, no. 1, pp. 44–50, 2022.

[17] T. Münzel, M. Molitor, M. Kuntic, O. Hahad, M. Röösli, N. Engelmann, M. Basner, A. Daiber, and M. Sørensen, "Transportation noise pollution and cardiovascular health," *Circulation research*, vol. 134, no. 9, pp. 1113–1135, 2024.

[18] Y. Yu, C. Dai, Y. Wei, H. Ren, and J. Zhou, "Air pollution prevention and control action plan substantially reduced pm2. 5 concentration in china," *Energy Economics*, vol. 113, p. 106206, 2022.

[19] S. A. Stansfeld, "Noise effects on health in the context of air pollution exposure," *International journal of environmental research and public health*, vol. 12, no. 10, pp. 12735–12760, 2015.

[20] I. Manisalidis, E. Stavropoulou, A. Stavropoulos, and E. Bezirtzoglou, "Environmental and health impacts of air pollution: a review," *Frontiers in public health*, vol. 8, p. 14, 2020.

[21] G. D'amato, R. Pawankar, C. Vitale, M. Lanza, A. Molino, A. Stanziola, A. Sanduzzi, A. Vatrella, and M. D'amato, "Climate change and air pollution: effects on respiratory allergy," *Allergy, asthma and immunology research*, vol. 8, no. 5, pp. 391–395, 2016.

[22] K. Smith, C. J. Fearnley, D. Dixon, D. K. Bird, and I. Kelman, *Environmental hazards: assessing risk and reducing disaster*. Routledge, 2023.

[23] F. Castelli and G. Sulis, "Migration and infectious diseases," *Clinical Microbiology and Infection*, vol. 23, no. 5, pp. 283–289, 2017.

[24] M. Nasar-u Minallah, M. Zainab, and M. Jabbar, "Exploring mitigation strategies for smog crisis in lahore: a review for environmental health, and

policy implications," *Environmental Monitoring and Assessment*, vol. 196, no. 12, p. 1269, 2024.

[25] G. Wielgosiński and J. Czerwińska, "Smog episodes in poland," *Atmosphere*, vol. 11, no. 3, p. 277, 2020.

[26] Q. Ying, M. P. Fraser, R. J. Griffin, J. Chen, and M. J. Kleeman, "Verification of a source-oriented externally mixed air quality model during a severe photochemical smog episode," *Atmospheric Environment*, vol. 41, no. 7, pp. 1521–1538, 2007.

[27] F. Dong, Y. Pan, Y. Li, and S. Zhang, "How public and government matter in industrial pollution mitigation performance: Evidence from china," *Journal of Cleaner Production*, vol. 306, p. 127099, 2021.

[28] M. Zhou, G. He, M. Fan, Z. Wang, Y. Liu, J. Ma, Z. Ma, J. Liu, Y. Liu, and L. Wang, "Smog episodes, fine particulate pollution and mortality in china," *Environmental research*, vol. 136, pp. 396–404, 2015.

[29] J. Chen, H. Chen, Z. Wu, D. Hu, and J. Z. Pan, "Forecasting smog-related health hazard based on social media and physical sensor," *Information Systems*, vol. 64, pp. 281–291, 2017.

[30] Z. Yang and J. Wang, "A new air quality monitoring and early warning system: Air quality assessment and air pollutant concentration prediction," *Environmental research*, vol. 158, pp. 105–117, 2017.

[31] G. Wielgosiński and J. Czerwińska, "Smog episodes in poland," *Atmosphere*, vol. 11, no. 3, p. 277, 2020.

[32] F. Dong, Y. Pan, Y. Li, and S. Zhang, "How public and government matter in industrial pollution mitigation performance: Evidence from china," *Journal of Cleaner Production*, vol. 306, p. 127099, 2021.

[33] I. Naureen, A. Saleem, S. Aslam, L. Zakir, A. Mukhtar, R. Nazir, and S. Zulqarnain, "Potential impact of smog on human health," *Haya Saudi J Life Sci*, vol. 7, no. 3, pp. 78–84, 2022.

[34] Q. Ying, M. P. Fraser, R. J. Griffin, J. Chen, and M. J. Kleeman, "Verification of a source-oriented externally mixed air quality model during a severe photochemical smog episode," *Atmospheric Environment*, vol. 41, no. 7, pp. 1521–1538, 2007.

[35] W. Raza, S. Saeed, H. Saulat, H. Gul, M. Sarfraz, C. Sonne, Z.-H. Sohn, R. J. Brown, and K.-H. Kim, "A review on the deteriorating situation of smog and its preventive measures in pakistan," *Journal of Cleaner Production*, vol. 279, p. 123676, 2021.

[36] G. Wielgosinski, J. Czerwinska, O. Namiecinska, and R. Cichowicz, "Smog episodes in the lodz agglomeration in the years 2014-17," in *E3S web of conferences*, vol. 28, p. 01039, EDP Sciences.

[37] J. S. Pastuszka, W. Rogula-Kozlowska, and E. Zajusz-Zubek, "Characterization of pm10 and pm2. 5 and associated heavy metals at the crossroads and urban background site in zabrze, upper silesia, poland, during the smog episodes," *Environmental Monitoring and Assessment*, vol. 168, no. 1, pp. 613–627, 2010.

[38] L. Zhang, Y. Yang, Y. Li, Z. M. Qian, W. Xiao, X. Wang, C. A. Rolling, E. Liu, J. Xiao, and W. Zeng, "Short-term and long-term effects of pm2. 5 on acute nasopharyngitis in 10 communities of guangdong, china," *Science of the Total Environment*, vol. 688, pp. 136–142, 2019.

[39] I. Kloog, B. Ridgway, P. Koutrakis, B. A. Coull, and J. D. Schwartz, "Long- and short-term exposure to pm2. 5 and mortality: using novel exposure models," *Epidemiology (Cambridge, Mass.)*, vol. 24, no. 4, p. 555, 2013.

[40] I. Manisalidis, E. Stavropoulou, A. Stavropoulos, and E. Bezirtzoglou, "Environmental and health impacts of air pollution: a review," *Frontiers in public health*, vol. 8, p. 14, 2020.

[41] S. Sivakumar and V. Ramya, "A review on air quality parameters for ambient pollution management framework," *REVISTA GEINTEC-GESTAO INOVACAO E TECNOLOGIAS*, vol. 11, no. 4, pp. 149–181, 2021.

[42] N. Boschi, *Defining an educational framework for indoor air sciences education*, pp. 3–6. Springer, 1999.

[43] I. Manisalidis, E. Stavropoulou, A. Stavropoulos, and E. Bezirtzoglou, "Environmental and health impacts of air pollution: a review," *Frontiers in public health*, vol. 8, p. 14, 2020.

[44] Y. Zhu, J. Xie, F. Huang, and L. Cao, "Association between short-term exposure to air pollution and covid-19 infection: Evidence from china," *Science of the total environment*, vol. 727, p. 138704, 2020.

[45] K. Cheung, N. Daher, W. Kam, M. M. Shafer, Z. Ning, J. J. Schauer, and C. Sioutas, "Spatial and temporal variation of chemical composition and mass closure of ambient coarse particulate matter (pm10-2.5) in the los angeles area," *Atmospheric environment*, vol. 45, no. 16, pp. 2651–2662, 2011.

[46] S. Fares, R. Vargas, M. Detto, A. H. Goldstein, J. Karlik, E. Paoletti, and M. Vitale, "Tropospheric ozone reduces carbon assimilation in trees: estimates from analysis of continuous flux measurements," *Global Change Biology*, vol. 19, no. 8, pp. 2427–2443, 2013.

[47] G. Lorenzini and C. Saitanis, "Ozone: a novel plant "pathogen"," in *Abiotic stresses in plants*, pp. 205–229, Springer, 2003.

[48] A. Ahuja and D. Mathpal, "An overview on effect of air pollution on human health," *ACADEMICIA: An International Multidisciplinary Research Journal*, vol. 11, no. 11, pp. 861–868, 2021.

[49] D. Zhan, M.-P. Kwan, W. Zhang, X. Yu, B. Meng, and Q. Liu, "The driving factors of air quality index in china," *Journal of Cleaner Production*, vol. 197, pp. 1342–1351, 2018.

[50] A. Abelsohn and D. M. Stieb, "Health effects of outdoor air pollution: approach to counseling patients using the air quality health index," *Canadian Family Physician*, vol. 57, no. 8, pp. 881–887, 2011.

[51] S. E. Mousavi, J. M. Delgado-Saborit, A. Adivi, S. Pauwels, and L. Godderis, "Air pollution and endocrine disruptors induce human microbiome imbalances: A systematic review of recent evidence and possible biological mechanisms," *Science of The Total Environment*, p. 151654, 2021.

[52] G. Xiong and Y. Luo, "Smog, media attention, and corporate social responsibility-empirical evidence from chinese polluting listed companies," *Environmental Science and Pollution Research*, pp. 1–14, 2021.

[53] H. Parsajou and T. Nasrabadi, "Evaluation of greenhouse gases emission and human health risk levels due to operation and maintenance of sareyn city wastewater treatment plant," *Journal of Environmental Studies*, vol. 47, no. 1, pp. 45–64, 2021.

[54] X. Sun, D. Li, B. Li, S. Sun, J. Geng, L. Ma, and H. Qi, "Exploring the effects of haze pollution on airborne fungal composition in a cold megacity in northeast china," *Journal of Cleaner Production*, vol. 280, p. 124205, 2021.

[55] T. Qin, F. Zhang, H. Zhou, H. Ren, Y. Du, S. Liang, F. Wang, L. Cheng, X. Xie, A. Jin, *et al.*, "High-level pm2. 5/pm10 exposure is associated with alterations in the human pharyngeal microbiota composition," *Frontiers in microbiology*, vol. 10, p. 422859, 2019.

[56] N. Qin, P. Liang, C. Wu, G. Wang, Q. Xu, X. Xiong, T. Wang, M. Zolfo, N. Segata, and H. Qin, "Longitudinal survey of microbiome associated with particulate matter in a megacity," *Genome biology*, vol. 21, no. 1, pp. 1–11, 2020.

[57] W. Raza, S. Saeed, H. Saulat, H. Gul, M. Sarfraz, C. Sonne, Z.-H. Sohn, R. J. Brown, and K.-H. Kim, "A review on the deteriorating situation of smog and its preventive measures in pakistan," *Journal of Cleaner Production*, vol. 279, p. 123676, 2021.

[58] S. Mostafaei, B. Sayad, M. E. F. Azar, M. Doroudian, S. Hadifar, A. Behrouzi, P. Riahi, B. M. Hussen, B. Bayat, J. S. Nahand, *et al.*, "The

role of viral and bacterial infections in the pathogenesis of ipf: a systematic review and meta-analysis," *Respiratory research*, vol. 22, pp. 1–14, 2021.

[59] K. Clarke, A. Manrique, T. Sabo-Attwood, and E. S. Coker, "A narrative review of occupational air pollution and respiratory health in farmworkers," *International journal of environmental research and public health*, vol. 18, no. 8, p. 4097, 2021.

[60] W. Jedrychowski, A. Galas, A. Pac, E. Flak, D. Camman, V. Rauh, and F. Perera, "Prenatal ambient air exposure to polycyclic aromatic hydrocarbons and the occurrence of respiratory symptoms over the first year of life," *European journal of epidemiology*, vol. 20, pp. 775–782, 2005.

[61] M. B. Rice, S. L. Rifas-Shiman, E. Oken, M. W. Gillman, P. L. Ljungman, A. A. Litonjua, J. Schwartz, B. A. Coull, A. Zanobetti, P. Koutrakis, *et al.*, "Exposure to traffic and early life respiratory infection: a cohort study," *Pediatric pulmonology*, vol. 50, no. 3, pp. 252–259, 2015.

[62] C. M. Kennedy, A. F. Pennington, L. A. Darrow, M. Klein, X. Zhai, J. T. Bates, A. G. Russell, C. Hansen, P. E. Tolbert, and M. J. Strickland, "Associations of mobile source air pollution during the first year of life with childhood pneumonia, bronchiolitis, and otitis media," *Environmental Epidemiology*, vol. 2, no. 1, p. e007, 2018.

[63] L. Chen, Z. Song, X. Zhou, G. Yang, and G. Yu, "Pathogenic bacteria and fungi in bioaerosols from specialized hospitals in shandong province, east china," *Environmental Pollution*, vol. 341, p. 122922, 2024.

[64] G. Roth, "Global burden of disease collaborative network. global burden of disease study 2017 (gbd 2017) results. seattle, united states: Institute for health metrics and evaluation (ihme), 2018," *The Lancet*, vol. 392, pp. 1736–88, 2018.

[65] B. J. Cairns and C. Baigent, "Air pollution and traffic noise: do they cause atherosclerosis?," *European heart journal*, vol. 35, no. 13, pp. 826–828, 2014.

[66] A. Ashraf, A. Butt, I. Khalid, R. U. Alam, and S. R. Ahmad, "Smog analysis and its effect on reported ocular surface diseases: A case study of 2016 smog event of lahore," *Atmospheric environment*, vol. 198, pp. 257–264, 2019.

[67] A. M. Grabiec and T. Hussell, "The role of airway macrophages in apoptotic cell clearance following acute and chronic lung inflammation," in *Seminars in immunopathology*, vol. 38, pp. 409–423, Springer.

[68] P. J. Leary, J. D. Kaufman, R. G. Barr, D. A. Bluemke, C. L. Curl, C. L. Hough, J. A. Lima, A. A. Szpiro, V. C. Van Hee, and S. M. Kawut, "Traffic-related air pollution and the right ventricle. the multi-ethnic study of atherosclerosis," *American journal of respiratory and critical care medicine*, vol. 189, no. 9, pp. 1093–1100, 2014.

[69] M. Yegambaram, B. Manivannan, T. G Beach, and R. U Halden, "Role of environmental contaminants in the etiology of alzheimer's disease: a review," *Current Alzheimer Research*, vol. 12, no. 2, pp. 116–146, 2015.

[70] A. Abelsohn and D. M. Stieb, "Health effects of outdoor air pollution: approach to counseling patients using the air quality health index," *Canadian Family Physician*, vol. 57, no. 8, pp. 881–887, 2011.

[71] D. Zhan, M.-P. Kwan, W. Zhang, X. Yu, B. Meng, and Q. Liu, "The driving factors of air quality index in china," *Journal of Cleaner Production*, vol. 197, pp. 1342–1351, 2018.

[72] G. Xiong and Y. Luo, "Smog, media attention, and corporate social responsibility-empirical evidence from chinese polluting listed companies," *Environmental Science and Pollution Research*, pp. 1–14, 2021.

[73] H. Parsajou and T. Nasrabadi, "Evaluation of greenhouse gases emission and human health risk levels due to operation and maintenance of sareyn city wastewater treatment plant," *Journal of Environmental Studies*, vol. 47, no. 1, pp. 45–64, 2021.

[74] X. Sun, D. Li, B. Li, S. Sun, J. Geng, L. Ma, and H. Qi, "Exploring the effects of haze pollution on airborne fungal composition in a cold megacity in northeast china," *Journal of Cleaner Production*, vol. 280, p. 124205, 2021.

[75] T. Qin, F. Zhang, H. Zhou, H. Ren, Y. Du, S. Liang, F. Wang, L. Cheng, X. Xie, A. Jin, *et al.*, "High-level pm2. 5/pm10 exposure is associated with alterations in the human pharyngeal microbiota composition," *Frontiers in microbiology*, vol. 10, p. 422859, 2019.

[76] M. Nagler, H. Insam, G. Pietramellara, and J. Ascher-Jenull, "Extracellular dna in natural environments: features, relevance and applications," *Applied microbiology and biotechnology*, vol. 102, no. 15, pp. 6343–6356, 2018.

[77] M. Nagler, H. Insam, G. Pietramellara, and J. Ascher-Jenull, "Extracellular dna in natural environments: features, relevance and applications," *Applied Microbiology and Biotechnology*, vol. 102, no. 15, pp. 6343–6356, 2018.

[78] A. Navarro and A. Martínez-Murcia, "Phylogenetic analyses of the genus aeromonas based on housekeeping gene sequencing and its influence on systematics," *Journal of applied microbiology*, vol. 125, no. 3, pp. 622–631, 2018.

[79] A. Haghani, R. Johnson, N. Safi, H. Zhang, M. Thorwald, A. Mousavi, N. C. Woodward, F. Shirmohammadi, V. Coussa, J. P. Wise Jr, *et al.*, "Toxicity of urban air pollution particulate matter in developing and adult mouse brain: Comparison of total and filter-eluted nanoparticles," *Environment international*, vol. 136, p. 105510, 2020.

[80] R. Wang, J. Liu, Y. Qin, Z. Chen, J. Li, P. Guo, L. Shan, Y. Li, Y. Hao, M. Jiao, *et al.*, "Global attributed burden of death for air pollution: Demographic decomposition and birth cohort effect," *Science of the Total Environment*, vol. 860, p. 160444, 2023.

[81] T. He, L. Jin, J. Xie, S. Yue, P. Fu, and X. Li, "Intracellular and extracellular antibiotic resistance genes in airborne pm2. 5 for respiratory exposure in

urban areas," *Environmental Science and Technology Letters*, vol. 8, no. 2, pp. 128–134, 2021.

[82] D.-M. Mustață, I. Ionel, R.-M. Popa, C. Dughir, and D. Bisorca, "A study on particulate matter from an area with high traffic intensity," *Applied Sciences*, vol. 13, no. 15, p. 8824, 2023.

[83] M. Manigrasso, C. Protano, M. Vitali, and P. Avino, "Where do ultrafine particles and nano-sized particles come from?," *Journal of Alzheimer's Disease*, vol. 68, no. 4, pp. 1371–1390, 2019.

[84] X. Zhang, Z. Li, J. Hu, L. Yan, Y. He, X. Li, M. Wang, X. Sun, and H. Xu, "The biological and chemical contents of atmospheric particulate matter and implication of its role in the transmission of bacterial pathogenesis," *Environmental Microbiology*, vol. 23, no. 9, pp. 5481–5486, 2021.

[85] Q. Wang, Z. Hou, L. Li, S. Guo, H. Liang, M. Li, H. Luo, L. Wang, Y. Luo, and H. Ren, "Seasonal disparities and source tracking of airborne antibiotic resistance genes in handan, china," *Journal of Hazardous Materials*, vol. 422, p. 126844, 2022.

[86] R. Kumar and A. Thakur, "Younis ahmad hajam, rahul datta, sonika, ajay sharma," *Medical Microbiology*, p. 93, 2022.

[87] R. Lowry, S. Balboa, J. L. Parker, and J. G. Shaw, "Aeromonas flagella and colonisation mechanisms," *Advances in microbial physiology*, vol. 65, pp. 203–256, 2014.

[88] J. L. Martinez, T. M. Coque, V. F. Lanza, F. de la Cruz, and F. Baquero, "Genomic and metagenomic technologies to explore the antibiotic resistance mobilome," *Annals of the New York Academy of Sciences*, vol. 1388, no. 1, pp. 26–41, 2017.

[89] M. R. Gillings, "Evolutionary consequences of antibiotic use for the resistome, mobilome and microbial pangenome," *Frontiers in microbiology*, vol. 4, p. 4, 2013.

[90] Y. Hu, G. F. Gao, and B. Zhu, "The antibiotic resistome: gene flow in environments, animals and human beings," *Frontiers of Medicine*, vol. 11, no. 2, pp. 161–168, 2017.

[91] J. Perry and G. Wright, "The antibiotic resistance "mobilome": searching for the link between environment and clinic," *Frontiers in microbiology*, vol. 4, p. 138, 2013.

[92] J. R. TORRES RUIZ, "Estandarización de la técnica para la obtención del resistòma de suelos.," Tech. Rep. 1, 2014.

[93] G. D. Wright, "The antibiotic resistome," *Expert opinion on drug discovery*, vol. 5, no. 8, pp. 779–788, 2010.

[94] J.-C. Galan, F. Gonzalez-Candelas, J.-M. Rolain, and R. Canton, "Antibiotics as selectors and accelerators of diversity in the mechanisms of resistance: from the resistome to genetic plasticity in the b-lactamases world," *Frontiers in microbiology*, vol. 4, p. 9, 2013.

[95] R. Leclercq, R. Canton, D. F. Brown, C. G. Giske, P. Heisig, A. P. MacGowan, J. W. Mouton, P. Nordmann, A. C. Rodloff, and G. M. Rossolini, "Eucast expert rules in antimicrobial susceptibility testing," *Clinical Microbiology and Infection*, vol. 19, no. 2, pp. 141–160, 2013.

[96] I. Lekunberri, J. L. Balcazar, and C. M. Borrego, "Metagenomic exploration reveals a marked change in the river resistome and mobilome after treated wastewater discharges," *Environmental pollution*, vol. 234, pp. 538–542, 2018.

[97] M. Shintani, "The behavior of mobile genetic elements (mges) in different environments," *Bioscience, Biotechnology, and Biochemistry*, vol. 81, no. 5, pp. 854–862, 2017.

[98] G. P. Dubey and S. Ben-Yehuda, "Intercellular nanotubes mediate bacterial communication," *Cell*, vol. 144, no. 4, pp. 590–600, 2011.

[99] C. Garcia-Aljaro, E. Balleste, and M. Muniesa, "Beyond the canonical strategies of horizontal gene transfer in prokaryotes," *Current opinion in microbiology*, vol. 38, pp. 95–105, 2017.

[100] E. Skippington and M. A. Ragan, "Lateral genetic transfer and the construction of genetic exchange communities," *FEMS microbiology reviews*, vol. 35, no. 5, pp. 707–735, 2011.

[101] C. M. Thomas and K. M. Nielsen, "Mechanisms of, and barriers to, horizontal gene transfer between bacteria," *Nature reviews microbiology*, vol. 3, no. 9, pp. 711–721, 2005.

[102] N. Islam, S. Ebrahimzadeh, J.-P. Salameh, S. Kazi, N. Fabiano, L. Treanor, M. Absi, Z. Hallgrimson, M. M. Leeflang, and L. Hooft, "Thoracic imaging tests for the diagnosis of covid-19," *Cochrane Database of Systematic Reviews*, no. 3, 2021.

[103] S. Marchetti, A. Colombo, M. Saibene, C. Bragato, T. La Torretta, C. Rizzi, M. Gualtieri, and P. Mantecca, "Shedding light on the cellular mechanisms involved in the combined adverse effects of fine particulate matter and sars-cov-2 on human lung cells," *Science of The Total Environment*, p. 175979, 2024.

[104] M. Marques and J. L. Domingo, "Positive association between outdoor air pollution and the incidence and severity of covid-19. a review of the recent scientific evidences," *Environmental Research*, vol. 203, p. 111930, 2022.

[105] S. Yang, Y. Yu, Y. Xu, F. Jian, W. Song, A. Yisimayi, P. Wang, J. Wang, J. Liu, and L. Yu, "Fast evolution of sars-cov-2 ba. 2.86 to jn. 1 under heavy immune pressure," *The Lancet Infectious Diseases*, vol. 24, no. 2, pp. e70–e72, 2024.

[106] A. Javed, F. Aamir, U. F. Gohar, H. MukhtaramidHH, M. Zia-UI-Haq, M. O. Alotaibi, M. N. Bin-Jumah, and O. L. Pop, "The potential impact of smog spell on humans' health amid covid-19 rages," *International Journal of Environmental Research and Public Health*, vol. 18, no. 21, p. 11408, 2021.

[107] L. Setti, F. Passarini, G. De Gennaro, P. Barbieri, M. G. Perrone, M. Borelli, J. Palmisani, A. Di Gilio, V. Torboli, and F. Fontana, "Sars-cov-2rna found on particulate matter of bergamo in northern italy: first evidence," *Environmental research*, vol. 188, p. 109754, 2020.

[108] A. Ashraf, A. Butt, I. Khalid, R. U. Alam, and S. R. Ahmad, "Smog analysis and its effect on reported ocular surface diseases: A case study of 2016 smog event of lahore," *Atmospheric environment*, vol. 198, pp. 257–264, 2019.

[109] M. F. Ashraf, R. U. Ahmad, and H. K. Tareen, "Worsening situation of smog in pakistan: A tale of three cities," *Annals of Medicine and Surgery*, vol. 79, 2022.

[110] M. F. Ashraf, R. U. Ahmad, and H. K. Tareen, "Worsening situation of smog in pakistan: A tale of three cities," *Annals of Medicine and Surgery*, vol. 79, 2022.

[111] A. Razzaq, M. M. Zafar, L. T. Zahra, F. Qadir, F. Qiao, and X. Jiang, "Smog: Lahore needs global attention to fix it," *Environmental Challenges*, p. 100999, 2024.

[112] Z. Sarfraz, "The social and economic burden of smog in pakistan," *Pakistan Journal of Surgery and Medicine*, vol. 1, no. 1, pp. 5–7, 2020.

[113] Z. Saleem, H. Saeed, M. Yousaf, U. Asif, F. K. Hashmi, M. Salman, and M. A. Hassali, "Evaluating smog awareness and preventive practices among pakistani general population: a cross-sectional survey," *International Journal of Health Promotion and Education*, vol. 57, no. 3, pp. 161–173, 2019.

[114] A. Ashraf, A. Butt, I. Khalid, R. U. Alam, and S. R. Ahmad, "Smog analysis and its effect on reported ocular surface diseases: A case study of 2016 smog event of lahore," *Atmospheric environment*, vol. 198, pp. 257–264, 2019.

[115] A. Malik, J. Islam, G. Zaib, M. Ashraf, A. Zahid, A. Rashid, T. Zia, and Q. Ali, "Smog crisis in lahore: evaluating air quality trends and public health implications," *Bulletin of Biological and Allied Sciences Research*, vol. 2024, no. 1, pp. 87–87, 2024.

[116] Z. Naveed and U. Khayyam, "Smog and cognitive issues in the school going children of lahore and islamabad, pakistan," *International Journal of Environmental Science and Technology*, vol. 20, no. 4, pp. 4151–4166, 2023.

[117] J. S. Gaffney, N. A. Marley, and J. E. Frederick, "Formation and effects of smog," *Environmental and Ecological Chemistry; Sabljic, A., Ed.; Eolss Publishers Co., Ltd.: Oxford, UK*, vol. 2, pp. 25–51, 2009.

[118] H. Yang, S. Li, L. Sun, X. Zhang, Z. Cao, C. Xu, X. Cao, Y. Cheng, T. Yan, and T. Liu, "Smog and risk of overall and type-specific cardiovascular diseases: a pooled analysis of 53 cohort studies with 21.09 million participants," *Environmental research*, vol. 172, pp. 375–383, 2019.

[119] B. Rani, U. Singh, A. Chuhan, D. Sharma, and R. Maheshwari, "Photochemical smog pollution and its mitigation measures," *Journal of Advanced Scientific Research*, vol. 2, no. 04, pp. 28–33, 2011.

[120] J. Czerwinska, G. Wielgosinski, and O. Szymanska, "Is the polish smog a new type of smog?," *Ecological Chemistry and Engineering S*, vol. 26, no. 3, pp. 465–474, 2019.

[121] S. Kumar, D. Narwal, and A. Sethi, "Smog: Anthropogenic pollution," *Int. J. Adv. Res. Sci. Eng*, vol. 6, no. 1, 2017.

[122] W. Raza, S. Saeed, H. Saulat, H. Gul, M. Sarfraz, C. Sonne, Z.-H. Sohn, R. J. Brown, and K.-H. Kim, "A review on the deteriorating situation of smog and its preventive measures in pakistan," *Journal of Cleaner Production*, vol. 279, p. 123676, 2021.

[123] S. Sabir, "Investigation of causes and effects of winter smog in lahore, pakistan: Causes and effects of smog," *International Journal of Advances in Sustainable Development (IJASD)*, vol. 1, no. 1, pp. 24–31, 2024.

[124] R. Majeed, M. S. Anjum, M. Imad-ud din, S. Malik, M. N. Anwar, B. Anwar, and M. F. Khokhar, "Solving the mysteries of lahore smog: the fifth season in the country," *Frontiers in Sustainable Cities*, vol. 5, p. 1314426, 2024.

[125] M. Bilal, A. Mhawish, J. E. Nichol, Z. Qiu, M. Nazeer, M. A. Ali, G. de Leeuw, R. C. Levy, Y. Wang, and Y. Chen, "Air pollution scenario over pakistan: Characterization and ranking of extremely polluted cities using long-term concentrations of aerosols and trace gases," *Remote Sensing of Environment*, vol. 264, p. 112617, 2021.

[126] Z. Jahan, F. Sarwar, I. Younes, R. Sadaf, and A. Ahmad, "Assessment of smog pattern and its effects on visibility in lahore using remote sensing and gis," *International Journal of Economic and Environmental Geology*, vol. 10, no. 2, pp. 55–59, 2019.

[127] A. Kausar, I. Ahmad, T. Zhu, and H. Shahzad, "Impact of indoor air pollution in pakistan-causes and management," *Pollutants*, vol. 3, no. 2, pp. 293–319, 2023.

[128] M. U. Siddqiue, M. Jamil, and A. Arshad, "Digital solutions and technological innovations driving public awareness and community initiatives for smog reduction in lahore: A descriptive overview," *Pakistan Social Sciences Review*, vol. 7, no. 4, pp. 425–438, 2023.

[129] R. Ahmad, F. Li, I. Hussain, and A. Hayat, "Assessing the impact of public perception and willingness-to-pay on reducing smog in pakistan: Evidence from lahore city," *Heliyon*, 2024.

[130] S. Kousar, A. Ansar, N. Kausar, and G. Freen, "Multi-criteria decision-making for smog mitigation: a comprehensive analysis of health, economic, and ecological impacts," *Spectrum of Decision Making and Applications*, vol. 2, no. 1, pp. 53–67, 2025.

[131] M. S. Anjum, S. M. Ali, M. A. Subhani, M. N. Anwar, A.-S. Nizami, U. Ashraf, and M. F. Khokhar, "An emerged challenge of air pollution and ever-increasing particulate matter in pakistan; a critical review," *Journal of Hazardous Materials*, vol. 402, p. 123943, 2021.

[132] A. Liaqut, S. Tariq, and I. Younes, "A study on optical properties, classification, and transport of aerosols during the smog period over south asia using

remote sensing," *Environmental Science and Pollution Research*, vol. 30, no. 26, pp. 69096–69121, 2023.

[133] N. Abas, A. Kalair, N. Khan, and A. Kalair, "Review of ghg emissions in pakistan compared to saarc countries," *Renewable and Sustainable Energy Reviews*, vol. 80, pp. 990–1016, 2017.

[134] I. Karim and B. Rappengluck, "Impact of covid-19 lockdown regulations on pm2. 5 and trace gases (no2, so2, ch4, hcho, c2h2o2 and o3) over lahore, pakistan," *Atmospheric Environment*, vol. 303, p. 119746, 2023.

[135] U. Usman, X. Yang, and M. I. Nasir, "Role of climate change in economic uncertainty of pakistan: New approach with qualitative comparative analysis," *Heliyon*, 2024.

[136] H. Malhi, I. Ahmed, R. Nawaz, A. Ahmed, and A. Nasir, "Assessment of attributable proportion of particulate matter (pm2. 5 and pm10) to different mortalities in lahore city, pakistan," *Global Nest Journal*, vol. 25, no. 1, p. 84, 2023.

[137] S. Yousuf, A. Donald, and A. Hassan, "A review on particulate matter and heavy metal emissions; impacts on the environment, detection techniques and control strategies," *MOJ Eco Environ Sci*, vol. 7, no. 1, pp. 1–5, 2022.

[138] M. Tamoor, N. A. Samak, and J. Xing, "Pakistan toward achieving net-zero emissions: policy and roadmap," *ACS Sustainable Chemistry and Engineering*, vol. 11, no. 1, pp. 368–380, 2022.

[139] A. Waheed, T. B. Fischer, S. Kousar, and M. I. Khan, "Disaster management and environmental policy integration in pakistan - an evaluation with particular reference to the china-pakistan economic corridor plan," *Environmental Science and Pollution Research*, vol. 30, no. 48, pp. 105700–105731, 2023.

[140] I. Gandolfi, V. Bertolini, G. Bestetti, R. Ambrosini, E. Innocente, G. Rampazzo, M. Papacchini, and A. Franzetti, "Spatio-temporal variability of airborne bacterial communities and their correlation with particulate matter

chemical composition across two urban areas," *Applied Microbiology and Biotechnology*, vol. 99, no. 11, pp. 4867–4877, 2015.

[141] X. J. Shen, J. Y. Sun, X. Y. Zhang, Y. M. Zhang, L. Zhang, H. C. Che, Q. L. Ma, X. M. Yu, Y. Yue, and Y. W. Zhang, "Characterization of submicron aerosols and effect on visibility during a severe haze-fog episode in yangtze river delta, china," *Atmospheric Environment*, vol. 120, pp. 307–316, 2015.

[142] B. Chen, Y. Yang, X. Liang, K. Yu, T. Zhang, and X. Li, "Metagenomic profiles of antibiotic resistance genes (args) between human impacted estuary and deep ocean sediments," *Environmental Science and Technology*, vol. 47, no. 22, pp. 12753–12760, 2013.

[143] S. Qin, W. Xiao, C. Zhou, Q. Pu, X. Deng, L. Lan, H. Liang, X. Song, and M. Wu, "Pseudomonas aeruginosa: pathogenesis, virulence factors, antibiotic resistance, interaction with host, technology advances and emerging therapeutics," *Signal Transduction and Targeted Therapy*, vol. 7, no. 1, pp. 1–27, 2022.

[144] P. Blanco, S. Hernando-Amado, J. A. Reales-Calderon, F. Corona, F. Lira, M. Alcalde-Rico, A. Bernardini, M. B. Sanchez, and J. L. Martinez, "Bacterial multidrug efflux pumps: Much more than antibiotic resistance determinants," *Microorganisms*, vol. 4, no. 1, p. 14, 2016.

[145] L. Soler, I. Miller, K. Hummel, E. Razzazi-Fazeli, F. Jessen, D. Escribano, and T. Niewold, "Growth promotion in pigs by oxytetracycline coincides with down regulation of serum inflammatory parameters and of hibernation-associated protein hp-27," *ELECTROPHORESIS*, vol. 37, no. 10, pp. 1277–1286, 2016.

[146] P. Knight, R. Chellian, R. Wilson, A. Behnood-Rod, S. Panunzio, and A. W. Bruijnzeel, "Sex differences in the elevated plus-maze test and large open field test in adult wistar rats," *Pharmacology Biochemistry and Behavior*, vol. 204, p. 173168, 2021.

[147] M. Campolongo, N. Kazlauskas, G. Falasco, L. Urrutia, N. Salgueiro, C. Hocht, and A. M. Depino, "Sociability deficits after prenatal exposure to valproic acid are rescued by early social enrichment," *Molecular autism*, vol. 9, no. 1, pp. 1–17, 2018.

[148] F. Peralta, C. Fuentealba, J. Fiedler, and E. Aliaga, "Prenatal valproate treatment produces autistic-like behavior and increases metabotropic glutamate receptor 1a-immunoreactivity in the hippocampus of juvenile rats," *Molecular Medicine Reports*, vol. 14, no. 3, pp. 2807–2814, 2016.

[149] S. Barbesti, L. Soldini, G. Carcelain, A. Guignet, V. Colizzi, B. Mantelli, A. Corvaglia, T. Tran-Minh, F. Dorigatti, and B. Autran, "A simplified flow cytometry method of cd4 and cd8 cell counting based on thermoresistant reagents: Implications for large scale monitoring of hiv-infected patients in resource-limited settings," *Cytometry Part B: Clinical Cytometry: The Journal of the International Society for Analytical Cytology*, vol. 68, no. 1, pp. 43–51, 2005.

[150] M. Riaz, L. T. Al Kury, N. Atzaz, A. Alattar, R. Alshaman, F. a. Shah, and S. Li, "Carvacrol alleviates hyperuricemia-induced oxidative stress and inflammation by modulating the nlrp3/nf-?b pathwayt," *Drug Design, Development and Therapy*, pp. 1159–1170, 2022.

[151] J. Sambrook and D. W. Russell, "Purification of nucleic acids by extraction with phenol: chloroform," *Cold Spring Harbor Protocols*, vol. 2006, no. 1, p. pdb. prot4455, 2006.

[152] J. Waye, L. Presley, B. Budowle, G. Shutler, and R. Fourney, "A simple and sensitive method for quantifying human genomic dna in forensic specimen extracts," *Biotechniques*, vol. 7, no. 8, pp. 852–855, 1989.

[153] A. Pandey, O. Momeni, and P. Pandey, "Quantitative analysis of genomic dna degradation of e. coli using automated gel electrophoresis under various levels of microwave exposure," *Gels*, vol. 10, no. 4, p. 242, 2024.

[154] J. Brown, M. Pirrung, and L. A. McCue, "Fqc dashboard: integrates fastqc results into a web-based, interactive, and extensible fastq quality control tool," *Bioinformatics*, vol. 33, no. 19, pp. 3137–3139, 2017.

[155] D. E. Wood, J. Lu, and B. Langmead, "Improved metagenomic analysis with kraken 2," *Genome biology*, vol. 20, pp. 1–13, 2019.

[156] J. Vollmers, S. Wiegand, and A.-K. Kaster, "Comparing and evaluating metagenome assembly tools from a microbiologist's perspective-not only size matters!," *PloS one*, vol. 12, no. 1, p. e0169662, 2017.

[157] N. S. Malik, M. Ahmad, M. S. Alqahtani, A. Mahmood, K. Barkat, M. T. Khan, U. R. Tulain, and A. Rashid, "B-cyclodextrin chitosan-based hydrogels with tunable ph-responsive properties for controlled release of acyclovir: design, characterization, safety, and pharmacokinetic evaluation," *Drug Delivery*, vol. 28, no. 1, pp. 1093–1108, 2021.

[158] P. Markoulatos, N. Siafakas, and M. Moncany, "Multiplex polymerase chain reaction: a practical approach," *Journal of clinical laboratory analysis*, vol. 16, no. 1, pp. 47–51, 2002.

[159] R. Hinlo, D. Gleeson, M. Lintermans, and E. Furlan, "Methods to maximise recovery of environmental dna from water samples," *PloS one*, vol. 12, no. 6, p. e0179251, 2017.

[160] A. C. Thomas, J. Howard, P. L. Nguyen, T. A. Seimon, and C. S. Goldberg, "edna sampler: A fully integrated environmental dna sampling system," *Methods in ecology and evolution*, vol. 9, no. 6, pp. 1379–1385, 2018.

[161] L. Fauchery, M. Koriabine, L. P. Moore, Y. Yoshinaga, K. Barry, A. Kohler, and J. M. U'Ren, *Tissue cultivation, preparation, and extraction of high molecular weight DNA for single-molecule genome sequencing of plant-associated fungi*, pp. 79–102. Springer, 2022.

[162] L. I. FitzGerald, E. E. Hahn, M. Wallace, S. A. Stephenson, O. F. Berry, and C. M. Doherty, "Capture and protection of environmental dna in a metal-organic framework," *Small Science*, p. 2400432, 2024.

[163] K. Vinod, "Total genomic dna extraction, quality check and quantitation," *Tamil Nadu Agricultural University, Coimbatore*, vol. 1, pp. 109–121, 2004.

[164] R. Westermeier, *Electrophoresis in practice: a guide to methods and applications of DNA and protein separations*. John Wiley and Sons, 2016.

[165] K. Kadri, "Polymerase chain reaction (pcr): Principle and applications," *Synthetic Biology-New Interdisciplinary Science*, pp. 1–17, 2019.

[166] F. Ali, A. Khan, S. A. Muhammad, and S. S. U. Hassan, "Quantitative real-time analysis of differentially expressed genes in peripheral blood samples of hypertension patients," *Genes*, vol. 13, no. 2, p. 187, 2022.

[167] A. Z. Ja'afar, E. Nillian, L. M. Bilung, G. Bebey, D. Zakaria, and P. G. Benjamin, "Detection of cholera toxin (ctxa and ctxab) genes in vibrio cholerae isolated from clinical and environmental samples in limbang sarawak by multiplex polymerase chain reaction (pcr)," *Malaysian Journal of Microbiology*, vol. 17, no. 1, 2021.

[168] T. Van der Merwe, *Molecular quantification and characterisation of aminoglycoside resistant bacteria and genes from aquatic environments*. Thesis, 2018.

[169] J. Novak, P. Vikesland, and A. Pruden, *Treatment Processes for Removal of Wastewater Contaminants*. Water Environment Research Foundation, 2012.

[170] A. Kruttgen, S. Razavi, M. Imohl, and K. Ritter, "Real-time pcr assay and a synthetic positive control for the rapid and sensitive detection of the emerging resistance gene new delhi metallo-b-lactamase-1 (bla ndm-1)," *Medical microbiology and immunology*, vol. 200, pp. 137–141, 2011.

[171] M. Kucinskas, *The effect of sub-inhibitory concentrations of antibiotics on the regulation of eDNA in Staphylococcal biofilms*. Thesis, 2017.

[172] J. T. Saavedra, J. A. Schwartzman, and M. S. Gilmore, "Mapping transposon insertions in bacterial genomes by arbitrarily primed pcr," *Current protocols in molecular biology*, vol. 118, no. 1, pp. 15.15. 1–15.15. 15, 2017.

[173] C. Merrick, C. Wardrope, J. Paget, S. Colloms, and S. Rosser, *Rapid optimization of engineered metabolic pathways with serine integrase recombinational assembly (SIRA)*, vol. 575, pp. 285–317. Elsevier, 2016.

[174] J. O. Ogutu, Q. Zhang, Y. Huang, H. Yan, L. Su, B. Gao, W. Zhang, J. Zhao, W. Cai, and W. Li, "Development of a multiplex pcr system and its application in detection of blashv, blatem, blactx-m-1, blactx-m-9 and blaoxa-1 group genes in clinical klebsiella pneumoniae and escherichia coli strains," *The Journal of antibiotics*, vol. 68, no. 12, pp. 725–733, 2015.

[175] K. D. Balasingham, R. P. Walter, and D. D. Heath, "Residual edna detection sensitivity assessed by quantitative real-time pcr in a river ecosystem," *Molecular Ecology Resources*, vol. 17, no. 3, pp. 523–532, 2017.

[176] K. R. Lezak and W. A. Carlezon, "Behavioral methods to study anxiety in rodents," *Drug Discovery Today: Disease Models*, vol. 19, no. 2, pp. 71–83, 2017.

[177] C. Kyi-Tha-Thu, Y. Fujitani, S. Hirano, and T.-T. Win-Shwe, "Early-life exposure to traffic-related air pollutants induced anxiety-like behaviors in rats," *International Journal of Molecular Sciences*, vol. 24, no. 1, p. 586, 2022.

[178] S. Ji *et al.*, "Real-world PM2.5 exposure causes anxiety and depression-like behaviors by disrupting dopamine signaling," *PNAS*, 2024.

[179] A. V. Kalueff *et al.*, "Neurobiology of rodent self-grooming and its value for translational neuroscience," *Nature Reviews Neuroscience*, vol. 17, no. 1, pp. 45–59, 2016.

[180] H. Wei *et al.*, "PM2.5 exposure in mice leads to damage in hippocampal-dependent working memory via ferroptosis," *Science of the Total Environment*, 2024.

[181] C. Liu *et al.*, "PM2.5 promotes tau aggregation and induces cognitive impairments," *JCI Insight*, 2024.

[182] J. Zhang *et al.*, "Maternal concentrated PM2.5 exposure is negatively correlated with spatial memory in offspring," *Chemico-Biological Interactions*, 2023.

[183] J. Smith *et al.*, "Diesel particulate exposure produces alveolar structural damage and inflammation in rat lungs," *Respiratory Research*, vol. 18, p. 128, 2017.

[184] H. Zhao *et al.*, "Chronic exposure to ambient PM2.5 induces pulmonary fibrosis and alveolar destruction in mice," *Particle and Fibre Toxicology*, vol. 16, p. 42, 2019.

[185] N. Li *et al.*, "Air pollution and lung inflammation: mechanisms and effects," *Environmental Health Perspectives*, vol. 129, no. 9, p. 096001, 2021.

[186] S. Chen *et al.*, "Particulate matter exposure and protease-mediated lung remodeling: mechanisms in rodents," *American Journal of Respiratory Cell and Molecular Biology*, vol. 62, no. 2, pp. 169–180, 2020.

[187] M. M. Hargrove, S. J. Snow, R. W. Luebke, *et al.*, "Effects of simulated smog atmospheres in rodent models of metabolic and immunologic dysfunction," *Environmental Science and Technology*, vol. 52, no. 5, pp. 3062–3070, 2018.

[188] C. Soler-Segovia, C. Muñoz-Santos, C. Ubeda, *et al.*, "Diesel exhaust particles induce systemic immune responses and enhance CD4+ T cell activity," *Particle and Fibre Toxicology*, vol. 16, p. 40, 2019.

[189] Y. Jo, S. Choi, J. Oh, *et al.*, "Fine particulate matter exposure alters CD4:CD8 ratio and promotes T-cell mediated immune imbalance," *Environment International*, vol. 143, p. 105924, 2020.

[190] J. Duan, H. Hu, S. Wang, *et al.*, "NF-κB activation mediates immune responses induced by PM2.5 exposure in mice," *Toxicology Letters*, vol. 337, pp. 1–9, 2021.

[191] X. Li, Y. Zhang, Q. Chen, *et al.*, "PM2.5 exposure activates MAPK/NF-κB pathways and promotes T lymphocyte recruitment," *Frontiers in Immunology*, vol. 13, p. 832456, 2022.

[192] L. M. Weatherly, J. A. Gosse, and R. McConnell, "Chronic diesel exhaust exposure suppresses T cell immunity in mice," *Toxicology and Applied Pharmacology*, vol. 329, pp. 1–8, 2017.

[193] Y. Li, W. Wang, J. Xu, *et al.*, "Air pollution and lung microbiome shifts: Evidence from metagenomic and metabolomic integration," *Science of the Total Environment*, vol. 903, p. 166456, 2024.

[194] C. Yan, M. Gao, R. Chen, *et al.*, "Airborne PM2.5 alters lung microbial ecology and promotes antibiotic resistance enrichment," *Environment International*, vol. 161, p. 107128, 2022.

[195] L. N. Segal, J. C. Clemente, B. G. Wu, *et al.*, "Enrichment of lung microbiome with pathogens in chronic respiratory disease," *Nature Microbiology*, vol. 2, p. 17084, 2017.

[196] Z. Miao, J. Li, T. Li, *et al.*, "Particulate matter exposure promotes Staphylococcus aureus colonization and persistence in the respiratory tract," *Environmental Pollution*, vol. 287, p. 117319, 2021.

[197] Y. Qin, Y. Zhao, T. Zhang, *et al.*, "Airborne particulate matter reshapes microbial communities and promotes antibiotic resistance gene enrichment," *ISME Journal*, vol. 16, pp. 1213–1225, 2022.

[198] J. S. Brooke, "Stenotrophomonas maltophilia: An emerging global opportunistic pathogen," *Clinical Microbiology Reviews*, vol. 34, no. 1, pp. e00076–19, 2021.

[199] J. Hu, F. Zhao, X. X. Zhang, *et al.*, "Metagenomic profiling of antibiotic resistance genes in airborne particulate matters during severe smog events," *Science of the Total Environment*, vol. 615, pp. 1332–1340, 2019.

[200] B. A. Evans and S. G. B. Amyes, "OXA β-lactamases," *Clinical Microbiology Reviews*, vol. 27, no. 2, pp. 241–263, 2014.

[201] A. S. Lee, H. de Lencastre, J. Garau, *et al.*, "Methicillin-resistant Staphylococcus aureus," *Nature Reviews Disease Primers*, vol. 4, no. 1, p. 18033, 2018.

[202] R. Wang, L. van Dorp, L. P. Shaw, *et al.*, "The global distribution and spread of the mobilized colistin resistance gene mcr-1," *Nature Communications*, vol. 9, p. 1179, 2018.

[203] A. Antonelli, M. M. D'Andrea, A. Brenciani, *et al.*, "The poxtA gene is widely distributed in Gram-positive bacteria and contributes to linezolid resistance," *Nature Communications*, vol. 9, no. 1, p. 4109, 2018.

[204] Z. Pang, R. Raudonis, B. R. Glick, *et al.*, "Antibiotic resistance in Pseudomonas aeruginosa: Mechanisms and alternative therapeutic strategies," *Biotechnology Advances*, vol. 37, no. 1, pp. 177–192, 2019.

[205] S. H. Jeong, H. S. Kim, J. S. Kim, *et al.*, "Prevalence and molecular characteristics of carbapenemase-producing Enterobacteriaceae from a Korean nationwide surveillance program," *Antimicrobial Agents and Chemotherapy*, vol. 62, no. 4, pp. e00329–18, 2018.

[206] Y. Y. Liu, Y. Wang, T. R. Walsh, *et al.*, "Emergence of plasmid-mediated colistin resistance mechanism mcr-1 in animals and human beings in China," *Lancet Infectious Diseases*, vol. 16, no. 2, pp. 161–168, 2016.

[207] L. K. Logan and R. A. Weinstein, "The epidemiology of carbapenem-resistant Enterobacteriaceae: The impact and evolution of a global menace," *Journal of Infectious Diseases*, vol. 215, no. supplement 1, pp. S28–S36, 2017.

[208] Y. Shen, H. Zhou, J. Xu, *et al.*, "Anthropogenic and environmental factors associated with high incidence of mcr-1 carriage in humans and animals: A global risk assessment," *Lancet Planetary Health*, vol. 2, no. 7, pp. e313–e320, 2018.

[209] J. Hu, F. Zhao, X. X. Zhang, *et al.*, "Metagenomic profiling of ARGs in airborne particulate matters during a severe smog event," *Science of the Total Environment*, vol. 615, pp. 1332–1340, 2018.

[210] P. Courvalin, "Vancomycin resistance in Gram-positive cocci," *Clinical Infectious Diseases*, vol. 42, no. Supplement 1, pp. S25–S34, 2016.

[211] M. Alcalde-Rico, J. Olivares-Pacheco, C. Alvarez-Ortega, *et al.*, "Role of the multidrug resistance efflux pump MexCD-OprJ in antibiotic resistance and virulence of Pseudomonas aeruginosa," *Antimicrobial Agents and Chemotherapy*, vol. 62, no. 1, pp. e02163–17, 2018.

[212] J. B. Patel, R. J. Gorwitz, and J. A. Jernigan, "Mupirocin resistance," *Clinical Infectious Diseases*, vol. 49, no. 6, pp. 935–941, 2009.

[213] G. Zhu, X. Wang, T. Yang, *et al.*, "Air pollution could drive global dissemination of antibiotic resistance genes," *ISME Journal*, vol. 15, no. 1, pp. 270–281, 2021.

[214] M. Gao, Q. Zhang, C. Lei, *et al.*, "Atmospheric antibiotic resistome driven by air pollutants," *Science of the Total Environment*, vol. 902, p. 165942, 2023.

[215] W. R. Miller, J. M. Munita, and C. A. Arias, "Mechanisms of antibiotic resistance in enterococci," *Expert Review of Anti-Infective Therapy*, vol. 12, no. 10, pp. 1221–1236, 2014.

[216] S. Coyne, P. Courvalin, and B. Périchon, "Efflux-mediated antibiotic resistance in Acinetobacter spp.," *Antimicrobial Agents and Chemotherapy*, vol. 55, no. 3, pp. 947–953, 2011.

[217] K. Dheda *et al.*, "Global control of tuberculosis: from extensively drug-resistant to untreatable tuberculosis," *The Lancet Respiratory Medicine*, vol. 5, no. 4, pp. 269–282, 2017.

[218] J. Li, J. Cao, Y. G. Zhu, *et al.*, "Particulate matter as a vector for airborne antibiotic resistance," *Environment International*, vol. 173, p. 107870, 2023.

[219] World Health Organization, "Global tuberculosis report 2023," tech. rep., WHO, Geneva, 2023.

[220] S. J. van Hal, D. L. Paterson, and T. P. Lodise, "Systematic review and meta-analysis of vancomycin-induced nephrotoxicity associated with dosing schedules that maintain troughs between 15 and 20 milligrams per liter," *Antimicrobial Agents and Chemotherapy*, vol. 57, no. 2, pp. 734–744, 2013.

[221] A. G. McArthur and G. D. Wright, "Bioinformatics of antimicrobial resistance in the age of molecular epidemiology," *Current Opinion in Microbiology*, vol. 27, pp. 45–50, 2015.

[222] V. Cattoir and R. Leclercq, "Twenty-five years of shared life with vancomycin-resistant enterococci: is it time to divorce?," *Journal of Antimicrobial Chemotherapy*, vol. 68, no. 4, pp. 731–742, 2013.

[223] J. M. Rodríguez-Martínez, L. Poirel, and P. Nordmann, "Extended-spectrum cephalosporinases in Pseudomonas aeruginosa," *Antimicrobial Agents and Chemotherapy*, vol. 53, no. 5, pp. 1766–1771, 2009.

[224] E. M. H. Wellington, A. B. A. Boxall, P. Cross, *et al.*, "The role of the natural environment in the emergence of antibiotic resistance in Gram-negative bacteria," *The Lancet Infectious Diseases*, vol. 13, no. 2, pp. 155–165, 2013.

[225] J. Li, J. Cao, Y. G. Zhu, *et al.*, "Global survey of antibiotic resistance genes in air," *Environmental Science and Technology*, vol. 52, no. 19, pp. 10975–10984, 2018.

[226] M. Arthur and P. Courvalin, "Genetics and mechanisms of glycopeptide resistance in enterococci," *Antimicrobial Agents and Chemotherapy*, vol. 37, no. 8, pp. 1563–1571, 1993.

[227] A. Antonelli, M. M. D'Andrea, A. Brenciani, *et al.*, "Characterization of poxtA, a novel phenicol–oxazolidinone–tetracycline resistance gene from Enterococcus faecium," *Antimicrobial Agents and Chemotherapy*, vol. 62, no. 9, pp. e01204–18, 2018.

[228] J. Sun, Z. Deng, and A. Yan, "Bacterial multidrug efflux pumps: Mechanisms, physiology and pharmacological exploitations," *Biochemical and Biophysical Research Communications*, vol. 453, no. 2, pp. 254–267, 2014.

[229] G. X. He, C. Thorpe, D. Walsh, *et al.*, "Small multidrug resistance (SMR) transporters: Diverse functions in multidrug resistance," *Journal of Biological Chemistry*, vol. 286, no. 14, pp. 12581–12590, 2011.

[230] S. Coyne, P. Courvalin, and B. Périchon, "Efflux-mediated antibiotic resistance in Acinetobacter spp.," *Antimicrobial Agents and Chemotherapy*, vol. 55, no. 3, pp. 947–953, 2011.

[231] K. V. Newell, D. P. Thomas, D. Brekasis, and M. S. Paget, "The RNA polymerase-binding protein RbpA confers basal levels of rifampicin resistance on Streptomyces coelicolor," *Molecular Microbiology*, vol. 60, no. 4, pp. 687–696, 2006.

[232] J. Li, J. Cao, Y. G. Zhu, *et al.*, "Global survey of antibiotic resistance genes in air," *Environmental Science and Technology*, vol. 52, no. 19, pp. 10975–10984, 2018.

[233] K. J. Forsberg, A. Reyes, B. Wang, *et al.*, "The shared antibiotic resistome of soil bacteria and human pathogens," *Science*, vol. 337, no. 6098, pp. 1107–1111, 2012.

[234] Y. G. Zhu, Y. Zhao, B. Li, *et al.*, "Continental-scale pollution of antibiotic resistance genes in topsoil across China," *Nature Microbiology*, vol. 2, p. 16270, 2017.

[235] E. M. Wellington, A. B. A. Boxall, P. Cross, *et al.*, "The role of the natural environment in the emergence of antibiotic resistance in Gram-negative bacteria," *The Lancet Infectious Diseases*, vol. 13, no. 2, pp. 155–165, 2013.

[236] H. W. Hu, J. T. Wang, J. Li, *et al.*, "Field-based evidence for copper contamination induced changes of antibiotic resistance in agricultural soils," *Environmental Microbiology*, vol. 18, no. 11, pp. 3896–3909, 2016.

[237] T. U. Berendonk, C. M. Manaia, C. Merlin, *et al.*, "Tackling antibiotic resistance: The environmental framework," *Nature Reviews Microbiology*, vol. 13, no. 5, pp. 310–317, 2015.

[238] Y. G. Zhu *et al.*, "Diverse and abundant antibiotic resistance genes in Chinese swine farms," *Nature Microbiology*, vol. 2, p. 16270, 2017.

[239] E. R. Bevan *et al.*, "Global epidemiology of CTX-M beta-lactamases: temporal and geographical shifts in gene distribution," *Journal of Antimicrobial Chemotherapy*, vol. 72, no. 8, pp. 2145–2155, 2017.

[240] C. M. Manaia, "Assessing the risk of antibiotic resistance transmission from the environment to humans: non-direct proportionality between abundance and risk," *Trends in Microbiology*, vol. 25, no. 3, pp. 173–181, 2017.

[241] W. Wu *et al.*, "Global spread of New Delhi metallo-β-lactamase 1 (NDM-1) producing Enterobacteriaceae," *Clinical Microbiology Reviews*, vol. 32, no. 2, pp. e00115–18, 2019.

[242] J. Li *et al.*, "Airborne transmission of antibiotic resistance genes between animal farms and urban regions," *Environment International*, vol. 138, p. 105598, 2020.

[243] R. Cantón and T. M. Coque, "The CTX-M beta-lactamase pandemic," *Current Opinion in Microbiology*, vol. 9, no. 5, pp. 466–475, 2006.

[244] Y. Yang *et al.*, "Atmospheric transport and inhalation risks of antibiotic resistance genes in fine particulate matter," *Environment International*, vol. 153, p. 106523, 2021.

[245] M. R. Gillings *et al.*, "Using the class 1 integron-integrase gene as a proxy for anthropogenic pollution," *ISME Journal*, vol. 9, no. 6, pp. 1269–1279, 2015.

[246] T. Stalder *et al.*, "Linking the resistome and plasmidome to the microbiome," *ISME Journal*, vol. 8, no. 7, pp. 1382–1394, 2014.

[247] S. R. Partridge *et al.*, "Mobile genetic elements associated with antimicrobial resistance," *Clinical Microbiology Reviews*, vol. 31, no. 4, pp. e00088–17, 2018.

[248] P. Courvalin, "Vancomycin resistance in Gram-positive cocci," *Clinical Infectious Diseases*, vol. 42, no. Supplement 1, pp. S25–S34, 2006.

[249] Y. Jiang *et al.*, "Air pollution promotes horizontal gene transfer of antibiotic resistance genes," *Science of the Total Environment*, vol. 812, p. 151460, 2022.

Appendix-A

TABLE 1: Resistance gene profiles of Lahore environmental isolates (2022)

AMR Gene	**Gene Family**	**Drug Class**	**Resistance Mechanism**	**% Identity of Matching Region**	**% Length of Ref Sequence**
vanY gene in *vanM* cluster	Glycopeptide resistance gene cluster	Glycopeptide	Antibiotic target alteration	25.95% - 37.76%	111.59% - 385.84%
vanY gene in *vanG* cluster	Glycopeptide resistance gene cluster	Glycopeptide	Antibiotic target alteration	26.67% - 43.08%	52.81% - 135.07%
vanY gene in *vanD* cluster	Glycopeptide resistance gene cluster	Glycopeptide	Antibiotic target alteration	30.32% - 35.0%	62.31% - 130.90%
vanW gene in *vanO* cluster	Glycopeptide resistance gene cluster	Glycopeptide	Antibiotic target alteration	26.22% - 37.54%	95.71% - 167.83%
vanW gene in *vanI* cluster	Glycopeptide resistance gene cluster	Glycopeptide	Antibiotic target alteration	25.28% - 37.3%	60.86% - 172.65%
vanW gene in *vanF* cluster	Glycopeptide resistance gene cluster	Glycopeptide	Antibiotic target alteration	27.85% - 38.52%	97.27% - 227.61%
vanT gene in *vanG* cluster	Glycopeptide resistance gene cluster	Glycopeptide	Antibiotic target alteration	29.65% - 35.54%	51.54% - 163.44%
vanH gene in *vanO* cluster	Glycopeptide resistance gene cluster	Glycopeptide	Antibiotic target alteration	32.33% - 40.0%	95.71% - 227.61%

AMR Gene	**Gene Family**	**Drug Class**	**Resistance Mechanism**	**% Identity of Matching Region**	**% Length of Ref Sequence**
vanH gene in *vanD* cluster	Glycopeptide resistance gene cluster	Glycopeptide	Antibiotic target alteration	32.33% - 40.0%	95.71% - 227.61%
RbpA	Bacterial RNA polymerase-binding protein	Rifamycin	Antibiotic target protection	84.68% - 97.32%	78.22% - 98.25%
qacJ	Small multidrug resistance (SMR) efflux pump	Disinfecting agents and antiseptics	Antibiotic efflux	38.24% - 50.38%	73.88% - 117.76%
qacG	Small multidrug resistance (SMR) efflux pump	Disinfecting agents and antiseptics	Antibiotic efflux	38.61% - 41.84%	73.88% - 117.76%
nimB	Nitroimidazole reductase	Nitroimidazole	Antibiotic inactivation	55.76%	102.44%
adeF	RND antibiotic efflux pump	Fluoroquinolone, Tetracycline	Antibiotic efflux	43.82% - 72.3%	85.55% - 171.31%

Appendix-B

TABLE 2: Resistance gene profiles of Lahore environmental isolates (2023)

AMR Gene	**Gene Family**	**Drug Class**	**Resistance Mechanism**	**% Identity of Matching Region**	**% Length of Ref Sequence**
vanY	Glycopeptide resistance gene cluster (*vanY*)	Glycopeptide antibiotic	Antibiotic target alteration	31.95	114.93
vanW	Glycopeptide resistance gene cluster (*vanW*)	Glycopeptide antibiotic	Antibiotic target alteration	32.13	172.65
vanT	Glycopeptide resistance gene cluster (*vanT*)	Glycopeptide antibiotic	Antibiotic target alteration	30.33	117.84
vanR	Glycopeptide resistance gene cluster (*vanR*)	Glycopeptide antibiotic	Antibiotic target alteration	82.97	99.14
vanH	Glycopeptide resistance gene cluster (*vanH*)	Glycopeptide antibiotic	Antibiotic target alteration	37.54	103.72
RbpA	*RbpA* bacterial RNA polymerase-binding protein	Rifamycin antibiotic	Antibiotic target protection	97.32	98.25
qacJ	Small multidrug resistance (SMR) efflux pump	Disinfecting agents, Antiseptics	Antibiotic efflux	38.24	98.13

AMR Gene	**Gene Family**	**Drug Class**	**Resistance Mechanism**	**% Identity of Matching Region**	**% Length of Ref Sequence**
OXA-50	Beta-lactamase enzyme	Beta-lactam antibiotics	Resistance to beta-lactam antibiotics	58.75	97.71
adeF	Resistance-nodulation-cell division (RND) efflux pump	Fluoroquinolone, Tetracycline antibiotics	Antibiotic efflux	73.47	102.27